endeavour

EUROC
EUROPEAN ROCKETRY CHALLENGE

Darwin III: The Great British Lift-off

Team 11 Technical Report to the 2022 EuRoC

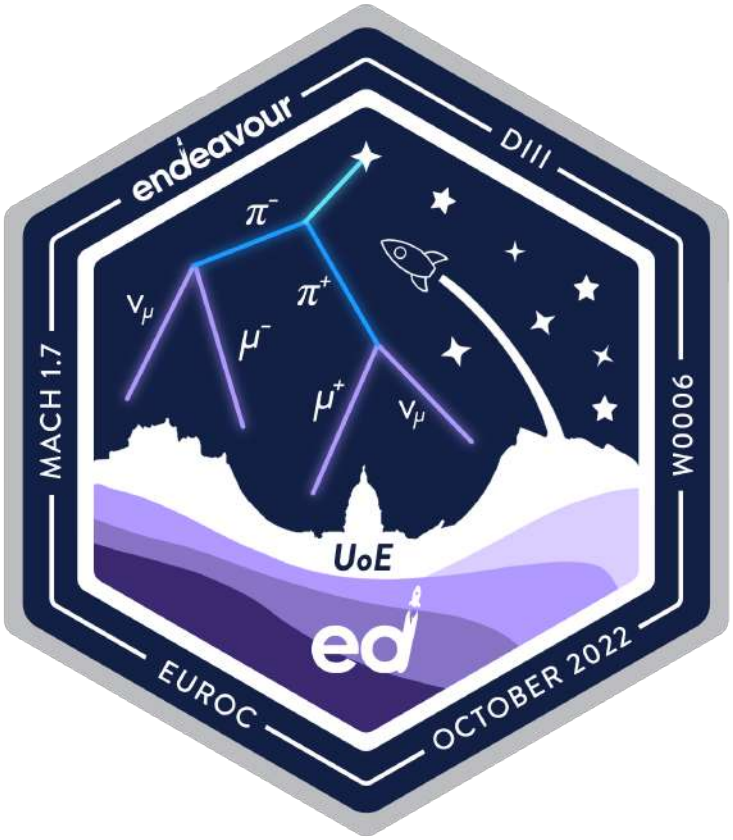

11 September 2022

Contents

1 Introduction **1**
- 1.1 Team Introduction . . . 1
  - 1.1.1 Team Ethos and Motivation . . . 2
  - 1.1.2 Stakeholders . . . 2
- 1.2 Legacy of Darwin II . . . 3
  - 1.2.1 Mission Objectives . . . 4

2 System Architecture **5**
- 2.1 Overview . . . 6
- 2.2 Propulsion subsystem . . . 9
  - 2.2.1 Motor Choice . . . 9
  - 2.2.2 Arming and Ignition . . . 10
- 2.3 Aerostructure subsystem . . . 11
  - 2.3.1 Mechanical Interfaces and Internal Components . . . 12
  - 2.3.2 Trajectory Simulation . . . 20
- 2.4 Recovery subsystem . . . 22
  - 2.4.1 Introduction . . . 22
  - 2.4.2 Components, Specifications and system overview . . . 22
  - 2.4.3 Recovery Subsystem Calculations . . . 23
  - 2.4.4 Detailed view of recovery bay and hardware . . . 25
  - 2.4.5 Parachute Shock Forces . . . 28
  - 2.4.6 Redundancy in recovery . . . 28
- 2.5 Payload Subsystem . . . 29
  - 2.5.1 Mission Aims and Success Criteria . . . 29
  - 2.5.2 Payload Architecture . . . 29
  - 2.5.3 Form Factor . . . 30
  - 2.5.4 Scientific Background and Context . . . 31
  - 2.5.5 Functionality . . . 31
  - 2.5.6 Dissemination of Results . . . 33
  - 2.5.7 Power Consumption . . . 34
  - 2.5.8 Deployment and Recovery . . . 34
- 2.6 Active flight control subsystem . . . 35
  - 2.6.1 Airbrake . . . 35
  - 2.6.2 In-Flight Abort/ Manual Recovery Initiation . . . 39
- 2.7 Special Subsystems . . . 40
  - 2.7.1 SRAD Avionics . . . 40
  - 2.7.2 Ground Station and the Endeavour Wireless Direct Link . . . 42

3 Mission Concept of Operations Overview **44**

4 Conclusions and Outlook **48**

A System Data **50**
- A.1 State and Event Definitions . . . 51
  - A.1.1 Actions during each state . . . 51

B Detailed Test Reports **55**
- B.1 Preliminary Ejection Mechanism Viability . . . 55
- B.2 Recovery Test - SRAD Ejection powered by SRAD Flight Computer . . . 56

B.3 Recovery Test - COTS Ejection system with external power supply . . . 57
B.4 Recovery Test - COTS Ejection powered by SRAD Flight Computer . . . 58
B.5 Recovery Test - COTS Ejection powered by COTS Flight Computer . . . 59
B.6 Recovery Test - COTS Main Release powered by COTS Flight Computer . . . 60
B.7 Recovery Test - COTS main release powered by SRAD Flight Computer . . . 61
B.8 Payload Muon Detector Test . . . 62
B.9 Payload Muon Detector Altitude Test . . . 63
B.10 Payload Muon Detector Climate Chamber Tests . . . 64
B.11 Payload Muon Detector Hodoscope Test . . . 65
B.12 Payload Power Board Electrical Load Test . . . 66
B.13 Payload Power Draw Test . . . 67
B.14 Payload Power Board Electrical Switch Test . . . 68
B.15 Payload Launch Load Test . . . 69
B.16 Integrated Test of Avionics Stack and Ground Station . . . 70
B.17 SRAD propulsion system testing . . . 71
B.18 SRAD pressure vessel testing . . . 72

C Hazard Analysis Report **73**
C.1 Motor assembly - explosives handling . . . 73
C.2 Recovery System Stored Energy Devices . . . 73
C.3 Avionics and Payload Lithium Battery Packs . . . 74

D Risk assessment **75**

E Checklists **83**
E.1 Shipping Checklist . . . 83
E.2 Edinburgh departure checklist . . . 85
E.3 Propulsion System Handling & Integration Procedure . . . 86
E.4 Recovery checklist/procedure . . . 88
E.5 Payload Assembly Procedure . . . 90
E.6 Pre-Flight Integration . . . 92
E.7 Countdown checklist . . . 94
E.8 Rocket search and rescue checklist . . . 95
E.9 Assembly Checklist . . . 96

F Engineering Drawings **97**

G Subsystem Details **111**
G.1 Payload Scientific Background . . . 111
G.1.1 CosmicWatch Muon Detector . . . 111
G.1.2 Slosh Experiment . . . 112

H Detailed Structural and Mechanical Calculations **113**
H.1 Payload 15G Liftoff Load . . . 113
H.2 Payload 180N Parachute Shock Force . . . 114

I Detailed Electrical Schematics **115**

J Final launch role definition **124**

Abstract

In the following report, the Endeavour sounding rocketry team Darwin, based in Edinburgh and composed of 30 members, will present the technical details and general mission profile of their 2022 challenger to the European Rocketry Challenge: Darwin III. The vehicle aims to achieve a 9000m apogee, propelled by the Cesaroni Technologies O3400 COTS motor, competing in the EuRoC S9-C category (aka "COTS-9k").

Darwin III (shortened to DIII) cannot be discussed without considering its predecessor, Darwin II. The DII mission was deemed a partial success - while the team gained valuable insights into the processes and complexity associated with international competitions, the vehicle did not fly. The failure to launch was subject to deep internal investigations, leading to a newfound emphasis on procedures and a more conservative manufacturing plan allowing for more testing and delay buffers.

Darwin III is a single-stage, composite construction experimental launch vehicle and seeks to improve on all aspects of DII while retaining commonality of fuselage diameter and solid motor. Particular attention was placed on increasing the stability margin by optimising mass distribution, and improving ease of assembly on launch day. Throughout, machined parts have been light-weighted by using aluminium 7075-T6, which provides up to 170% improvement in specific yield strength. The fully redesigned SRAD Avionics interface with several high current outputs, both servo-motors and pyrotechnic, giving flexibility in recovery systems and deployment of the active control surfaces of the airbrake. A brand new, fully SRAD telemetry stack enables robust, two-way communication with a ground station suitable for rough terrain. Flight data and abort options are clearly displayed on a high-definition graphical interface and data is pushed to a remote server for ubiquitous smartphone access during recovery efforts. For the first time, the team has developed a servo-actuated drogue ejection system inspired by the CO_2-powered Raptor system. The SRAD system is cross-braced with a COTS CO_2 ejection system, improving the likelihood of a successful ejection event. To further improve the reliability of the recovery system, the cable management between Avionics and Recovery Bays has been consolidated into robust, simple harnesses.

A 2U CubeSat, housed within the team's first all CFRP nosecone, will be conducting physics experiments validated in collaboration with the School of Physics at The University of Edinburgh, and gathering valuable engineering data for the team's future vehicles. An open-source muon detector was adapted for the harsh environment of launch, and calibrated against state-of-the-art detectors and literature values, in a range of conditions within a climate chamber, such that it will produce results accurate enough that the team will be able to independently confirm the validity of Einstein's Theory of Special Relativity. The secondary experiment features a high-definition slow motion camera used to study the sloshing dynamics of fluids held in slender vessels, as an analogue for fuel slosh in Endeavour's future bi-liquid vehicles.

Acknowledgement

First off, we would like to thank the School of Engineering, School of Physics and Astronomy, and School of Informatics at The University of Edinburgh for their support. The staff at the university, in particular our academic advisors Dr. Francisca Martinez-Hergueta and Dr. David Garcia-Cava have helped us immensely in many technical and pastoral aspects from simulation of composite materials, to overseeing the countless risk assessments while always representing and supporting the team within the School of Engineering.

An additional, heartfelt thank you goes out to the School of Engineering technicians that have made Darwin III possible. Steve Gourlay contributed his experience to optimising our initial designs for the machining facilities available at the University. Jamie Brown dedicated weeks of his time to creating the intricate geometries of our parts on both manual machines and 5-axis CNC mills. On top of their constant support and unmistakable humour, Andrew Brown supported our team through the fabrication of the airbrake in under a week, and Calum Melrose assisted with countless questions around fabrication - we appreciate you technicians of G.20! And to Tom Bolland, thank you for opening up our lab at odd hours and for caringly engaging with us regarding the future of the university's MakerSpace facilities.

To guide us on the electrical/avionics side, special recognition goes out to the patient and knowledgeable technicians of TLD: Iain Gold for showing the team the ropes on high-powered microscopes and solder-paste dispensers, Rom Correa for promptly spinning up PCBs and always being able to source the one component we forgot to order and Alasdair Chrsitie for never backing away from even the smallest QFN packages.

We are grateful to the Student Innovation Advisory Group members, in particular Chris Sturgeon, Sally Morgan, Dr. Edward McCarthy and the Edinburgh Innovations group for creating a positive environment conducive to student-led innovation and providing advice and logistics and advanced composite additive manufacturing capabilities.

On top of the invaluable support of technicians, professors and advisers, we would like to mention our sponsors and industrial partners, who allowed us to build Darwin III using high-quality components and using modern tools, preparing our team to enter the workforce. We are grateful to Skyrora's support and mentoring, and greatly appreciated ZOT and M-Carbo's in-kind contribution of high-quality PCB and custom, filament-wound CFRP tubing. Thank you to Altium, Solidworks and nTopology for supporting us with access to your cutting edge Computer Aided Engineering software products.

Finally, and most importantly, thank you to our alumni and current team members for making Endeavour what it is. This team is a special collection of individuals, and the bonds of trust, friendship and respect we have built over our missions will hold strong for years to come. No matter the obstacles we have faced, and the ones that lie ahead, this team will undoubtedly remain a point of reference for passionate, driven students from every faculty of our University.

Our hard work brought us all the way here. Now, let's light this candle.

List of Abbreviations

AB - Airbrake

AFB - Air force base

ALS - Above launch site

BJT - Bipolar junction transistor

BMS - Battery management system

BP - Black Powder

CATO - Catastrophe at take-off

CFD - Computational Fluid Dynamics

CFRP - Carbon fibre reinforced polymer

CNC - Computer numerical control

CONOPS - Concept of operations

COTS - Commercial off the shelf

DII - Darwin II

DoF - Degrees of freedom

EMI - Electromagnetic interference

EWDL - Endeavour wireless direct link

FC - Flight computer

FEA - Finite element analysis

FEM - Finite element method

FET - Field effect transistor

FoS - Factor of safety

GFRP - Glass fibre reinforced polymer

GPS - Global positioning system

GSO - Ground Station Operator

HDPE - High-density polyethylene

IMU - Inertial measurement unit

LiPo - Lithium-polymer batteries

LOS - Line of sight

LV - Launch vehicle

MOSFET - Metal oxide semiconductor field-effect transistor

NMEA - National Marine Electronics Association

OR - OpenRocket

OS - Operating System

PCB - Printed circuit boards

PID - Proportional–integral–derivative controller

PLA - Polylactic acid

PMD - Propellant Management Device

PMT - Photomultiplier Tube

PRB - Power routing board

RAS - RASAero

RF - Radio frequency

RSO - Range safety officer

SARA - Scottish Aeronautics and Rocketry Association

SHSS - Shoulder Head Socket Screw

SiPM - Silicon Photomultiplier

SPI - Serial Peripheral Interface

SRAD - Student research and developed

STEM - Science, Technology, Engineering, and Mathematics

TD - Tender descender

UKRA - United Kingdom Rocketry Association

Nomenclature

Δv	Change in velocity [m/s]
ρ	Density [kg/m^3]
σ	Stress [Pa]
a	Acceleration [m/s^2]
a_{peak}	Maximum acceleration [m/s^2]
F	Force [N]
F_a	Axial force [N]
F_D	Drag force [N]
g	Gravitational acceleration [m/s^2]
I	Muon Flux [muons cm^{-2} s^{-1} steradian^{-1}]
m	Mass [kg]

m_{BP} Mass of BP [g]

m_{lower} Lower body mass [kg]

m_{motor} Motor mass [kg]

m_{total} Total mass [kg]

P Pressure [Pa]

P_{out} Power output [dBm]

R Combustion Gas Constant [ft lbf/lbm°R]

r Parachute area [m^2]

r Parachute radius [m]

T Combustion gas temperature [°R]

V Volume [in^3]

v Velocity [m/s]

v_{tar} Target speed range [m/s]

1 — Introduction

1.1 Team Introduction

Endeavour is the student-run rocketry team at The University of Edinburgh in Scotland, United Kingdom. Darwin III is the third vehicle designed and built by the team since its formation in 2019. The Darwin team is one of the three technical groups within Endeavour, with around 30 members actively involved. The Team Lead is responsible for engaging with all stakeholders, making decisions on various projects that Endeavour is involved with, along with other tasks required for the functioning and long term viability of the team. The Operations Lead assists the Team Lead in their work, doing various administrative tasks and planning logistics. The Finance Manager keeps an eye on the budgets, processes purchases, and records our spending for future information. Social media and sponsorships are overseen by the Partnership and Marketing Manger.

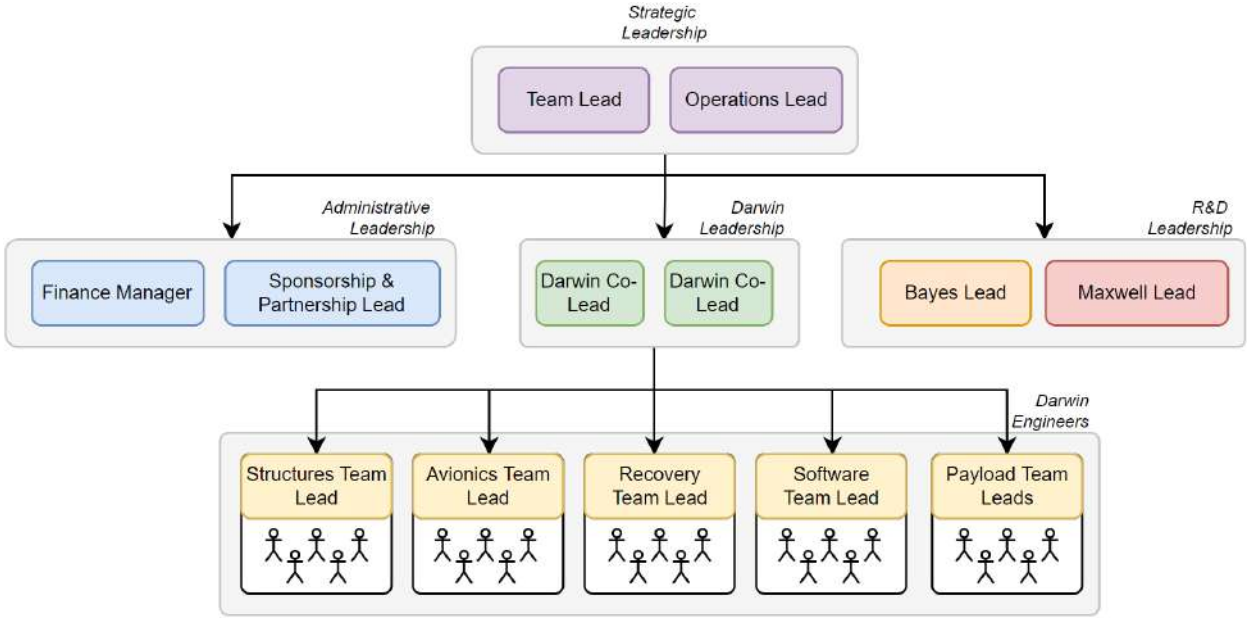

Figure 1.1: Endeavour Organisation Chart.

The Darwin group is comprised of five sub-teams responsible for Structure, Avionics, Software, Recovery, and Payload. These groups are coordinated by the Darwin Co-Leads - this year the role was taken up by the Structures Lead and the Systems Lead. The former ensured hardware integration between teams (i.e. mechanical compatibility interfaces, as well as management of the mass budget). The latter oversaw the integration of all avionics hardware and software, as well as the general operational compatibility of all subsystems, with special consideration of the EuRoC launch site conditions and timing (i.e. ease of assembly, launch day CONOPs, general and specific mission profile). Given the multidisciplinary and high complexity of the Payload, the team is managed by a Mechanical Lead and an Payload Avionics Lead.

Most of our students are from the School of Engineering in the university, with the majority of them studying mechanical engineering and are responsible for the rocket's structure. Many of our software and avionics team study electrical and mechanical engineering, electronics and computer science, and electronics and electrical engineering. Some are from the School of Informatics, focusing purely on computer science and are a part of our software team. We have many students from the School of Physics, studying theoretical physics and astrophysics. We also have members from School of Mathematics, Economics, Business, and GeoSciences.

1.1.1 Team Ethos and Motivation

Endeavour aspires to encourage the pursuit of careers in STEM, particularly aerospace, from the grassroots level. We give students at the university opportunities to experiment, gain engineering design and manufacturing experience, engaging with real challenges of aerospace vehicle design, as well as the many soft skills required to function as an independent student team, from fundraising and networking, to project management, conflict resolution and strategic decision-making. By taking our passion, hardware, and our experiences to classrooms in local schools (from primary up to the high school level) we aim to inspire young people to get excited about space, rocketry and STEM, along with a glimpse of what they could achieve in higher education.

The two other technical groups, Maxwell and Bayes give students with more experience an exciting project to work on. Our Maxwell team is designing a liquid rocket engine that will participate in an UK rocket engine competition in 2023, and students involved can gain an in-depth understanding of the chemistry and pressure systems. Our Bayes team is more focused on software and controls, attracting students who are more interested in data-science, control systems and high-fidelity simulations. The Bayes hopper vehicle is looking forward to their first test flight within the year.

1.1.2 Stakeholders

As a university society, our biggest stakeholders are the students and staff of the university. We offer a way for the prospective students to apply the theoretical knowledge they have learned in the classroom, teach them soft skills, and give them a taste of the aerospace sector which they would otherwise not get in our university, which lacks an aerospace department. The academic and technical staff give us valuable advice in improving

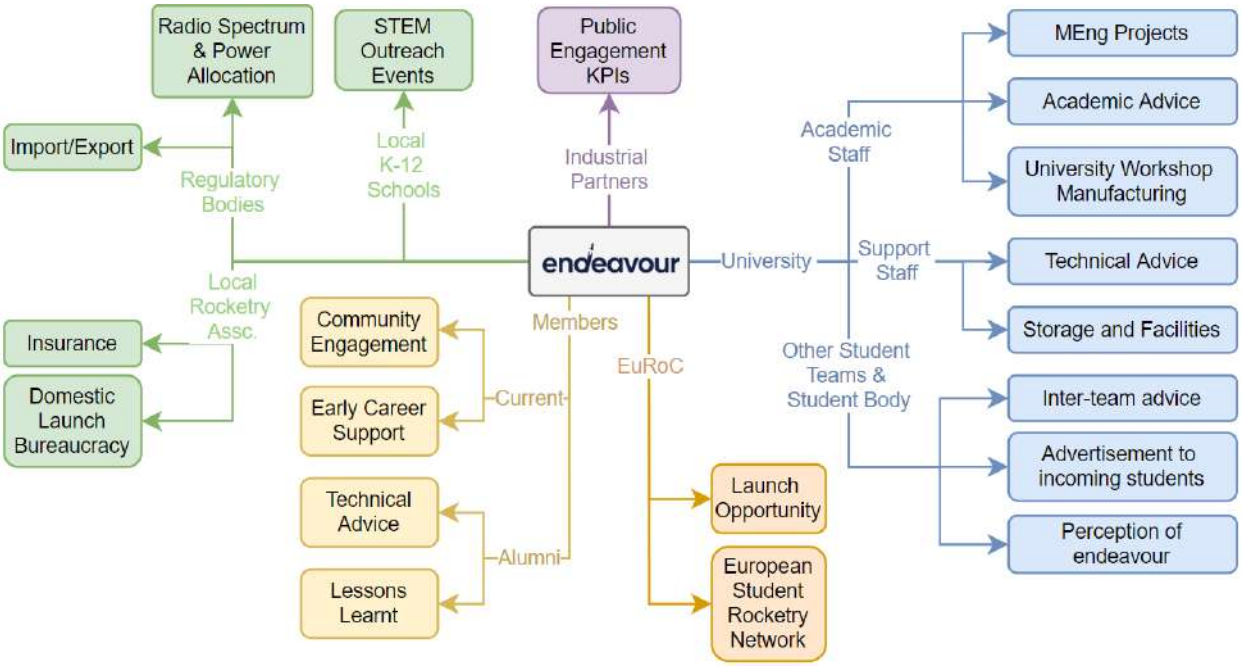

Figure 1.2: Endeavour stakeholders.

our design and manufacturing procedures, and help us through many logistical issues. Endeavour, in turn, offers the university an increase in student satisfaction through enriching student life and topics for final year projects. Many of our suppliers are based in the UK and is affiliated with the university. The School of Engineering, School of Physics and Astronomy, and School of Informatics have granted us funding to enhance the student experience. The School of Engineering, in particular, is our main connection to the university, and supports us in manufacturing, obtaining components, and staff advice. We have also received the Student Experience Grant, a grant that supports university societies and individuals from alumni donations, to fund EuRoC logistics. Edinburgh Innovations has given us logistical support, from business representation to supervising our in-house manufacturing in the university's MakerSpace. Edinburgh Innovation, alongside

with the Science and Technology Facilities Council, operate the Higgs centre, where we will be conducting vibration testing and material testing for our Maxwell engine with the STFC IAA funding. Data-Driven Innovation, a business group for the School of Informatics, has helped us engage with industry sponsors, and provided locations for our various events. Our external sponsors have supported us both financially and



Figure 1.3: Endeavour sponsors

in-kind. Altium, nTopology, and Dassult Systems have given us their software for industry-level design for our avionics PCBs and structures, while ZOT Engineering and M-Carbo have manufactured our PCBs and CFRP components as an in-kind donation. Their work has allowed use of cutting edge manufacturing techniques to create reliable subsystems of the highest standard, and we are grateful for their support. EasyComposites have given a discount in our purchasing, and with this, we were able to incorporate more in-house composites manufacturing to build our knowledge. Skyrora, a space company based in Edinburgh, have given us financial support and advice on our Maxwell engine.

1.2 Legacy of Darwin II

Darwin II was a successful vehicle in terms of design and some aspects of manufacturing, and it allowed us to gain experience in design process, manufacturing, and logistics. However, due to a current spike caused by an unlabelled power connector, the recovery systems were energised prematurely and the parachutes were ejected on the launch rail. EuRoC officials offered DII a second launch window, which was scrubbed at t-2 hrs due to adverse weather conditions. We have taken the lessons we've learnt through the experience and has made massive improvements to DIII. The Darwin team was re-structured to integrate the mechanical and electrical design better, more thorough planning to allow for any unexpected delays, and placing more emphasis on procedures and checklists.

Building on the lessons learnt in DII and the confidence gained at EuRoC 2021, the team is thrilled to present Darwin III. This single-stage, composite-construction experimental launch vehicle improves on all aspects of DII, while retaining some key parameters such as the fuselage diameter, choice of solid motor and parachute dimension. The stability margin is increased by redistributing mass between the aft and forward body sections and increasing the number of fins to 4. The fin dimensions, geometry, thickness and reinforcement were optimised to balance survivability in the supersonic regime, drag characteristics, and flight safety. The specific yield strenght has been increased by 170% and the mass has been reduced with 7075-T6 aluminium.

Servo-driven airbrake have been redesigned for a lower-friction and more predictable deployment, and have been paired with a computationally-efficient algorithm for correction of manufacturing variances in the total

impulse of the motor. Above the airbrake, the completely redesigned avionics bay houses the COTS and SRAD flight computers, as well as a 4k camera, telemetry computers and a novel umbilical system allowing for indefinite holds on the launch pad, radically simplifying launch-day CONOPs. The redesigned SRAD avionics are paired with a ground station with robust, two-way communication based on SRAD protocol. The ground station allows for clear insight of the behaviour of the rocket with advnaced graphical interface and easy access from mobile devices with an AWS server.

The flight computer features five high-current output channels, enabling flexibility in recovery strategy. For the first time, the team has developed a servo-actuated drogue ejection system inspired by the CO2-powered Raptor system. The SRAD system will be cross-braced with an unmodified, Raptor piston with the aim of improving the reliability of the recovery system. Furthermore, the cable management between the avionics and recovery bay has become more robust with harnesses. The payload contains two experiments that can bridge the gap between theoretical knowledge, and that can be used for Endeavour in the future. The first experiment, the Open-Source Cosmic Perspective muon detector, is adapted to survive and successfully collect data during a launch, and the modifications has been verified under various conditions in a climate chamber. It was calibrated with standard detectors to ensure that the data collected is accurate, and therefore the results will allow students to see Einstein's Theory of Special Relativity based on Muon Decay for themselves. The seconda experiment, the slosh experiment, films sloshing dynamics of fluid in slow-motion to study the fluid behaviour over the flight of a rocket, and will be used for Endeavour's future bi-liquid vehicles.

1.2.1 Mission Objectives

1. Validate flexible, resilient procedures, increase the overall safety and improve the standard of testing.
2. Flight-test a novel avionics architecture based on modular boards.
3. Flight-test a novel black-powder-less deployment architecture.
4. Successfully store flight data for engineering analysis and outreach projects.
5. Accurately reach apogee of 9000m by deploying airbrake.
6. Connect to, and learn from the student groups participating in the competition.

2 — System Architecture

Endeavour has reflected long and hard on its journey to EuRoC '21, and has attempted to distil the many lessons learnt into Darwin III. The vehicle attempts to address some of the major technical shortcomings of Darwin II, namely the avionics integration, testing procedures and ease of assembly. The areas for improvement identified did not limit themselves to the hardware, but extended to the team structure and processes including, but not limited to, greater consideration of launch-day CONOPS, and a much accelerated design phase, allowing for more thorough and transparent testing campaigns. The key innovations brought forward this year are the redesigned airbrake, with an overhauled, real-time control scheme, vastly upgraded avionics and ground-station systems featuring a custom telemetry protocol and a robust SRAD recovery device for the apogee separation event.

Table 2.1 lays out the top-level requirements delineated at the start of the Darwin III program. These requirements derive from competition regulations (EuRoC), financial or logistical limitations, and preliminary engineering analysis.

Table 2.1: High Level Requirements for Darwin III LV.

Req.	Description	Criterion	Level	Margin	Source	Validation
HLR01	Match Category Apogee	Altitude	9000m	-300/+300m	EuRoC	Simulations and Test Flight
HLR02	Stable throughout flight	Stability off launch rail [S_{LR}]	1.75	1.5¡S_{LR}¡4.0	EuRoC	Simulations and Test Flight
HLR03	Contain functional payload	Payload Mass [M_{PLD}^{MAX}]	2kg	2kg¡M_{PLD}^{MAX} ¡2.3kg	EuRoC	3D model mass tracking and Weigh-in before flight
HLR04	Safe recovery	Number of deployment events	2	0/+2	EuRoC	CONOPs and SRAD/COTS ground tests
HLR05	Safe recovery	Number of deployment events	2	0/+2	EuRoC	CONOPs and SRAD/COTS ground tests
HLR06	Mass optimisation	Mass	36kg	-5kg/0	Systems Lead	3D model mass tracking and Weigh-in before flight
HLR07	Size Optimisation	Length	3000mm	0/-500mm	Operations Manager	Must fit existing crate to simplify shipping operations.
HLR08	Size Optimisation	Inner Diameter	152mm	0	Finance Manager	Must conform to mandrel used for previous vehicle.
HLR09	Budget Constraints	GBP	£10000	-2000/+1000	Finance Manager	Internal bookkeeping

2.1 Overview

Darwin III's high-level technical Specifications are presented in Table 2.5.

Table 2.2: Main Technical Specifications of Darwin III.

Parameter	Figure
Wet Mass	34,333 g
Dry Mass	23,061 g
	9,220m (OR)
Predicted apogee	8,998m (RAS)
	pending (RocketPy)
Motor	CTI 21062-O3400-IMax
All-out Length	2890mm
Outer Diameter (OD)	156mm
Fins	4x, Swept, 4-5.5mm thickness, 0.5 in fillet
Drogue Descent Speed	30 m/s (@500m AGL)
Main Descent Speed	6 m/s (@0m AGL)
Active Flight Control	Yes, apogee control
Payload Form Factor	2U CubeSat
Payload Mass	2,200g

The vehicle is divided into 4 main assemblies. Starting aft, these are the Lower Body (1), Avionics Bay (2), Recovery Bay (3), and Nosecone (4). A view of the entire vehicle where the body sections have been made transparent can be seen in Figure 2.1. To accompany this visual aid, a flow diagram showing the main paths of forces, electrical signals and radio signals is shown in Figure 2.3. The Lower Body section

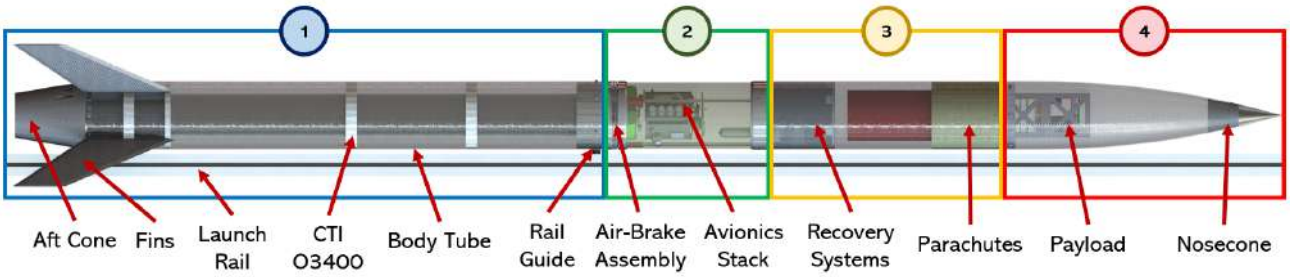

Figure 2.1: View of the major parts and assemblies of Darwin III. Aerostructure opacity reduced for clarity.

is a purely mechanical subsystem, with no SRAD or COTS avionics modules. Its primary function is to house and transfer the thrust from the Cesaroni O3400 Imax motor (P/N: 21062O3400-6GXL). The rocket's four fins are affixed to the lower body via a through-body construction with a double Araldite 2015 fillet reinforced by CFRP wet layup. According to simulations conducted in OpenRocket, FinSim, and RasAero, the aggressive sweep angle of the fins raises our stability margin off the launch rail by 35% while improving drag characteristics compared to the 3 much larger fins on Darwin II. The exact geometry, bonding and reinforcement is the result of careful simulation across FinSim and RasAero, aiming to provide a balance of performance and safety against the aero-elastic effects of flutter and divergence, as discussed in depth in Section **??**.

The Avionics Bay houses most of the SRAD avionics and all COTS avionics, as well as the airbrake module. The loads from aerodynamic forces and motor thrust are transferred from the motor bulkhead through the airbrakes module and into the stainless steel avionics bay rods, which resist compression and bending loads. The torsional loads are supported by a glass fibre, radio-frequency transparent body tube section. To ensure that the glass fibre tube is only loaded in torsion, the base of the tube "floats" above the airbrake Cap (D3-209), while interlocks with female angular cutouts. This system plays to the strengths of each design element: the steel rods are strong in compression but may buckle and twist under torsion loads, whereas glass fibre is strong in torsion but has unpredictable behaviour under compressive loads. The combination of these two structural elements is more than adequate to withstand the loads expected in flight. Within the Avionics bay, 5 SRAD PCBs are attached to a 3D-printed, highly integrated module. This central module also houses 2 COTS Flight Computers (FCs), a 4K camera, arming switches and all the antennas and wire harness attachment points. The SRAD Avionics are broken up into 5 different boards:

- *CLB* (Charging Logic Board) enables all on-board avionics to be powered by a ground power supply and switch to internal power on command.
- *Papa* distributes and converts power from the battery voltage (8.4V max) to 6V, 5V and 3V3.
- *Alpha* tracks the current state machine by fusing and filtering raw data from redundant accelerometers and barometers. Based on the trajectory and a robust set of conditions laid out by a Finite State Machine, it can actuate the Air-Brakes to regulate apogee, and can execute both recovery events by detecting apogee and monitoring barometric altitude, respectively.
- *Bravo* handles telemetry, including the SRAD eWDL (endeavour Wireless Direct Link) to the ground station as well as GPS. Bravo receives and communicates ground station commands to Alpha
- Contrary to COTS FCs like the EggFinder, the *GPS Board* has a large groundplane (70x60mm) which boosts sensitivity by -10dB.

The Recovery Bulkhead separates the Avionics Bay from the Recovery Bay, providing attachment points for all recovery lines, as well as locating the various recovery mechanisms and providing attachments for wiring harnesses. Darwin III carries 4 independent recovery devices, including a SRAD ejection mechanism. The mechanism pierces a CO2 canister without employing Black Powder (BP). In order to accomplish this, a servo motor advances a lead screw with a sharp, hollow tip. The tip punctures the canister and the CO_2 escapes through the centre of the screw. The remaining deployment mechanisms are COTS: a Raptor piston for ejection and two L2 Tender Descender in parallel for Main Chute Release. A high-level overview of the recovery systems is given in Figure 2.2. Once ejected, the 24-inch drogue will slow DIII's descent, and a 96-inch main will be released at 450m ALS (above launch site), bringing the vehicle to a landing at a descent speed just below 6 m/s. The ejection and release mechanisms are separated by the parachutes and a polycarbonate disk with perforations through which the parachute lines pass. This disk protects the mechanisms from jamming against parachutes or getting tangled in the lines, which are likely to shift from their packed position due to the violent launch acceleration. Finally, in the Nosecone section, Darwin III

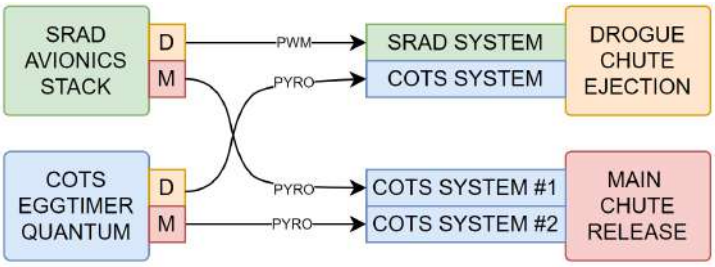

Figure 2.2: Schematic Representation of the cross-braced recovery system layout.

will be launching a new 2U CubeSat developed with the support of the University of Edinburgh School of Physics, carrying a SRAD muon detector. The instrument has undergone extensive characterisation and its results will be calibrated against a high-fidelity system provided by the University. The payload will also be collecting engineering data by relating IMU data to images from a high-resolution, slow-motion camera capturing the sloshing behaviour of liquids in a slender cylindrical tank. The images will inform the design

of PMD (Propellant Management Devices) for geometrically similar tanks of Endeavour's bi-liquid vehicle projected for EuRoC 2024.

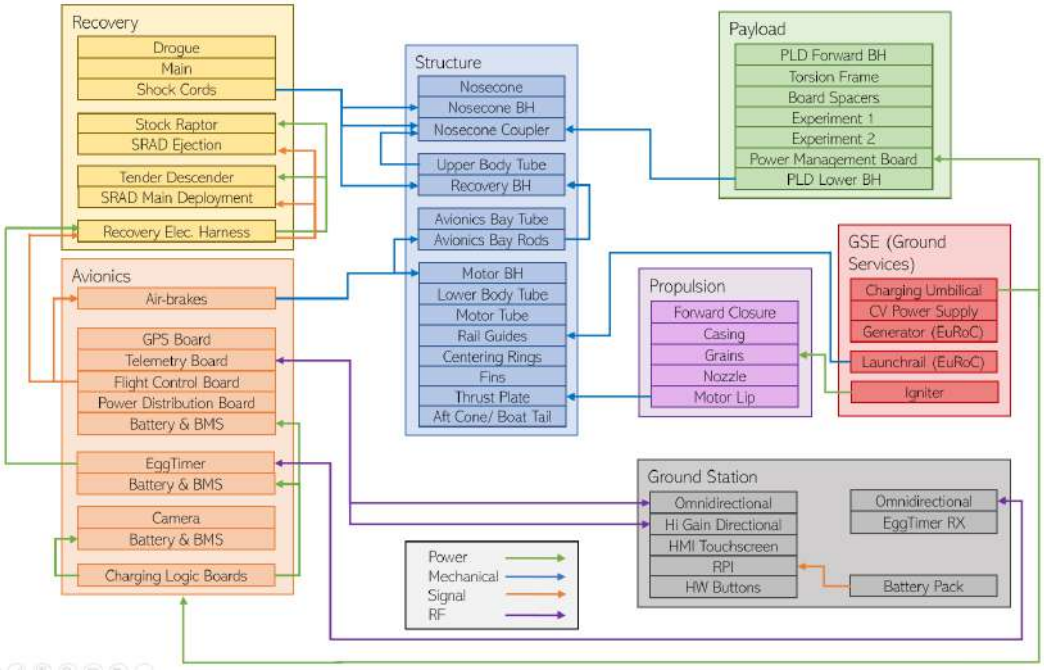

Figure 2.3: Flow Diagram of Loads, Signals and Power through the vehicle and GSE.

2.2 Propulsion subsystem

The first major step in Darwin III's design process was selecting an appropriate motor. This decision prescribes the total impulse available throughout the flight, as well as the maximum thrust at liftoff and maximum loading of the structure (Max-Q). The motor thus defines the flight envelope, generating engineering requirements for the rocket's overall mass, aerodynamic properties and structural integrity.

2.2.1 Motor Choice

With regulations in the UK making the possessions of solid rocket motors highly restricted and their manufacturing illegal, the team uses COTS solid motors imported from abroad, specifically products of Cesaroni Technologies Inc. (CTI). Given last years scrubbed launch, the team was in possession of an un-used Pro98-6GXL casing for Darwin II's motor - a 21062O3400-6GXL. Since the casing represents as much as 40% of the cost of a new motor, it was decided to order a new reload for the 2021 casing. The original 2021 reload was disposed of on the advice of the technical personnel of EuRoC, who had witnessed CATO (Catastrophic failure At Take-Off) due to poorly stored grains.

The selected reload uses *Imax* propellant, which packs the maximum total impulse for a given motor casing class. The total impulse of Imax reloads is 15% higher than that of other 6GXL reloads, and burns with a long flame with a hint of green. It releases a large volume of dense smoke. Despite the favourable total impulse, the *specific* impulse is lower due to the higher density of the propellant.

In order to fit a 2U payload (a key requirement), the outer diameter of the vehicle was chosen to be 152mm. This diameter also simplified the procurement of coupler tubes and mandrels for the composite body sections, as imperial 6 inch sections are readily available. The effect of the vehicle's outer diameter dominates other factors in terms of drag. Thus, it was possible to conduct preliminary OpenRocket simulations to ascertain which reloads available through the EuRoC approved reseller would allow Darwin III to achieve a 9km apogee. Figure 2.4 shows a comparison between the thrust curves of two motors which, according to these initial calculations provides sufficient total impulse to achieve our target apogee while fitting the unused Pro98-6GXL casing: Cesaroni's 21062O3400-P and 20146N5800-P.

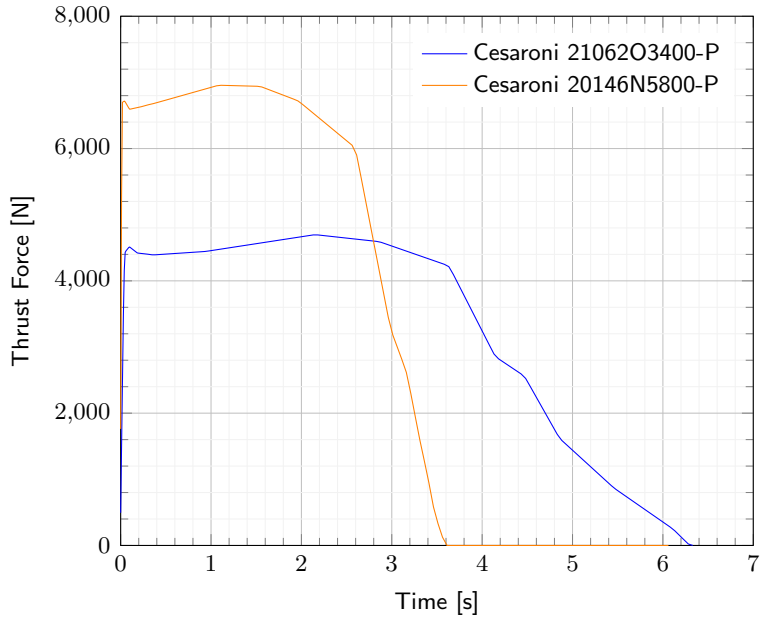

Figure 2.4: Rocket motor thrust curve comparison.

Ultimately, the Cesaroni 21062O3400-P was selected as Darwin III's first choice motor. As is visible in Figure 2.4, it has lower peak thrust compared to the 20146N5800-P, which results in reduced loads on the load-bearing assemblies, lowering risk of structural failure and allowing for more light-weight assemblies. Additionally, the O3400 requires more time to reach to maximum thrust, resulting in lower inertial forces on

the vehicle structure. The decision flow leading to this choice is presented in Figure 2.17.

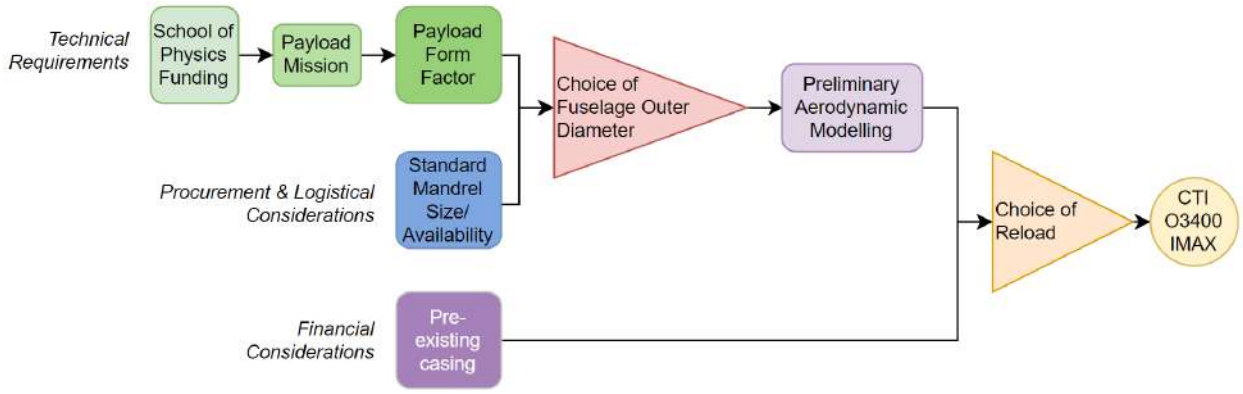

Figure 2.5: Decision Flow-chart for Reload Decision.

2.2.2 Arming and Ignition

No special arming or ignition sequences are necessary for the motor. Cesaroni Technologies Inc. recommends the use of an e-match (igniter) introduced from the aft of the motor, ensuring that it travels forward until it is in contact with the forward closure. Once in place, the igniter will be secured to the motor nozzle with tape or the supplied plastic cap. Igniter wires are then passed through one of the vent holes. Before evacuating the launch-pad, it must be visually confirmed that a vent for igniter gases is present, as this prevents premature ejection of the igniter. Once the launch area is clear, control is handed over to the Pyrotechnic and Range Safety personnel for launch authorisation and execution as per EuRoC's launch system protocol. When the e-match is activated by an electrical signal, the rocket's solid propellant begins its chemical reaction and the rocket takes off.

2.3 Aerostructure subsystem

Darwin III is composed of four main functional sectors that must be joined together with stiff yet lightweight structural joints, and enclosed by aerodynamic cowlings, fairings, or tube-sections. These sectors and their respective sub-assemblies are:

- **Lower Body (D3-SEC-1.0)**
  - COTS Solid Motor casing (D3-COTS-1)
  - Aft-cone (D3-102)
  - Fin-can (D3-ASSY-1.1)
  - CFRP Body Tube & centering rings (D3-ASSY-1.2i)
  - Motor Bulkhead (D4-111)
- **Avionics Bay (D3-SEC-2.0)**,
  - Air-Brakes system (D3-ASSY-2.1)
  - GFRP Avionics Tube (D3-306)
  - Stainless Steel Axial "Force Rods" (D3-301)
  - SRAD and COTS Avionics, including batteries.
  - Recovery Bulkhead (D3-401)
- **Recovery Bay (D3-SEC-3.0)**
  - Aft Coupler (D3-402)
  - CFRP Recovery Tube (D3-405)
  - COTS and SRAD ejection/release systems.
  - Main and Drogue Parachutes
- **Payload Bay (D3-SEC-4.0)**
  - Forward Coupler (D3-402)
  - Payload Bulkhead (D3-501)
  - CFRP Nosecone
  - 2U CubeSat Payload (D3-ASSY-4.1)
  - Main and Drogue Parachutes

This section of the report will initially focus on the exterior elements forming part of the aerodynamic shell, then move on to discuss the interfaces that combine the four sectors and finally present structural analysis and FEA results.

CFRP Components

The exceptionally high strength-to-weight ratio of CFRP made it the obvious choice of material for the majority of Darwin III's air-frame. Due to the time and monetary investments necessary to develop a custom filament winding machine, the manufacture of most CFRP components were outsourced to one of our industry sponsors, M-Carbo. The 2mm thick body tube and the motor-sleeve were manufactured with a winding angle 15° as per manufacturer's recommendation, to provide the best compromise strength under axial and bending loads. The flat CFRP components used throughout the Lower Body assembly (Fins (D3-106-REVB) and Thrust Ribs (D3-103)) were also manufactured by M-Carbo using 2mm thick CFRP sheets, consisting of a 3k tow, precision-milled using a CNC cutter.

The nosecone of DIII is a tangent shape, with a total length of 640mm and a radius of curvature of 2430mm. Its main CFRP section was fully manufactured by students using pre-impregnated (pre-preg) CFRP laid up within twin female moulds. The moulds were machined out of Epoxy Tooling Board and sanded to a smooth finish, and finally mould sealer and mould release chemical agents were applied to obtain a glossy texture. Six plies of pre-preg were applied onto each mould following a 0°, 45°, 0°, 0°, 45°, 0° angular schedule created attempting to resist the buckling failure mode, considered most likely. Following an overnight oven cure in a vacuum-sealed bag, the Nosecone was polished to obtain a glossy texture and reducing skin-friction drag

in this aerodynamically significant sector of the vehicle. The Stainless Steel tip is fastened to the tube by means of two mating conical/tapered inserts printed in Nylon-CFRP filament on a Markforged Two printer. The high glass transition temperature of this engineering-grade filament (145° C) ensures the heat caused by an extended stay on the launch-pad, or the small amount of aerothermal heating experienced by DIII will not cause any deflections.

Fin Assembly

Darwin III's fins were designed and manufactured to provide sufficient aerodynamic stability, while also withstanding the forces of supersonic flight. The core is a CNC machined 2mm CFRP plate. To increase strength and stiffness, both vital in combating flutter, the fins are designed to be connected through the body - that is, they are bonded to both the fin can (a 98mm ID CFRP tube which centres the motor casing, supported by Nylon 66/CFRP 3D fin rings), and the body tube. The bonding takes the form of 1/2" Araldite 2015 fillets on the inner tube, and 3/4" fillets on the outer tube. The inner assembly is shown in Figure 2.3. This through-body construction limits the repairability and modularity of the fin assembly, but contributes to a great increase in the stiffness of their connection to the fuselage and should prevent the tear-out failure mode witnessed on more than one test flight at EuRoC '21. To further improve their resilience, they are laid up by 3 layers of woven carbon fibre plies tip-to-tip, and 2 layers mid span to mid span, resulting in an overall thickness of 4mm at the tip and 5.5mm at the root (without accounting for the fillet).

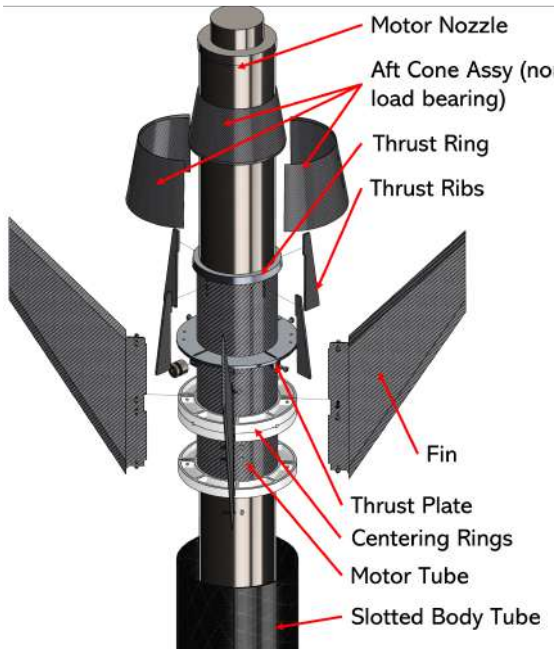

The process of tip-to-tip layup involves laying up CFRP from the tip of a fin, along its surface, across the fuselage, to the tip of the neighbouring fin. After all 4 fins were laid up, the resin was left to cure in a vacuum bag to minimise internal voids and consolidate the plies. After the curing has finished, both the leading and trailing edges of the fins were sanded, providing razor-sharp edges which reduce the drag coefficient of this assembly. The tip-to-tip layup increases the stiffness of the fins, which is crucial given their aggressively swept-back angle. Laminating the fins using a tip-to-tip layup was preferred over simply using a thicker CFRP core because a more granular control of the modes of flutter can be achieved by customising the orientation of each individual ply. This makes the use of material more efficient, reducing the thickness of the fins and improving the drag characteristics compared to an equally stiff monolithic core.

GFRP RF Transparent Section

Carbon filaments within CFRP composites act as millions of tightly woven conductive wires, creating a Faraday cage and blocking RF signals, so a fuselage constructed entirely of CFRP would result in a complete lack of RF transparency. To reach RF transparency and therefore allow communication between the flight-computer and the ground station, the EuRoC '22 Design, Test, and Evaluation guideline prescribes the use of RF-transparent windows at least 2 calibres in length to be used around RF sensitive equipment. DIII conforms to these regulations by enveloping the avionics bay in a 2mm thick, 304mm long filament wound GFRP outer shell in the midsection of the LV, acting as a bridge between the lower body and the recovery and payload bays. This shell and its mechanical integration with the other section of the LV forms integral part of the load path of the vehicle, and is discussed further in Sections 2.3.1 and 2.3.1/

2.3.1 Mechanical Interfaces and Internal Components

The mechanical assemblies that join the four main sectors of Darwin III are aimed at reducing the susceptibility of the LV to the axial loads of take-off and recovery, as well as the significant bending and torsional dynamic

effects generated by high speed flow.

Interface 1: Motor Bulkhead - Figure 2.6 Machined Aluminium 7075-T6, the Motor Bulkhead (D3-111) was designed with a robust shoulder feature, which telescopically slides within the Body Tube by half of a body-diameter (3" or 75mm), and is secured to it permanently by 6 M4 bolts. The shoulder feature creates a stiff connection to resist bending, while the M4 bolts retain the Body Tube and Fin Assembly during recovery events. The Motor Bulkhead features a lip which extends to the outer diameter of the vehicle, allowing the Body Tube to butt up against it, efficiently transmitting the thrust directly into the aluminium. The forward face of the bulkhead also acts as the point of connection for the airbrake, contains the motor retention mechanism (see Section 2.3.1) and three "Force Blocks", housing the three load-bearing "Force Rods" (D3-301) which transmit axial forces through the avionics bay.

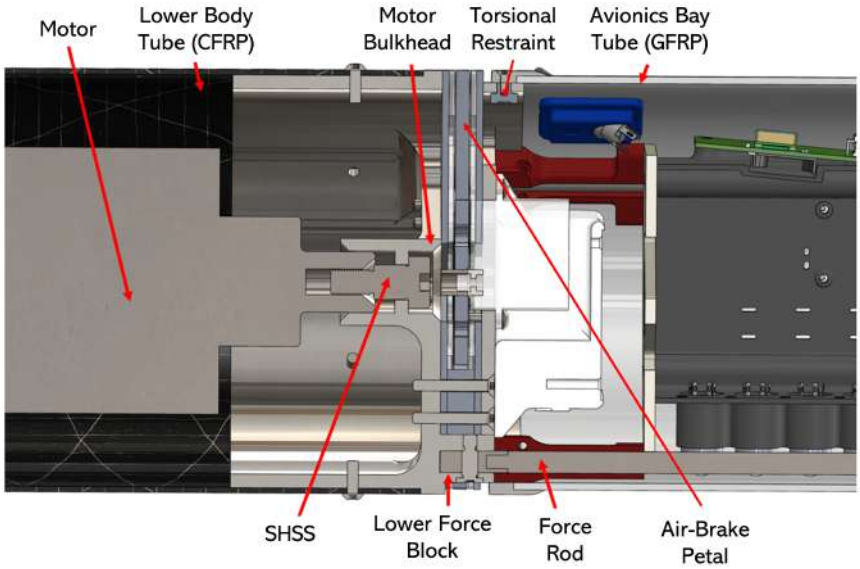

Figure 2.6: Interface 1: Motor Bulkhead Section View

Interface 2: Recovery Bulkhead - Figure 2.8 The aft face of the Recovery Bulkhead (D3-401) houses three identical "Force Blocks", retaining the forwards end of the "Force Rods". On the forward face of the bulkhead, a one body-diameter long GFRP coupling tube is bonded and screwed to a 15mm Aluminium shoulder feature. This coupling tube is the interface between the recovery section's CFRP fuselage and the recovery bay and provides rigidity in bending. The recovery bulkhead also acts as the point of connection for the recovery system - the RAPTOR ejection system, the M10 and M6 eye bolts and the servos.

Interface 3: Payload Bulkhead - Figure 2.8 The payload bulkhead features a lip on its aft face bonded and screwed to a one-calibre long GFRP coupling tube. This coupler is secured to the CFRP fuselage of the recovery section with four shear pins, acting as a predictable shear-points when the recovery sequence is initiated. This bulkhead is also responsible for locating the 2U CubeSat with the threaded features on the payload's aft bulkhead, and the ballasts that may be used to the stability of the rocket. Finally, the nosecone is bolted via 6 M4 bolts onto a 20mm lip on the forward face of the bulkhead, so that the payload may be easily accessed. This bulkhead also seals the recovery bay from the nosecone, meaning additional pressure can be generated by a 33g cartridge of CO_2.

Motor Retention & Thrust Path

The motor is positively retained to keep it securely attached to the rocket during flight. A 3/8" socket head set screw (SHSS) attaches into the motor through a centre-hole in the Motor Bulkhead. This screw is secured in place via an aluminium plate with a hexagonal extrusion, which drastically simplifies the assembly process. The rocket will not have to be disassembled when securing the motor: instead of screwing the fastener into the stationary motor, the motor will be screwed onto the stationary fastener. The SHSS is only responsible for securing the motor, and transfers no thrust. Centering the motor is of paramount importance as it reduces

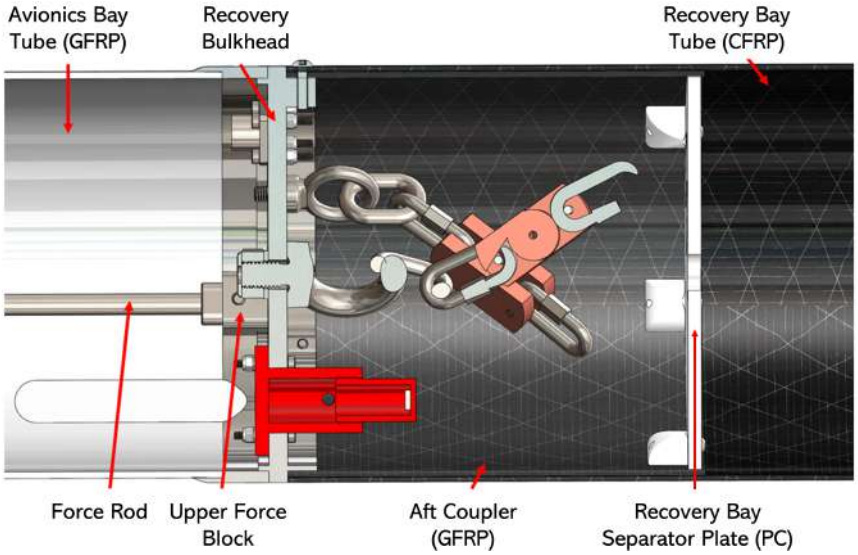

Figure 2.7: Interface 2: Recovery Bulkhead Section View

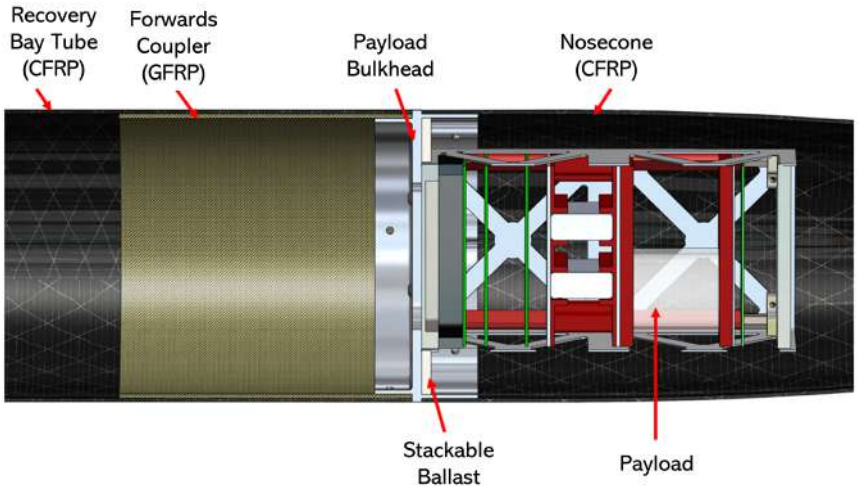

Figure 2.8: Interface 3: Payload Bulkhead Section View

off-axis oscillatory forces. The Fin-Can has a 300mm long filament-wound CFRP tube which provides the majority of the alignment at the aft end of the vehicle. To ensure that concentricity is maintained throughout the entire lower body, two additional centring rings, manufactured with Nylon-CF Markforged filament and reinforced with short sections of CF tube, are bonded to the inner face of the Body Tube. The combination of these techniques provides a solid mount for the motor, retaining it axially and radially.

At the aft of the Pro98-6GXL casing, a small lip feature on the Nozzle Retention Ring transfers the motor's thrust to the LB structure. The thrust from this lip is transferred to the aft face of the Thrust Ring (D3-102), a machined Al 7075-T6 component, sitting directly on top of the lip. The main purpose of this part is to increase the surface area from the motor's lip, thus distributing the force and decreasing the stress on the following parts on the thrust path.

The forward face of the Thrust Ring butts up against 4 CFRP ribs and the 300mm CFRP Motor Tube. The thrust travels up the ribs (which are slotted and bonded to the Motor Tube) and is transferred into the Thrust Plate (D3-105). The ribs are epoxied into the CFRP tube and the machined Al 7075-T6 thrust plate, the cylindrical inner face of which is epoxied onto the CFRP tube. The purpose of this assembly is to spread the thrust radially, from near the motor's casing (98mm OD), into to the Body Tube (156mm OD). The thrust is then transferred through the lower body's CFRP fuselage into the Motor Bulkhead's lip, as described in Section 2.3.1 on Mechanical Interfaces.

As the GFRP tube encasing the Avionics Bay is relatively weak and unpredictable in compression, it was decided to transfer thrust and bending loads through this section using stainless steel rods. These three 8mm thick bars have welded-on end caps, which slide into the motor and recovery bulkheads "Force Block" features and are pinned in place by Ultra-Low Head Shoulder bolts (further details in Section 2.3.1). The thrust from the Recovery Bulkhead is transferred into the Recovery Bay's CFRP fuselage, using a similar lip to that of the Motor Bulkhead's. Similarly to the other two bulkheads, the thrust to the payload bulkhead is transferred through its lip. From the payload bulkhead, the thrust goes into the CFRP nosecone through the bulkhead's shoulder, which then transfers it into the nosecone tip, completing the thrust path.

Since these parts experience high loads, all of the metal parts have undergone numerous iterations of FEA. The designs are strengthened and lightweighted until every part achieves a FoS of at least 3. The FoS of the metal components with their yield strengths and highest expected stresses are presented in Table 2.3. The more critical simulations are reported in Section 2.3.1.

Table 2.3: Summary of FEA simulations and Safety Factor on Machined Components.

Part Name	Part ID	Material	Yield Strength [MPa]	Peak Stress Ascent [MPa]	FoS Ascent	Peak Stress Descent [MPa]	FoS Descent
Thrust Plate	D3-105	Al 7075-T6	572	181	3.2	n/a	n/a
Motor BH	D3-111	Al 7075-T6	572	79.8	7.2	58.3	9.8
Recovery BH	D3-401	Al 7075-T6	572	13.5	42.4	141	4.1
Payload BH	D3-501	Al 7075-T6	572	6.9	82.9	53.8	10.6

Avionics Bay



One significant challenge for DIII was to design an avionics bay that would be simple to assemble and maintain while safely transmitting the significant forces created by the motor during the rocket's flight. The solution improves on Darwin II in several ways. Both designs use 8mm steel rods to transmit the force from the motor bulkhead at the aft of the bay to the recovery bulkhead forwards of the bay. While such rods are adequate to transmit forces running parallel to the main axis of the rocket, they have the potential to bend or buckle under torques about that axis. Last year's design used cold-rolled steel cross-bracing attached to the rods to prevent this bending, and the PCBs were attached to those brackets. DII's design made it extremely difficult to assemble the PCBs once the rocket was assembled, as well as as accessing batteries, cameras and servo-motors. This year's design uses a combination of materials to achieve the same effect while leaving the avionics bay free of bracing which increases the available volume. The steel rods are attached directly to the motor bulkhead and are pinned in place by shoulder bolts from the outside of the LV, allowing for rapid disassembly.

The glass fibre tube enclosing the avionics bay is then used to transmit angular forces from the lower body of the rocket to the upper body. Since GFRP is weak in compression, the tube does not touch the top of the motor bulkhead. A small gap is left between the tube and the bulkhead, and the connection is made instead with three female protrusions on the base of the glass tube which slide into corresponding slots around the perimeter of the Motor Bulkhead. This method of connection ensures that only rotational forces

are transmitted through the glass tube.

Numerical Simulations

FEA was performed on every machined part with a non-trivial geometry. The pass criteria was internally agreed to be a minimum safety factor of 3 on worst-case scenario loads. Analyses were performed in nTopology, based on the Abaqus solver.

The forces acting on the parts are due to the inertia of the mass being accelerated by that part - this means that the force acting on each part can be calculated using the following equation:

$$F = m_{\text{inertia}} \cdot a_{peak}, \tag{2.1}$$

where F is the inertia force, $m_{inertia}$ is the mass of the rocket that is being accelerated by the specific part and a_{peak} is the peak acceleration at ascent and descent. During ascent, the peak acceleration is due to the thrust, while at descent it is due to the main parachute opening (see Table 3.1 for maximum acceleration values). The masses accelerated and the resulting forces acting on each analysed components are shown in Table 2.4. The values for recovery forces are based on calculations shown in Section 2.4.3.

Table 2.4: Summary of Inertial Forces experienced by Machined Components.

Part Name	Part ID	Mass Accelerated Ascent [kg]	Force applied Ascent [N]	Mass Decelerated Descent [kg]	Force Applied Descent [N]
Thrust Plate	D3-105	16.98	2326	0.9	107
Motor Bulkhead	D3-111	13.46	1843	10.98	1318
Recovery Bulkhead	D3-401	7.99	1095	14.30	1718
Payload Bulkhead	D3-501	4.49	615	4.49	540

Thrust Plate The thrust plate is restrained by the CFRP Body Tube, and the fixed geometry was chosen as the outer lip of the plate. While the fins would also transfer some of the thrust as they are bonded onto both the plate and into the fuselage, it was assumed to have no loading capabilities to ensure that the thrust plate has sufficient FoS. With the restraints set, and knowing that the forces both during ascent and descent are transferred to the plate by the CFRP Motor Tube and the Thrust Ribs, the simulation were run with results presented in Table 2.3 and Figure 2.9.

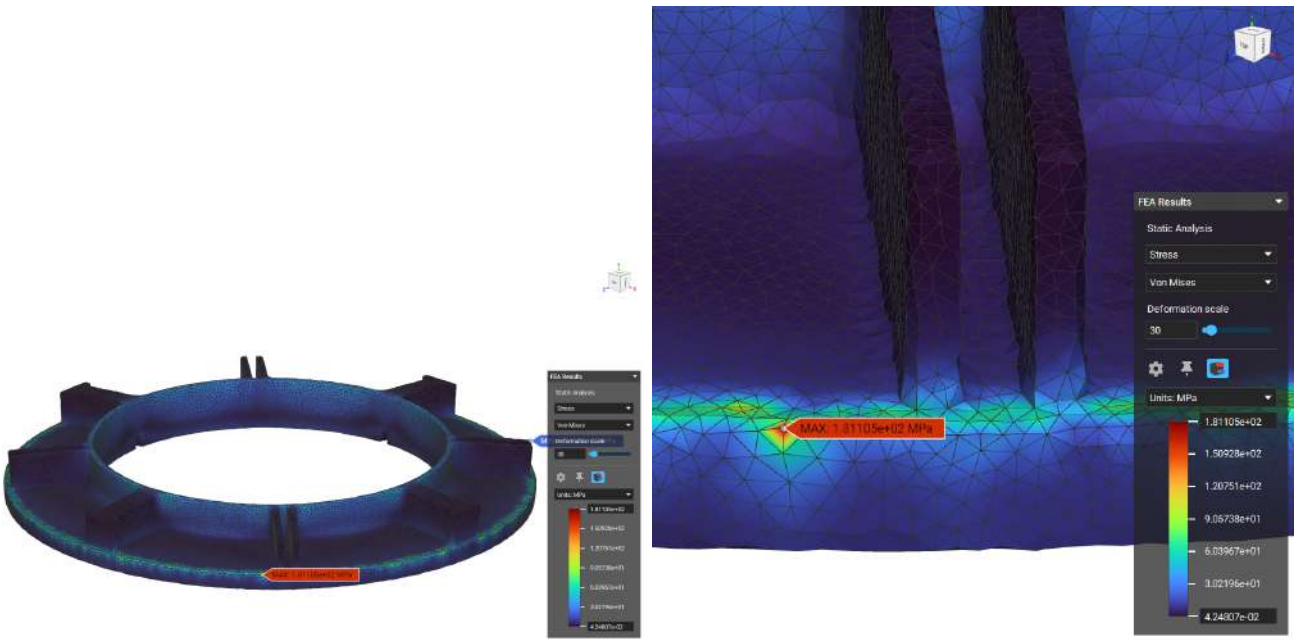

(a) (b)

Figure 2.9: Results of FEA for the thrust plate.

Motor Bulkhead During ascent, the forces acting on the Motor Bulkhead are through its shoulder, and it is restricted from moving by the flat face of the pockets in the force blocks and by the web (that carries the avionics stack). During descent, the snatch force acts on the connection between the shoulder bolts and the force blocks, while the motor is restrained from moving by the SHSS in the centre and the rest of the lower body by the 12 radial M4 bolts (similarly to ascent, the web stops the avionics stack from moving). Using these setups, the simulations were run with the results are presented Table 2.3 and Figure 2.10 and 2.11.

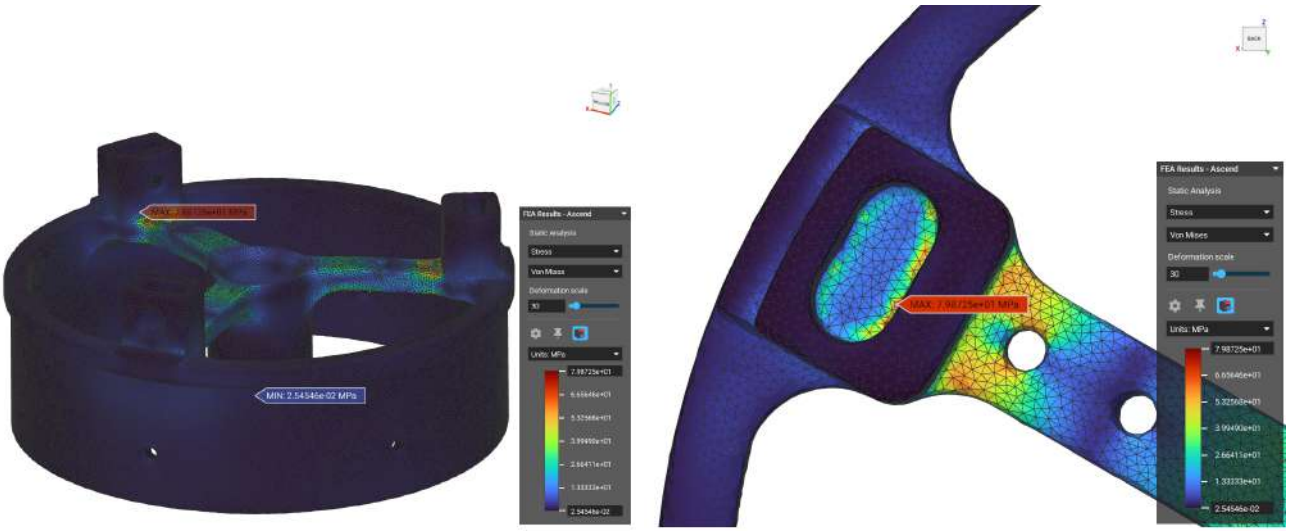

(a) (b)

Figure 2.10: Results of FEA for the motor bulkhead during ascent.

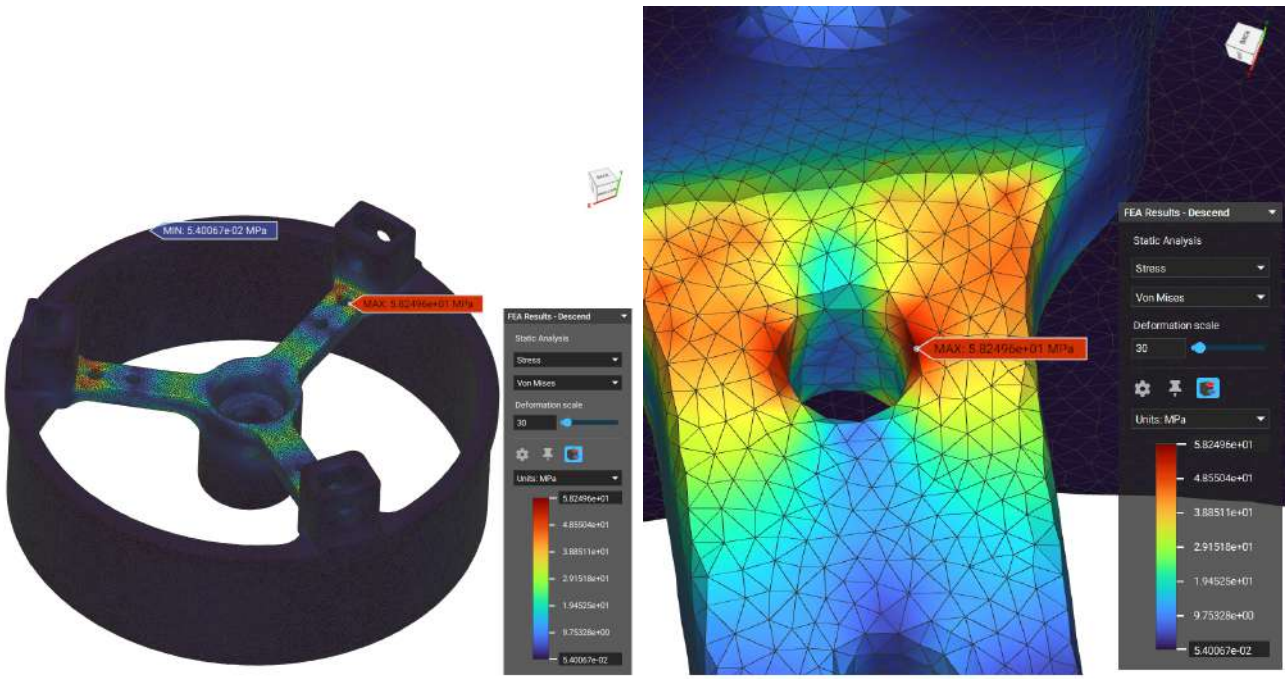

(a) (b)

Figure 2.11: Results of FEA for the motor bulkhead during main parachute deployment.

Recovery Bulkhead The loading is similar to the Motor Bulkhead, but inverted with respect to the phases of flight: during ascent, the forces are acting on the flat face in the pocket of the force blocks, while its displacement is restrained by its outer lip. During descent, the snatch force is acting on the central hole by the M10 eye bolt while its movement is restricted by the pinned shoulder bolts in the force blocks. The simulations results are presented Table 2.3 and Figure 2.12 and 2.13.

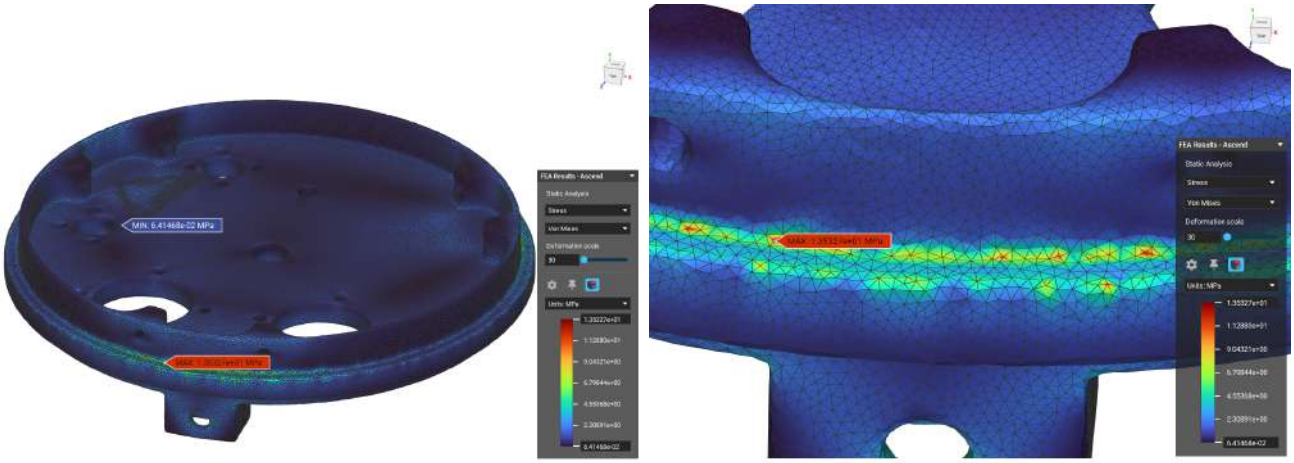

(a) (b)

Figure 2.12: Results of FEA for the recovery bulkhead during ascent.

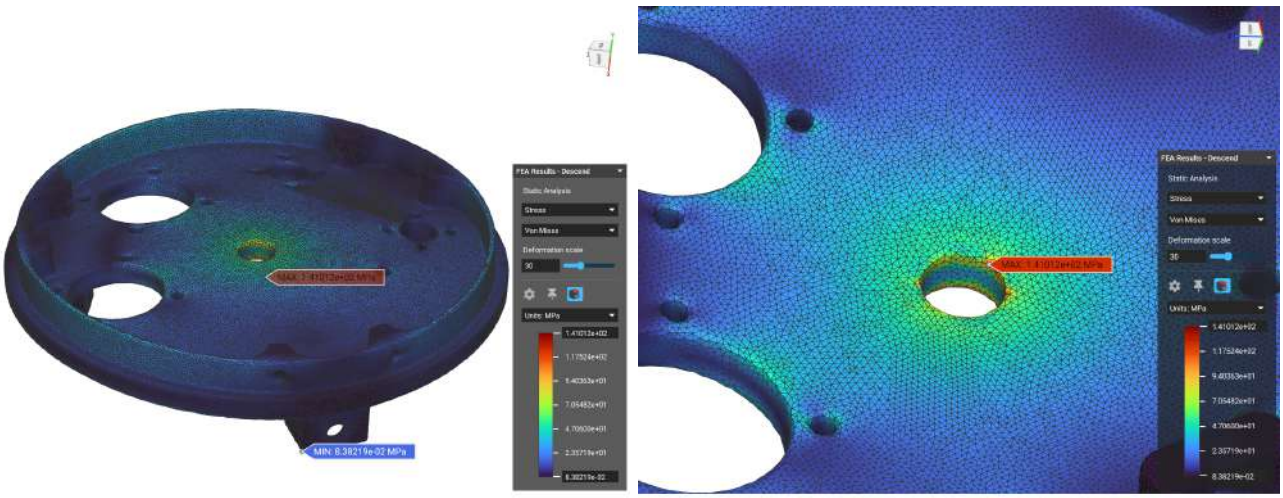

(a) (b)

Figure 2.13: Results of FEA for the recovery bulkhead during main parachute deployment.

Payload Bulkhead The thrust force is transferred into the Payload Bulkhead through its shoulder. The masses it accelerates during ascent are in contact with the bulkhead by many surfaces, namely the shoulder for the nosecone and the web for the ballast and the payload. These surfaces are used as restraints for ascent. During descent, the snatch force is acting on the bulkhead by the two M6 eye bolts. The part being accelerated by this force, are connected to the bulkhead by 6 M4 bolts for the nosecone, two M5 bolts for the ballasts and four M4 bolts for the payload. The results shown in Table 2.3 and Figure 2.14 and 2.15.

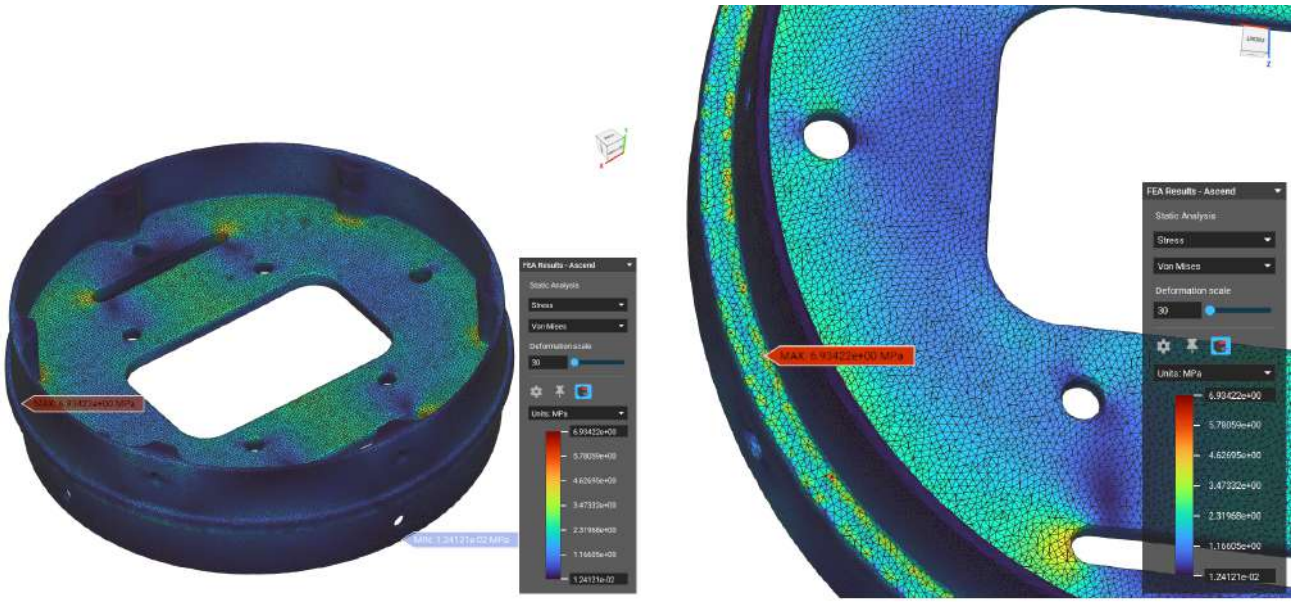

(a) (b)

Figure 2.14: Results of FEA for the payload bulkhead during ascent.

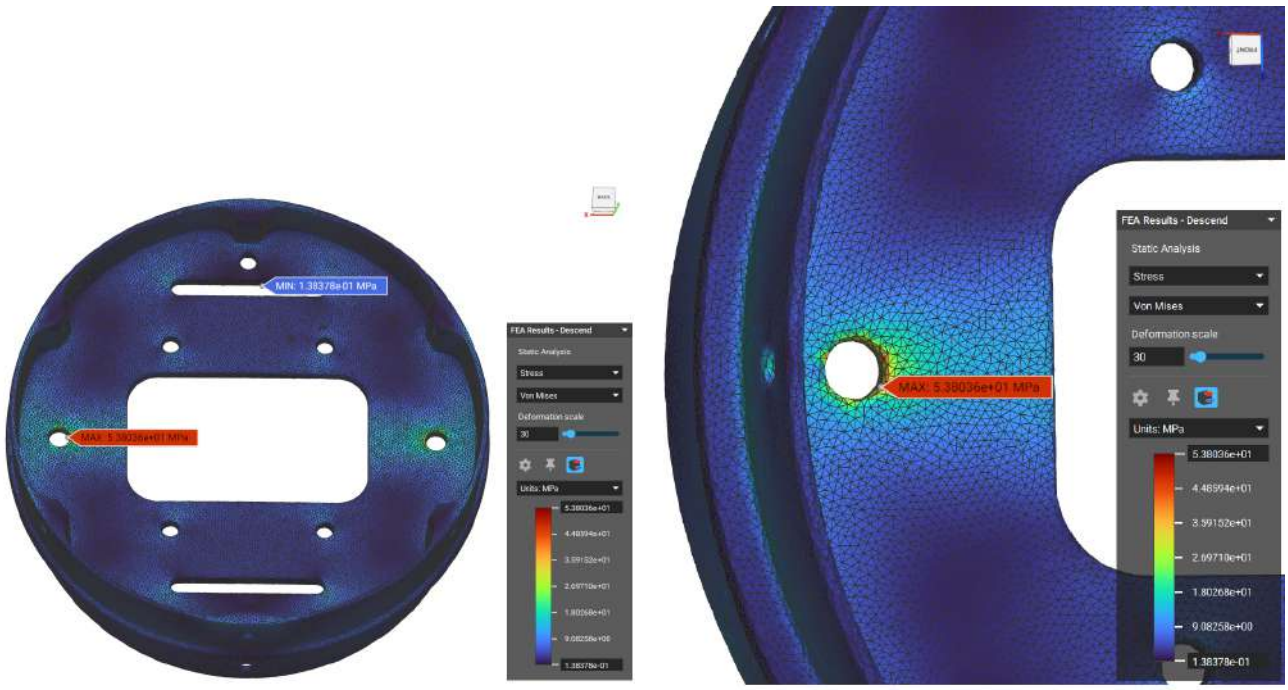

(a) (b)

Figure 2.15: Results of FEA for the payload bulkhead, during main parachute deployment.

The force rods are cylinders with a diameter of 8mm and two caps on either ends. As the are made out of 316L stainless steel annealed bars, each of them is able to carry the total axial loading distributed among the three of them. However, as these rods are quite slender and have no cross-bracing, they can be prone to buckling, which would be catastrophic. To ensure that they won't buckle, Euler's formula is presented below to calculate buckling:

$$F_{\text{critical}} = \frac{\pi^2 EI}{(KL)^2}, \tag{2.2}$$

where F_{critical} is the critical compressive loading when buckling occurs, E is the material's Young's Modulus (E = 193GPa), I is the cross-section's second moment of inertia (I = 201mm^4), K is the effective length factor (K = 0.65 for rigidly supported beam) and L is the rod's length (L = 302mm). Using these values, a critical load of $F_{\text{critical}} = 9.94MN$ is obtained and then divided by the rods cross-sectional area of A = 50.27mm^2 to get the buckling stress of 198GPa, which is far beyond the material's yield strength, meaning that it will fail due to yield far before buckling would occur.

While designing the fins, our highest priority was to reach an off-the-rail stability of 1.8, while also being safe from fin flutter. Combating flutter requires adequate damping as it is a vibration phenomenon. To achieve this, many different aspects of the fins have to be considered, such as their geometry, material, and how they are attached to the rocket. Their attachment to the rocket is difficult to quantise, and most developed equations assume that they are not through-the-body and not tip-to-tip layup - both of these should increase damping and therefore increase the velocity where flutter occurs. Using the equation developed by Rasuo and Dinulovic [1], a maximum safe speed of 889m/s was calculated for Darwin III's fin geometry. A precise geometry of the fins is presented in Appendix F (part ID: D3-106)

As the peak velocity is expected to be 572m/s (M1.71), the fins are deemed safe for flutter. Additionally, as the fins are through-the-body and are tip-to-tip laid up, their maximum safe speed will be even larger.

2.3.2 Trajectory Simulation

To validate that Darwin III's design is capable of exceeding its target apogee with the chosen motor and airframe design described above (including masses for payload, recovery and avionics subsystems) for airbrake deployment, flight trajectory simulations were performed and compared using two software: OpenRocket and

RASAero II. OpenRocket benefits from a superior UI and integration of optimisation features, which were utilised throughout the design process. However, in the transonic and supersonic regimes, OpenRocket suffers from lower accuracy as a result of various assumptions used in its calculation of drag. The results for velocity, acceleration, altitude and stability obtained from OpenRocket and RASAero II are presented and discussed further in Section 3.

Stability was specifically tracked throughout the development of DIII to avoid the low off-the-rail stability. The CG is controlled by the mass distribution, with mass closer to the nosecone being beneficial and mass closer to the aft-cone being detrimental. With this in mind, most of the mass-optimisation happened near the aft sections - especially with the thrust plate and the motor bulkhead. As an additional measure, we introduced the ballast, steel plates that can be stacked on top of each other in the nosecone, to shift the CG upwards, in case of low stability. As the outer diameter of the rocket cannot be changed, the only way of increasing the stability is moving the CP closer to the aft. The fin geometry was carefully chosen to achieve the desired CP location. We settled with four relatively small swept fins that are designed with a goal of achieving maximum stability while also being stiff enough to combat flutter and the bending stresses. To simulate the stability of the vehicle, we used both OpenRocket and RASAero II, and the results of which are shown in Figure 3.1 in Section 3.

Looking at the graphs, it can be seen that RASAero II predicts a higher stability than OR. As with the velocity increasing, the aerodynamic forces increases as well, meaning that the most critical point from a stability standpoint is when the rocket leaves the rail. The off-the-rail stability predicted by OR is 1.79 cal, while RASAero II predicted 2.85 cal.

2.4 Recovery subsystem

2.4.1 Introduction

The Darwin III recovery system is a dual deployment two-chute design consisting of a 24-inch drogue parachute, a 96-inch main parachute, an SRAD CO_2 canister powered ejection mechanism and a COTS main parachute recovery stage.

2.4.2 Components, Specifications and system overview

Table 2.5: Recovery hardware for Darwin III.

Hardware	Quantity
Rocketman 96-inch High Performance Parachute	1
Rocketman 24-inch Elliptical Parachute	1
SRAD CO_2 Ejection System	1
Tinder Rocketry RAPTOR CO_2 Ejection System	1
Rocketman 10ft Nylon Shock Cord	1
Rocketman 20ft Nylon Shock Cord	1
Rocketman Kevlar 6ft Y-harness	1
Eye Bolt and nylock nut M10	1
Eye Bolt and nylock nut M6	1
Polycarbonate separator plate	1
33g CO_2 Canister	2
Tender Descender L2 Recovery Tether	2

As apogee is detected, the flight computers will initiate their ejection sequence. The ejection systems will activate, ejecting the nosecone, pulling the drogue parachute from the recovery bay. The rocket will descend at 43m/s at peak altitude, slowing to 26m/s as air pressure increases. At 450m, the main parachute will be released by activation by either one or both TD. The drogue parachute will pull the main parachute out of the recovery bay, causing it to inflate. The rocket will descend at 6m/s until it reaches the ground, minimising damage to the air frame.

Figure 2.16 shows an overview of the system at different deployment stages. In the first stage, the rocket is in its ground state where nothing has been deployed. At the second stage, the nosecone is ejected, pulling out and inflating the drogue parachute. The main parachute is held in place by a shock cord that is connected to the main release shared ring, which cannot travel upwards, unless one or both TDs has been activated. In the third stage, the TDs are activated, letting the drogue parachute pull the ring up and out, which itself pulls the main parachute bag out of the recovery bay and deploys the main parachute.

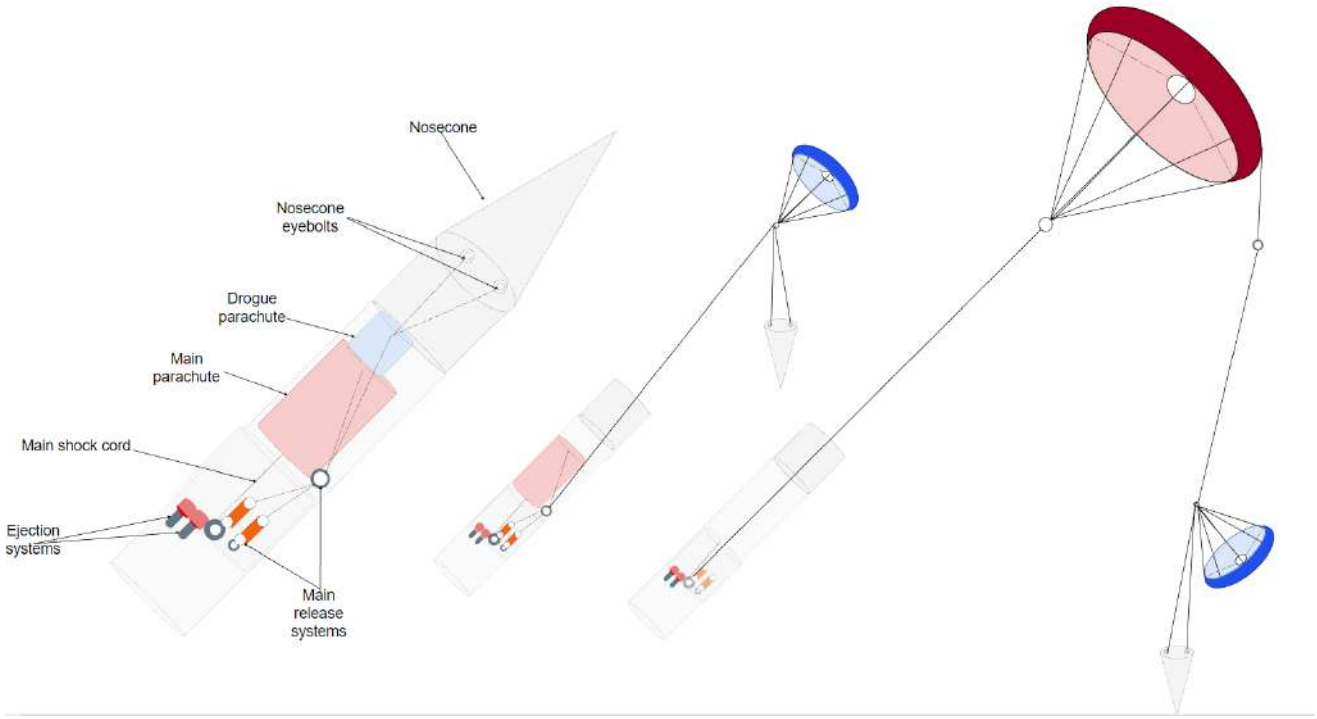

Figure 2.16: Recovery CONOPS.

2.4.3 Recovery Subsystem Calculations

Parachute calculations

The parachute sizes were calculated from solving the drag equation (2.3) as follows:

$$F_D = \frac{C_D \pi \rho r^2 v^2}{2}. \tag{2.3}$$

Where the symbols correspond to the following physical parameters:

- F_D - Drag force acting on the parachute measured in Newtons [N]
- C_D - Drag Coefficient [-]
- ρ - Air Density for a given altitude in kilograms per cubic metre [kg/m^3]
- r - Radius of the parachute in metres [m]
- v - Descent speed of the rocket in metres per second [m/s]

Equating the drag force to the rocket's weight and rearranging for r, we have Equation (2.4):

$$r = \sqrt{\frac{2mg}{\pi \rho v^2 C_D}}. \tag{2.4}$$

Where:

- m - Mass of the rocket in kilograms [kg]
- g - Acceleration due to gravity in metres per square second [m/s^2]

The results are given in Table 2.6. The range of C_D values was based upon what was quoted in commercially available parachutes.

The team already owns a 96" annular parachute with a C_D of 2.2 and a 24" elliptical parachute with a C_D of 1.6. A recovery was simulated to test whether they would be suitable candidates. The mass of the rocket used was 23kg, in-line with the expected dry mass of the rocket and the drag from the body of the rocket was also included. The main parachute gave a descent velocity of 5.6-6.2m/s, below the maximum 9m/s

Table 2.6: Parachute sizing table for Darwin III.

Parameter	Drogue	Main	Units
Deployment Altitude	9000	450	m
Range of C_D values	$1.6<C_D<2.2$		N/A
Air Density	0.41	1.225	kg/m^3
Target Speed	$23<v_{tar}<46$	$5<v_{tar}<9$	m/s
Parachute radius	**$0.16<r<0.37$**	**$0.81<r<1.71$**	**m**

mandated by the competition and above the minimum 5m/s set by the team to reduce the drift upon the main parachute opening. The drogue parachute gives a descent velocity of 30-43m/s, once again, within the range. This confirms that the parachute selection is compliant with competition rules. Both parachutes have built in swivel links to reduce the incidence of tangling and reefing.

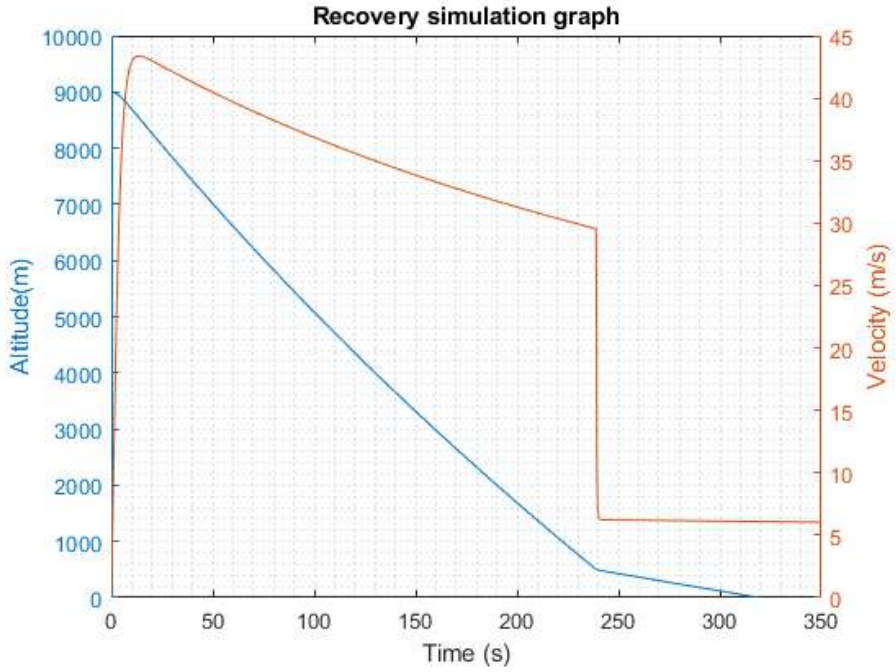

Figure 2.17: Simulation for descent through the recovery phase.

Ejection calculations

To understand the size of the CO_2 charge required for successful ejection, there are a few key areas that need to be accounted for:

1. Volume of the recovery bay.
2. Shear strength of the shear pins.
3. The friction force between the nosecone and the coupler
4. The outside pressure at apogee.
5. The force of the pressure difference due to the rapidly changing atmospheric pressure.

To begin with, the shear pins must strong enough to prevent early ejection due to the rapidly changing atmospheric pressure during launch, as well as being weak enough to shear during the ejection phase. By taking the dimensions the minimal diameter of an M3 shear pin and the shear strength of Nylon 6-6, the

force required to shear the pin in single shear can be estimated using Equation (2.5).

$$F_{sp} = \frac{k\tau D^2 \pi}{4}. \tag{2.5}$$

Where:

- F_{sp} - Total shear pin force [N]
- τ - Shear strength [Pa]
- D - Minimal diameter of the shear pin [m]
- k - Number of shear pins [-]

To calculate the potential maximum force from pressure difference, Equation (2.6) is used.

$$F_P = [(P_0 - P_1) \times A]. \tag{2.6}$$

Where:

- F_P - Force from pressure difference [N]
- P_0 - Pressure at sea level [Pa]
- P_1 - Pressure at apogee [Pa]
- A - Inside cross-sectional area of the recovery bay [m^2]

As long the force to overcome the shear pins is greater than the force exerted due to pressure change, there should not be an early ejection. The volume of the recovery bay is given in Equation (2.7):

$$V = \frac{\pi D^2 L}{4}. \tag{2.7}$$

Where:

- V - Volume of recovery bay [m^3]
- D - Inside diameter of recovery bay [m]
- L - Length of the recovery bay [m]

In order for the recovery system to deploy, the CO_2 gas has to exert enough pressure given in Equation (2.8).

$$F_{CO_2} = \frac{nRTA}{V}. \tag{2.8}$$

Where:

- F_{CO_2} - Force from CO_2 release [N]
- n - Moles of CO_2
- R - Molar gas constant [$JK^{-1}mol^{-1}$]
- T - Temperature at apogee [K]
- A - Inside cross-sectional area of the recovery bay [m^2]
- V - Volume of the recovery bay [m^3]

As long as the force produced is greater than the shear pin force and the coupler friction, there should be an ejection of the nosecone.

2.4.4 Detailed view of recovery bay and hardware

Figure 2.18 shows the internals of the recovery bay including the SRAD and COTS ejection systems and the COTS main parachute releases. The SRAD system can be seen on the left side of the render. The servo being used for recovery purposes is the SPT5325LV-360. The servo is encapsulated by the white servo holder. The servo holder provides a surface for the servo to push against, forcing the servo to pull itself down instead, boring into the CO_2 cartridge. The servo holder also helps to keep the servo upright under operation



Figure 2.18: Render showing the overview of the recovery bay hardware.

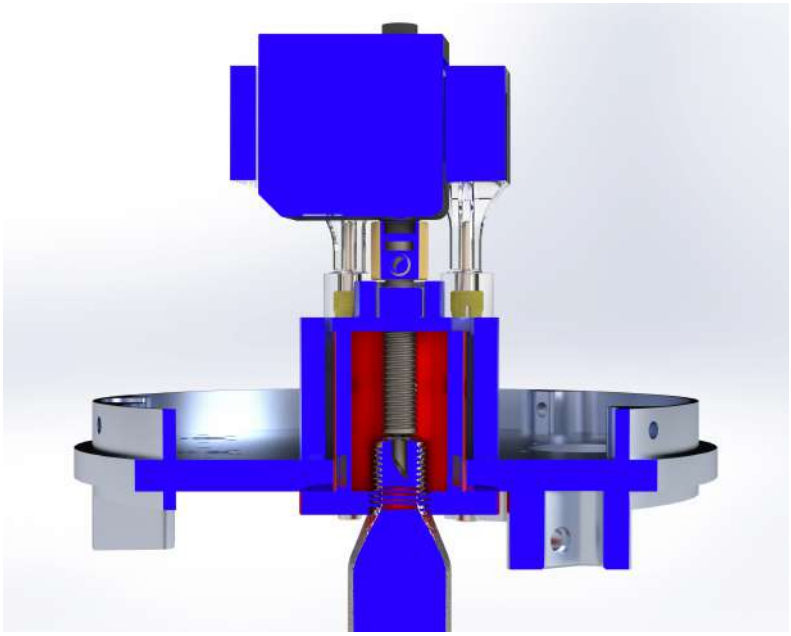

Figure 2.19: Render showing the overview of the recovery bay hardware.

so it punctures vertically, which will help to stop the tip from 'skating' on the top of the cartridge. This can be seen more clearly in Figure 2.19. Figure 2.19 shows the structure of the SRAD ejection system. The repurposed RAPTOR mount is locked in place with long bolts that pass into the servo holder. The servo holder has threaded inserts in the feet, seen in yellow, which provide strong retention of the mount and the servo holder. The blue cover around the RAPTOR mount provides a guide for the bolts and a mounting point for the servo holder. There are vent holes allowing the CO_2 to escape instantly. The cross-section also shows how the puncture device bores into the cartridge.

Figures 2.20a and 2.20b show the design of the puncture device. The sharp tip allows the head to pierce the canister, while the central hole leads to two escape vents. These vents allow the CO_2 to escape quickly, pressurising the recovery bay quickly and ejecting the nosecone. The cutter is made from stainless steel due to its high yield strength, ease of machining, and resistance to rust build up. The cutter threads into an M8 nut which is lubricated with a PTFE dry lubricant to allow for low-temperature operation and increase force

output.



(a) (b)

Figure 2.20: Design of the cutter head.

To provide a linear force to puncture the CO_2 cartridge while using the servo, a Lead Screw design is being used, translating the torque from the servo into a linear force. To find the linear force produced, equation 2.9 is used.

$$F_{ls} = \frac{2T_s}{d_m \tan(\phi + \lambda)}. \tag{2.9}$$

Where:

- F_{ls} - Force from the leadscrew [N]
- T_s - Servo torque [Nm]
- d_m - Diameter of leadscrew [m]
- ϕ - Angle of friction [rad]
- λ - Lead angle [rad]

A balance must be struck between the force output from the mechanism to the linear speed of the puncture device. This is due to a smaller diameter increasing the force output, shown in Figure 2.21a, but also requiring a smaller thread pitch, reducing its speed as shown in Figure 2.21b. From these values, an M8 thread profile was chosen, as it produces over 800N of linear force at 2.5Nm of torque and moves at over 1.1mm/s. With the small area of contact that the puncture device has combined with the high force and rotational motion, the CO_2 cartridges are easily pierced.

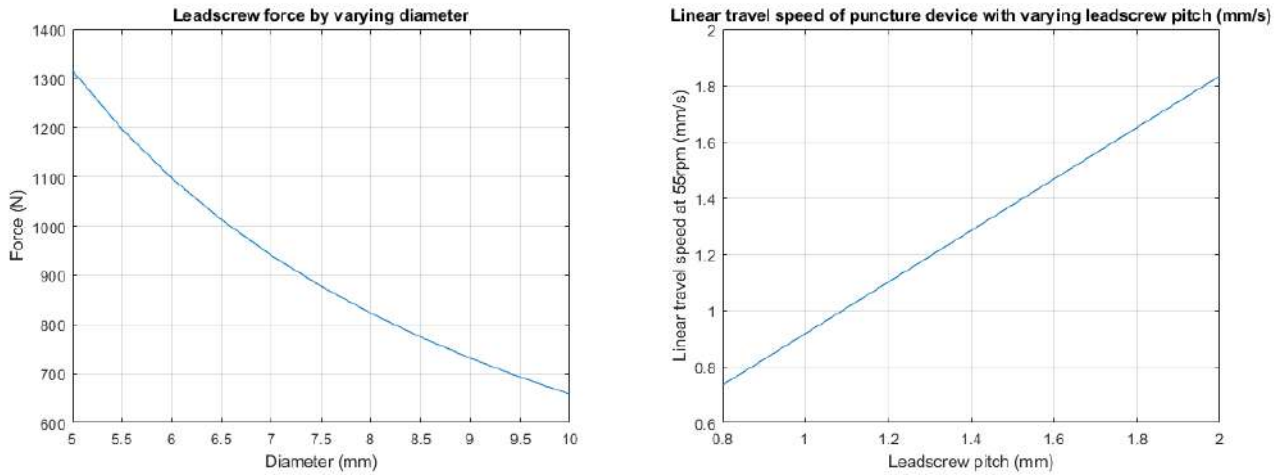

(a) (b)

Figure 2.21: Characterisation of lead screw forces and travel speeds.

The effectiveness of this SRAD mechanism was proven in a series of ground tests. Initially, preliminary tests

were carried out on the existing DII upper body to fine tune the cutter geometry and validate sufficient power delivery to the servo. Then, final validation tests were conducted on the as-flown upper body of DIII. Test reports available at Section B.1 and B.2.

2.4.5 Parachute Shock Forces

To work out the maximum forces experienced by the recovery equipment. To estimate the shock loads on the rocket, we use a program called OSCALC. OSCALC allows us to input our basic recovery parameters and it will output upper and lower bounds of the expected shock load. For recovery, ensuring that there is sufficient room for sub-optimal operating conditions is critical, as it gives a larger scope for recovering the rocket successfully. Table 2.7 provides the input parameters used and the final output for the shock loads. The values of shock factor are taken from historical data that OCSALC has collated, allowing for a more accurate estimation. Table 2.8 lists the safety factors of all the components that come under load during recovery. It

Table 2.7: OSCALC shock load calculations for Darwin III.

Parameter	**Drogue**	**Main**	**Units**
Deployment speed max	80	35	m/s
Deployment speed expected	50	26	m/s
C_D	1.6	2.2	N/A
Air Density	0.41	1.225	kg/m^3
Shock factor	1<Ck<2	0.5<Ck<0.8	N/A
Shock force max	**602<r<1205**	**3720<r<5950**	**N**
Shock force expected	**235<r<470**	**2050<r<3280**	**N**

includes safety factors for the expected loads, as well as pass/fail characterisation. A component is deemed to have passed if it features a safety factor of *at least* 1.5. As seen from Table 2.8, every component has

Table 2.8: Safety factors with respect to expected nominal loads as predicted by OSCALC.

Component	**Rated load [N]**	**Load [N]**	**Safety factor**	**Pass/fail**
Main parachute bridle	6690	3280	2.04	Pass
Drogue parachute bridle	6690	470	14.2	Pass
Shock cords	9810	3280	2.99	Pass
Shared TD shock cord	1080	470	2.30	Pass
3mm quicklinks	3530	470	7.51	Pass
Tender Descender L2	9810	470	20.9	Pass
8mm quicklink	34000	3280	10.4	Pass
10mm eyebolt	13500	3280	4.12	Pass
6mm eyebolt	4415	470	9.4	Pass

a safety factor of at least 2 with respect to the upper end of the predictions for nominal operation ("Shock Force Expected" in Table 2.7). Additionally the components can survive the absolute worst case scenario loads ("Shock Force Max" from Table A.2) which gives room for safe recovery under off-nominal recovery events such as as a torn drogue.

2.4.6 Redundancy in recovery

Redundancy is a critical aspect of recovery systems, as it is not guaranteed that a single design will work by itself. For the ejection stage, the SRAD flight computer will activate the SRAD CO_2 ejection system and has a separate connection to the backup RAPTOR. The COTS flight computer will activate the backup RAPTOR. Another layer of redundancy can be found in the design of the SRAD ejection system. As it is based off the

RAPTOR mount, in an event before launch where the SRAD design is found to be non-functional, it can be swapped out for a full RAPTOR and remain fully functional and redundant.

For the main release, there are two L2 TDs, with each controlled by a separate flight computer. They are also connected in parallel by using a shared connection to the drogue parachute. By doing this, only one of the TDs has to activate to release the main parachute. By using these methods, the recovery systems have sufficient redundancy in-line with the competition rules.

2.5 Payload Subsystem

2.5.1 Mission Aims and Success Criteria

Darwin III's payload consists of two scientific experiments: a student built muon detector (a modified version of MIT's CosmicWatch Muon Detector) and a fluid dynamics slosh experiment. The mission aims for the payload are as follows:

1. Collect muon count data using our modified CosmicWatch muon detector during flight to explore how muon detection rate changes with altitude, along with correlating it to temperature and pressure data the payload collects independently
2. Compare the muon rate during flight to the rate at sea level to explore Einstein's theory of special relativity and the efficiency of the detector
3. Using a wide-angle lens camera, observe how propylene glycol (a fluid with a higher viscosity than water) behaves during flight and how this relates to the wave fluid dynamics, with focus on the potential points of micro-gravity.
4. Using the IMU acceleration data, attempt to reproduce the recorded fluid behaviour in a Computational Fluid Dynamics (CFD) simulation.

Both of these experiments have been researched extensively and characterised during a Summer Internship conducted in collaboration with the School of Physics focusing on testing the limits of the muon detector. The conclusions of these tests can be found in the appendix. For the payload missions to be considered successful, criteria must be met:

1. The intact recovery of both payload hardware and electronics, with the SD cards having the relevant data on them and are able to be read into a laptop for data processing.
2. The muon detector will have detected a rate deemed reasonable with respect to the previous tests.
3. The slosh experiment will remain intact, producing a clear video to observe the slosh effect, with the potential of microgravity and the CFD simulation will emulate the mechanics of the observed fluid.

2.5.2 Payload Architecture

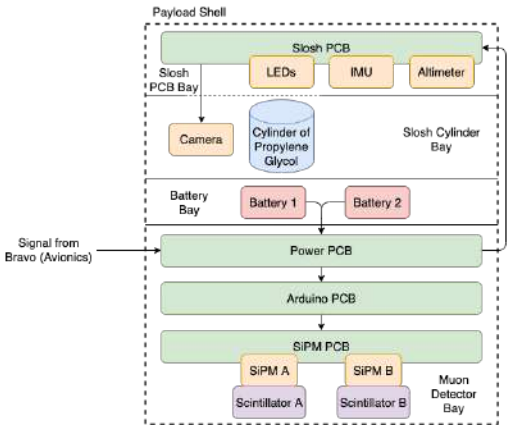

Figure 2.22: Payload Architecture

An overview of the the main components of the payload is given in Figure 2.22.

2.5.3 Form Factor

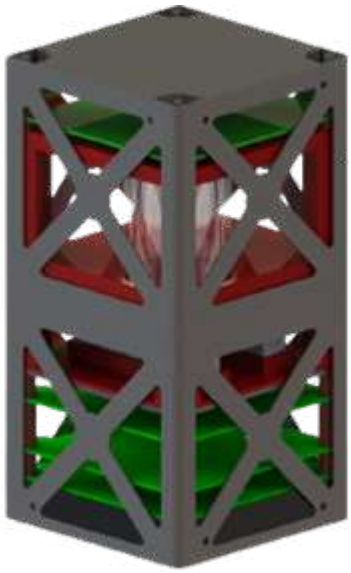

(a) CubeSat with the aluminium shell visible. The triangular features on the frame resist torsional forces while reducing its mass.

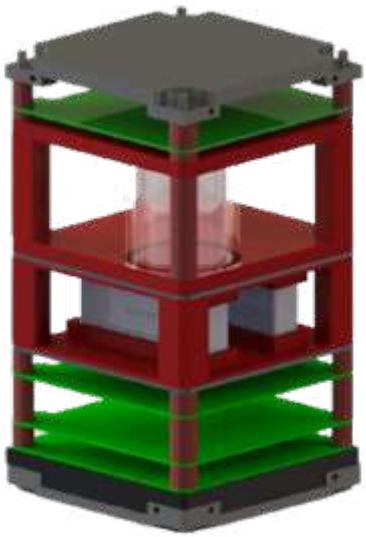

(b) The assembled CAD of the payload without the outer shell for clarity. The lower section houses the muon detector while the upper section has the fluid dynamics slosh experiment.



(c) Assembled payload without the shell.

As seen in Figure 2.23a, the payload is a 2U CubeSat so has the dimensions of 100 x 100 x 200 mm including fasteners. The CubeSat design was necessary for the muon detector design, as the boards had to be large enough to hold all the components dictated by CosmicWatch. As discussed in Section 2, the payload form factor was a deciding factor in the choice of the outer diameter of Darwin III's body tubes.

The vertical stack, centred on four stainless steel M4 threaded rods, was chosen for ease of assembly and disassembly. 3D printed spacers fit around the rods and carry the compressive forces of launch, while the threaded rods carry the tension loads experienced during the recovery events. The outer shell (fastened to the aft and forward bulkheads (PLD-502 and PLD-503)) was designed to provide torsional stiffness to the assembly - the cross triangular design is optimal for this, and the use of only two bolts along the diagonal of two sides both accounts for the torsional twisting of the shell away from the bulkheads while simplifying of assembly. The other faces have four bolts, with one panel being fully removable to allow easy access to critical components such as switches, cables and batteries. By using the same M3 bolts for the shell and M4 nylon locking nuts on the four rods, we reduce the number of tools required to assemble the CubeSat, along with using very easily sourced fasteners for modularity.

Another feature of modularity is splitting the payload into sections. By using insets in the 3D printed spacers of the battery brace and the slosh experiment frame, these sections can be easily removed as one piece, reducing the time for assembly and disassembly. By using tight tolerances on the prints, the design is still able to be dismantled enough to allow full access to components in case of any breakages/other emergencies. The CubeSat's mass budget is detailed in Table 2.9.

Finite element analysis was performed on the CAD to analyse how the materials involved would perform under the loads from ascent and the parachute deployment shock. Further details can be found in Appendix H.1. The results show a maximum stress on the aft bulkhead (PLD-502) (316L stainless steel). The FoS on the bulkhead at lift off with a load of 15G is 3.23. The aft payload bulkhead (PLD-502) takes the maximum stress from the parachute shock force (180N in this case), giving a FoS of 8.63. Both of these values are sufficient to remain confident in the bulkhead throughout all stages of flight. See Appendix H.2 for details. In addition to the FEA, a physical test was performed on the assembled payload to test the 3D spacers under

Table 2.9: Mass budget for Darwin III payload.

Component	Material	Mass (g)	Contingency Mass (g)
Bulkheads	316 Stainless Steel	1017	1017
Aluminium Plates	Aluminium	111	111
Rods	Steel	57	57
Shell	Stainless Steel	356	374
Electronics	Mixed	400	400
3D Printed Spacers and Braces	PLA	236	236
Slosh Fluid	Propylene Glycol	44	50
Fasteners	Stainless Steel	24	30
Total Mass		2180	2218

load. Results can be found in Appendix B.15.

To ensure the safety of the electronics within the CubeSat and rocket, several steps were taken to prevent leaks and breakages from the slosh experiment. The acrylic tube is 3mm thick, which will ensure it does not crack, along with the spacers around the slosh bay taking all of the compressive force from lift off. The tube and acrylic window are sealed with silicon and epoxy to the PLA brace, which itself is 3D printed with 4 "roof" layers, ensuring no leaks across its surface. The functionality of the window located between Slosh PCB and the tube is to diffuse the light emitted by the LEDs on the PCB above, reducing glare and allowing the camera to see the waves in the liquid. The liquid was chosen to be propylene glycol, due to its higher viscosity correlating to slower slosh dynamics, making it easier to be seen on the camera's video. Its viscosity of 5.2×10^{-5} m^2s^{-1} is similar to that of kerosene ($\nu = 2.39 \times 10^{-4}$ m^2s^{-1}) in comparison to water ($\nu = 1 \times 10^{-6} m^2s^{-1}$), making it analogous to rocket fuel. As the temperature during flight can drop to $-40°C$, propylene glycol was chosen as it has a freezing point of $-59°C$. The propylene glycol will have added pigmentation and reflective particulates inside to again reflect the light and again make the observations in the video easier to see. Propylene glycol is a very safe, inert liquid.

Interface, Configuration and Removal

The CubeSat is attached with M5 eyebolts at two points to the payload bulkhead (D3-501) and sits inside the nosecone throughout the ascent. The aft payload bulkhead (PLD-502) of the CubeSat has four threaded M5 holes to ensure a tight fixation to the bulkhead below. The other two holes on the bulkhead are used to attach one arm of the Y-harness from the recovery system to the nosecone and the CubeSat inside.

2.5.4 Scientific Background and Context

See Appendix G.1 for details the motivation behind the muon experiment, and the work done to characterise it in full.

2.5.5 Functionality

The two scientific experiments are comprised of three microcontrollers over four PCBs. The system is powered through two 1300mAh 7.4V 35C LiPo batteries in parallel (full power analysis in Section 2.5.7). The output voltage of the batteries is stepped down to the 5V required to power each of the microcontrollers and surrounding sensors. This voltage conversion is performed on a separate Power PCB to minimise interference from the EMI that arises from the onboard DC-DC Buck. Figure 2.24 shows the electrical architecture detailing how the voltage conversion and each experiment is arranged over four PCBs.

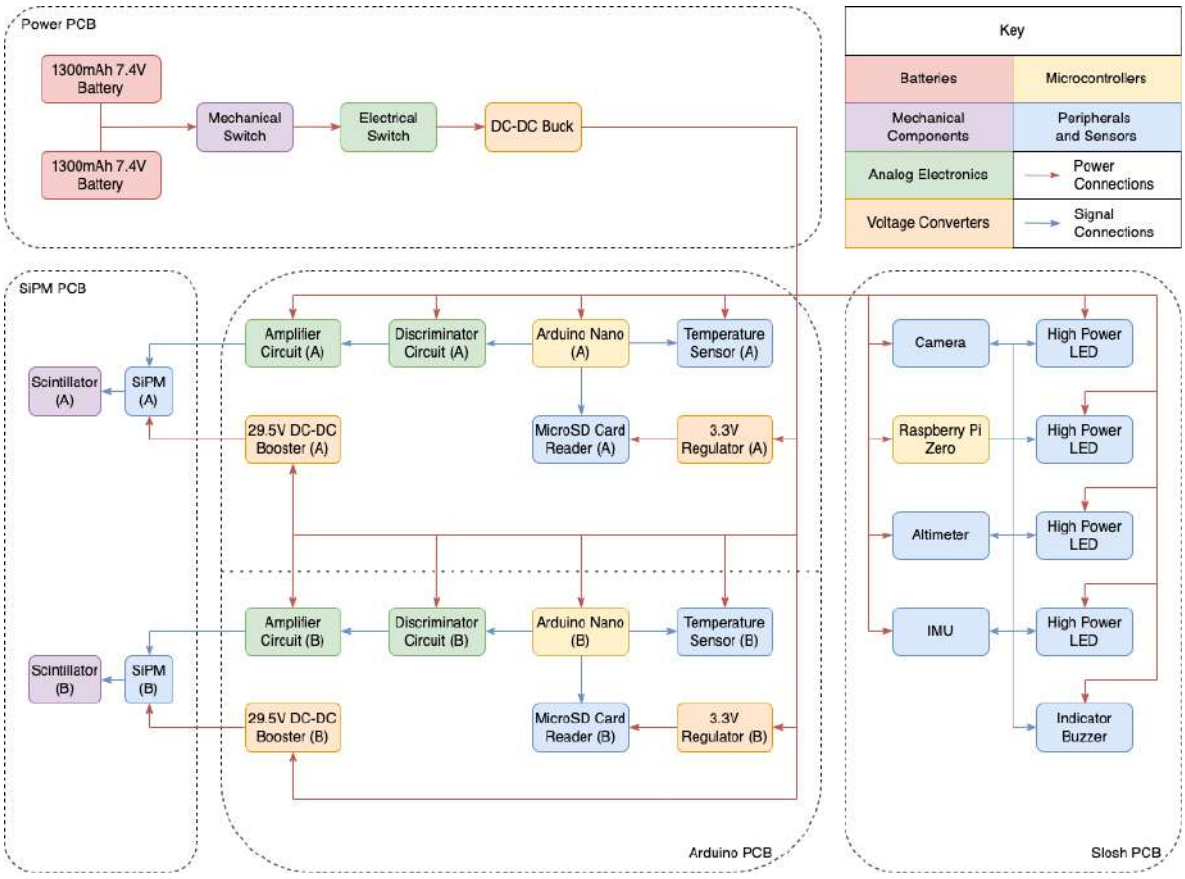

Figure 2.24: CubeSat Electrical Diagram.

Power PCB: Voltage Conversion

The Power PCB was designed to isolate the high power components from the data signals. Nominally, the 7.4V supplied by the batteries is stepped down by a DC-DC Buck with maximum efficiency of 96% to 5V (actual LiPo voltage range is between 6.4V to 8.4V). The stepped-down voltage is passed to each experiment though JST connectors. To provide electrical safety, the system can be isolated by a mechanical switch. The system is further protected by an electrical switch to conserve power whilst the system is idle on the launch pad. The electrical switch is controlled through a signal provided by Bravo (the avionics telemetry PCB) and uses a NAND gate with its inputs tied together to invert the incoming signal, then the negated signal is used to turn on a PMOS high side switch. The switch is normally open, meaning that the payload batteries will be connected to the payload experiments if a logic LOW is presented at its input. Thus, when the vehicle is waiting to launch, avionics will assert a logic HIGH, disconnecting the batteries and preserving power. At t-180s before launch, the GSO (Ground Station Operator) will command the avionics subsystem to pull the signal LOW, thus, connecting the batteries and allowing the payload experiments to boot up. Upon drogue ejection, an aux cable connection to the avionics bay will be disconnected, but an internal pull-down resistor will ensure the switch input is kept LOW; hence keeping the experiments powered. The connection between the payload and avionics bay is made through a shielded Aux cable, chosen for its EMI tolerance and low disconnection force (3N) required during the drogue ejection event. A detailed plan of the harness between the payload and avionics bay is given in Figure 2.25.

This circuitry - with particular attention to the electrical switch - has been verified through simulations, breadboarding and load tests on the final system. The final tests verifying the Power board's ability to drive high loads and turn off when the signal from avionics is asserted are detailed in Appendix B.12 and B.14. Additionally, a full test of the Power PCB powering both boards was performed in Appendix B.13

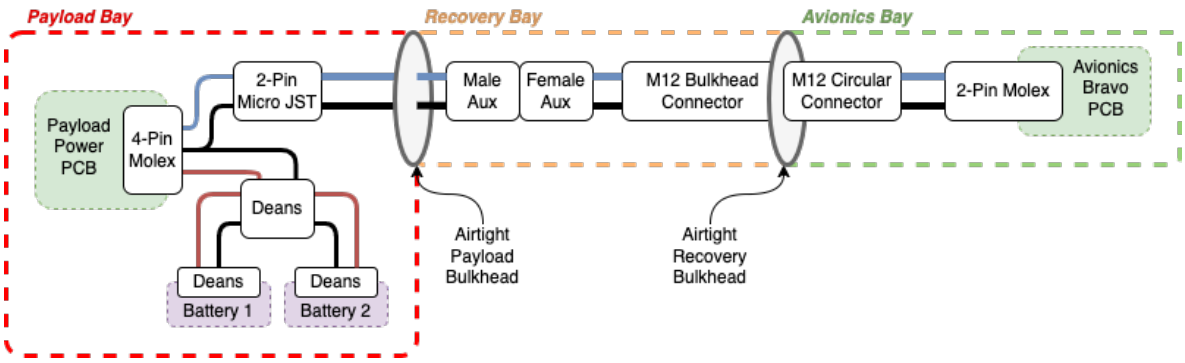

Figure 2.25: Electrical Connection between Payload and Avionics.

Arduino and SiPM PCBs: CosmicWatch Muon Detector

The Muon Experiment contains two adjacent muon detectors. The design of the detectors, inspired by MIT's CosmicWatch Detector, were chosen due to their compact design and affordability. To have both detectors to be on the same PCB (the Arduino PCB) the CubeSat form factor was required. The SiPM PCB contains the SiPM (Silicon Photomultiplier) chip for each detector. SiPMs are components that convert the photons (created by the scintillators) into electrons. The Arduino PCB contains the remainder of the circuitry for each detector, which amplifies and discriminates the signal from the SiPMs before passing it to its respective Arduino Nano. The microcontroller determines when a muon has been detected by comparing the voltage received against a threshold (50ADC in this case). All data is written to an SD card for evaluation upon recovery. Temperature values will accompany the data to help calibrate the results.

As the SiPM chips are prone to being noisy, the second detector is used to determine if the detected signal is indeed a muon. The detectors are placed side by side for statistics purposes (i.e if the detectors detect the a particle at the same time, it is most likely a muon as opposed to noise).

The detector has been tested at great lengths to determine its accuracy. The detector detects muons at a reasonable rate (0.224 muons per second) for the surface area of scintillator (20cm^2 on each) [2]. See Appendix B.8, B.10, B.9 and B.11 for further details including tests at different temperatures and altitudes.

Slosh PCB: Slosh Experiment

The Slosh PCB contains a camera to observe the fluid along with 4 high power LEDs to illuminate the payload when its is inside the rocket. An IMU and altimeter will also record flight data alongside this to support both experiments, providing a log of how the system performs during different stages of the flight. A RaspberryPi Zero will communicate with the sensors over I2C storing the data on the microcontroller's internal memory. The microcontroller was chosen for its simple compatibility with cameras and a 64GB SD card will be used to store the Operating System (OS) to ensure memory will not be a limiting factor. At a resolution of 1080x720 (the maximum the camera module can provide) it is estimated that 49 hours of video can be achieved. The video data will be saved every 10 seconds to ensure partial data is still available if damage occurs to the camera during flight.

The system has been tested to ensure the image quality is high, and to observe the fluids performance at different temperatures. A wider lens has been chosen to observe the full tube in the small distance of the camera and fluid.

2.5.6 Dissemination of Results

CosmicWatch Muon Detector

The purpose of having a muon detector in Darwin III is ultimately to write a scientific paper and publish it in an undergraduate journal of physics. This goal has been greatly helped by one of the payload leads undertaking an 8-week physics internship to explore the efficiency of the student built muon detector. Tests

included putting the muon detector in a climate chamber to find a relationship between dark currents (thermal noise produced by the environment and the detector itself) and the use of two other standard muon detectors to help reduce the noise on the CosmicWatch detector. See Appendix B.11 for further details.

Slosh Experiment

The slosh experiment data collection is instrumental in our development of a liquid rocket engine, by another subteam - Maxwell. This will be the first slosh test done within Endeavour of how a fuel like substance behaves during flight and at apogee, and so simulations produced from this video will be used for years to come. The IMU data will be manipulated to identify the rockets orientation, acceleration and altitude. The altitude will be compared against the values read by the altimeter to verify their accuracy. This flight data will be used to observe the behaviour of the fluid during different stages of flight, with the aim of identifying micro-gravity at apogee.

2.5.7 Power Consumption

To ensure the lifetime of the battery meets the 6hours required by the Demand, Test and Evaluation guide the power consumption of the system was tested (see Appendix B.13). The system draws a peak power of 2.9W whilst the camera is recording. The two batteries 1300mAh each at a nominal 7.4V, this would allow the experiments to run for 6.6 hours. Though this value is close to the limit specified by the EuRoC Design, Test and Evaluation Guide, the electrical switch will be open until t-180s before launch. Thus, no power will be drawn until then, increasing the power safety margin.

2.5.8 Deployment and Recovery

Darwin III's payload is not deployable and thus remains integral to the Nosecone Assembly throughout the mission. As it will be recovered with the rest of the LV, it does not have its own recovery or GPS system.

2.6 Active flight control subsystem

Darwin III features redesigned airbrake and an Abort system, which are described in detail below. The airbrake will correct any manufacturing imperfections in the COTS CTI reload which may cause Darwin III to exceed target apogee of 9000m. The abort functionality, enabled by a robust SRAD half-duplex RF interface to the ground station, will help limit risks in case of structural, recovery or propulsion failures.

2.6.1 Airbrake

Mechanical Subsystem



Endeavour's third set of airbrake were designed with the challenges of the previous two designs in mind. One fundamental difference between this year's design and those of the previous years is the deployment mechanism. In previous years, the airbrake were actuted by a servo-motor, and deployed linearly, radially from the body; this simplified calculations relating to partial deployment but introduced practical and implementation challenges due to the manufacturing methods available to the team. The airbrake that presented with DII were deemed unsuitable for flight and deactivated ahead of the launch attempt due to significant friction between the moving and stationary parts. To overcome these challenges, a rotary design is used on DIII.

A centre gear drives three rotationally symmetrical petals which open out from the side of the rocket. To reduce friction under load, thrust bearings are placed above and below the petals. The petals rotate freely on brass bushings through their centers.

Manufacturability was a primary design criteria for these airbrake. Despite the teams manufacturing capabilities improving later in the year, all components are planar and designed to be cut out of 3 mm aluminum with a waterjet or laser cutter. At the top and bottom, two plates hold the whole structure together. These are bolted together around the periphery, meaning the entire is structurally self-sufficient and may be easily removed for servicing. Sheets of high-density polyethylene (HDPE) fill in the gaps between the plates and the petals. The whole assembly is modular and can easily be removed from the rocket if necessary.

The center gear is powered and held in place by a 6V, high-torque SPT-360LV servo-motor. For the safety of the rocket, it is essential to make sure that the airbrake do not prematurely deploy. If the LV enters a high-frequency roll caused by unexpected aerodynamic forces, the centrifugal forces acting on the petals of the airbrake could cause them to prematurely deploy. This would happen if the torque acting on the petals exceeded the stall torque of the servo. Given that the stall torque of the motor is 29kg-cm (2.8N-m) and that there are 3 symmetrical petals, the torque acting on each petal must exceed 0.9N-m. The petal has a mass of 44g and may be modelled as a single point at the centre of mass, yielding the following free-body diagram: Here, M represents the centre of mass of the petal, C the centre of the rocket, and O the centre of the gear. r thus represents the radius of rotation of the centre of mass of the petal. The angular velocity equation (2.10) is:

$$\omega = \sqrt{\frac{F_c}{mr}}. \tag{2.10}$$

Where:

- F_c Centripetal force acting on the petals [N]
- ω Angular velocity [rad/s]
- m Mass of the petal [kg]
- r Radius of rotation [m]

F_t is obtained by projecting F_c onto a perpendicular to the centre of mass; to overcome the stall torque at that point, a force of 47 N is required. This corresponds to a centrifugal force of 48 N and an angular velocity of 140 rad/sec or 8105 deg/sec. This number is well outside of the expected range of rotational

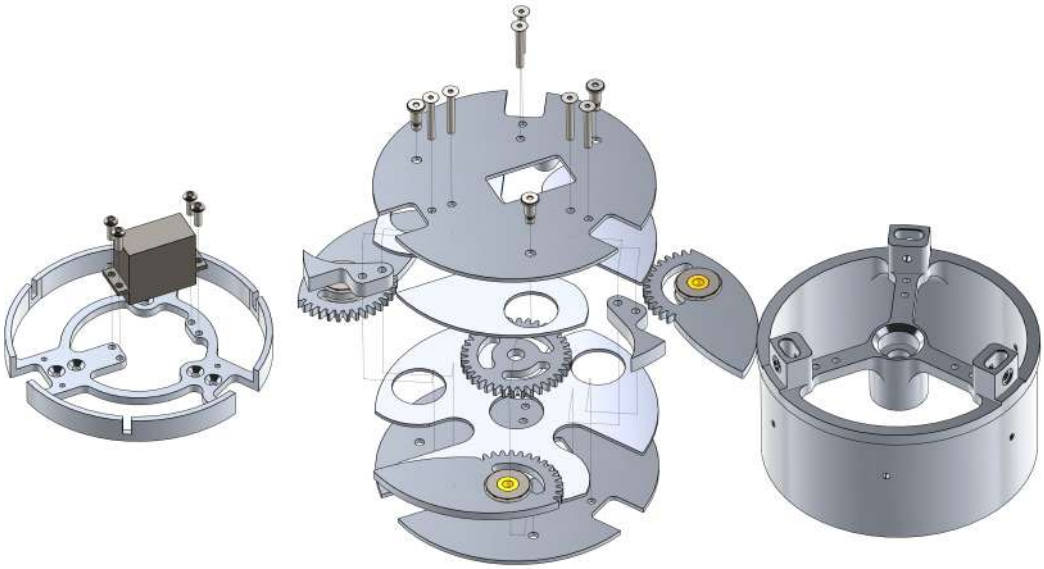

Figure 2.26: An exploded view of the entire assembly.

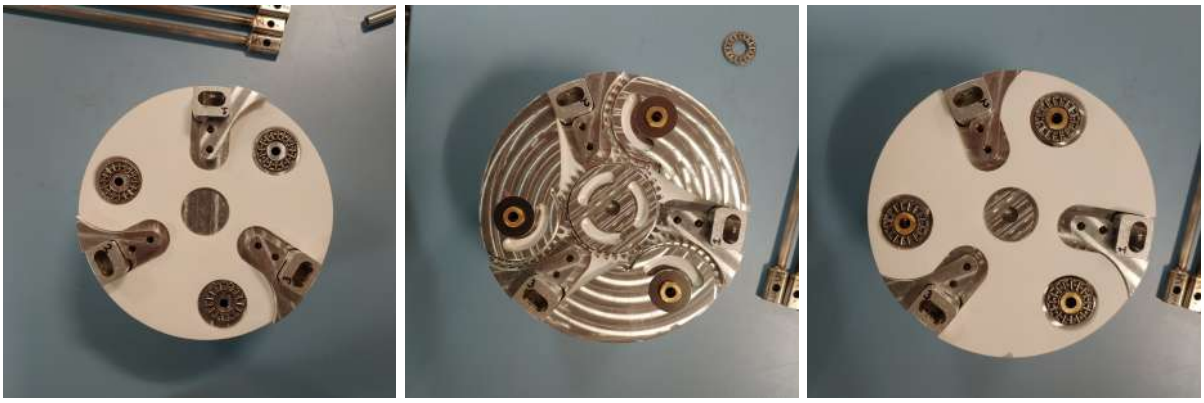

Figure 2.27: The assembly of the airbrake section, completed in stages.

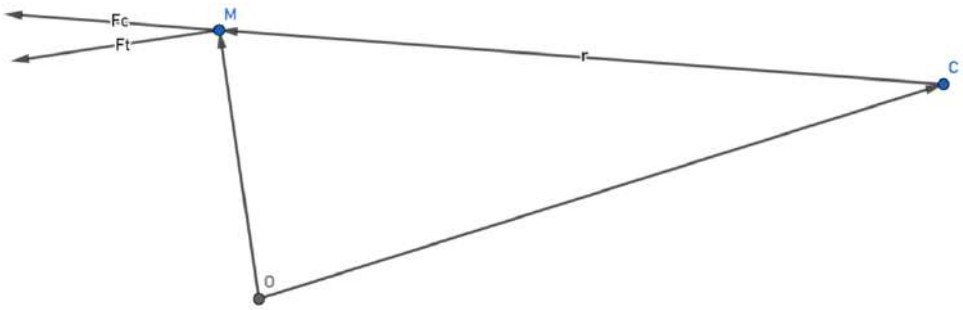

Figure 2.28: Free body diagram of one petal.

speeds predicted by OpenRocket, even for fin misalignment as drastic as 3° , ensuring that the airbrake

cannot deploy prematurely.

Deployment Logic

The main goal behind the airbrake is to have a system that can reduce the final altitude reached by the rocket in the case of a predicted overshoot. This is done by increasing the drag of the rocket in a controlled manner. For it to work, a control system is needed that monitors the current speed and altitude of the rocket and one that can predict the apogee of the rocket.

Onboard the rocket, the SRAD flight computer (Alpha) received high-frequency (¡100Hz) data from a set of accelerometers and barometers. Using a Kalman Filter as the sensor fusion algorithm, the flight computer is then able to compute and update the current speed and altitude of the rocket at every timestep. Thus, the main hurdle to overcome was how to obtain an accurate prediction of the apogee given this data. An additional engineer challenge was ensuring the method was lightweight and rapid, thus suitable for embedded micro-controllers without causing slow-downs in their program loops.

The first step was to model the trajectory of the rocket as a system of non-linear ODE's that could be numerically solved. The system was modelled as a projectile in 2D motion subject to a drag force which opposes the direction of travel, shown by equation (2.11).

$$F_D = \frac{C_D \rho A v^2}{2}. \tag{2.11}$$

Where:

- F_D - Drag force acting on the rocket measured in Newtons [N]
- C_D - Drag coefficient of the rocket, whose value is dependent on the current speed of the rocket [-]
- ρ - Air density modelled as a function of the current altitude of the rocket [kg/m^3]
- A - The area of the perpendicular cross section of the rocket [m^2]
- v - The current velocity of the rocket [m/s]

Values for C_D were obtained by introducing our 3D model of the rocket into the program OpenRocket. Thus, the predicted apogee of the rocket can be calculated by numerically solving the system and finding the altitude at which the vertical velocity of the rocket decreases to zero.

Additionally, the effect of opening the airbrake can be mathematically modelled as an increase of the drag coefficient C_D of the rocket. Thus, predicting the apogee when the airbrake have been deployed is simply a matter of taking into account the increase in C_D during the period in which they are open. The complexity lies in obtaining reliable information regarding the C_D - this is discussed further in Section 2.6.1.

The fourth order Runge-Kutta method is the numerical integrator chosen to solve the ODE system. A timestep of 0.5 seconds was found to be a sufficiently good compromise between processing resources and accuracy obtaining predicted apogee values within 20 metres of the OpenRocket result. By optimising the solver, the 600MHz Teensy 4.1 MCU used for processing on the Alpha board can produce apogee predictions within less than half a millisecond. This control system for controlling apogee is encapsulated in the block diagram illustrated in Figure 2.29. In order to preserve the structural integrity of the rocket, the airbrake do not deploy until the rocket has reached subsonic speeds. It is beneficial to predict apogee only after motor burnout has been achieved - at that point, the vast majority of energy will have already been introduced to the system. At burnout, the flight computer begins performing the necessary calculations to obtain predictions for the apogee. It is not necessary to conduct these calculations at high frequency, as the frequency of events which might cause the trajectory to change drastically are not expected. When the process confirms five independent times that the rocket will overshoot the desired target by at least 100 m, the flight computer must then calculate how long to leave the airbrake open for in order to achieve the necessary correction.

In the subsonic region a sensible value to deploy the airbrake at is 200 m/s. This number is within the structural limits that the LV can withstand and it is also large enough for the airbrake to introduce a significant enough correction to the apogee. To start off, the flight computer assumes that the airbrake will be open for a very short time; that is, the airbrake will close when the speed of the rocket dips below

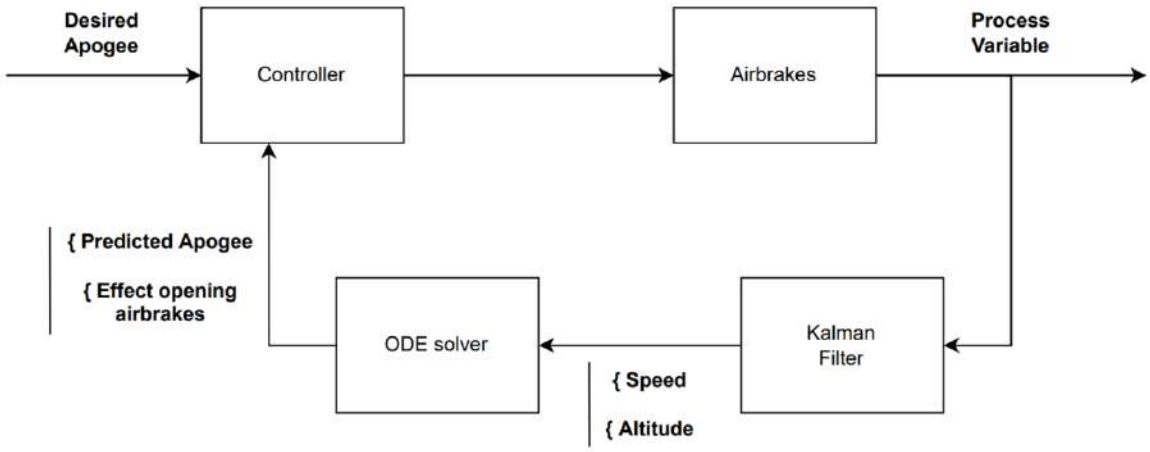

Figure 2.29: Block diagram of the control system behind the deployment of the airbrake.

190 m/s. If the correction introduced by this short opening time is not enough, then the speed at which the airbrake will close is reduced by 10 m/s. This happens successively until the correction introduced is sufficient. Otherwise, the airbrake will remain open.

Our algorithm was tested and results validated using data provided by the NTNU Propulse rocketry team (Trondheim, NOR), to which we extend our deepest and friendliest thanks. The flight NTNU provided data came from the SAC flight of their Project Birkeland LV, which successfully completed a perfect mission.

The sensor data provided was then read line by line and the Kalman Filter was updated sequentially on this data, simulating real flight conditions. When the rocket's speed dropped below 250 m/s, the ODE system was then numerically solved for different deployment scenarios of the airbrake. The results are shown in Figure 2.30. When no airbrake are deployed, the rocket reaches apogee at an altitude of 9638m. When airbrake are deployed at the speeds of 150 m/s, 200 m/s and 250 m/s, apogee is reached at altitudes of 9557m, 9411m and 9159m; respectively.

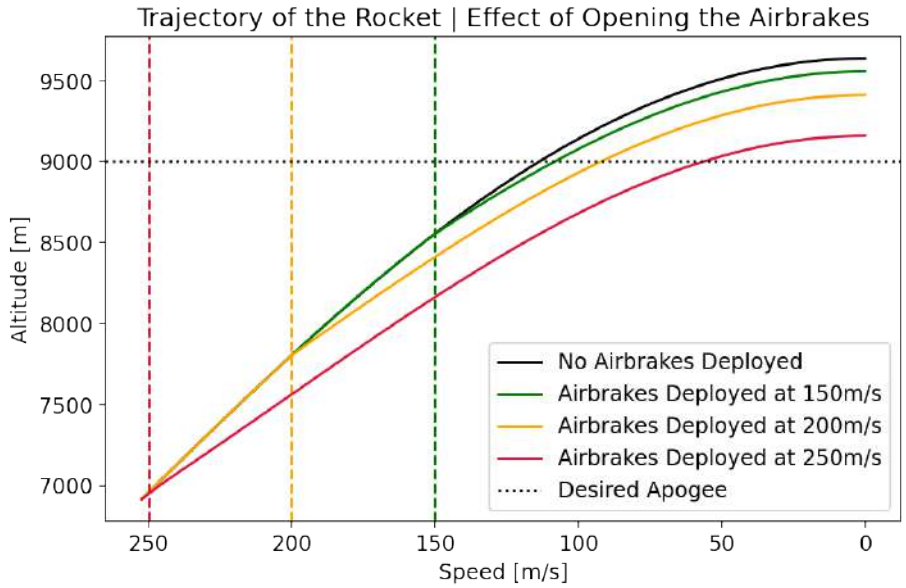

Figure 2.30: Effect of opening the airbrake on the trajectory of the rocket. The dashed lines indicate at what speed the airbrake were opened for each particular case. Once open, they remain open until apogee is reached.

CFD results

While there is some literature related to coefficient of drag of surfaces that are similar to the airbrake, most of it only reports experimental data. Analytical solutions are hard to obtain since the airbrake interact heavily with the boundary layer, and therefore the coefficient of drag differs from the one of a simple flat plate in a flow. A CFD analysis was conducted with a simplified model of the rocket for free-stream condition at approximately 6700 m travelling at 200 m/s. The behaviour was analysed as a steady problem and was solved with SolidWorks Flow Simulator, and it reached convergence after around 40 elements for global average values of density, velocity, and force. At 6700 m, the pressure and temperature varies significantly from

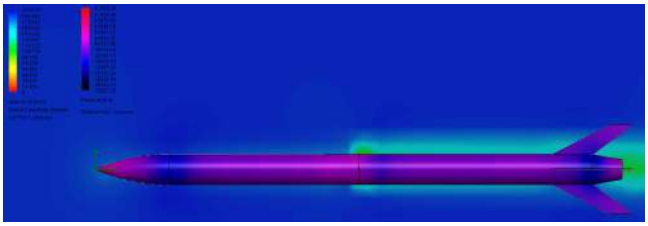

(a) Velocity and pressure along length of rocket.

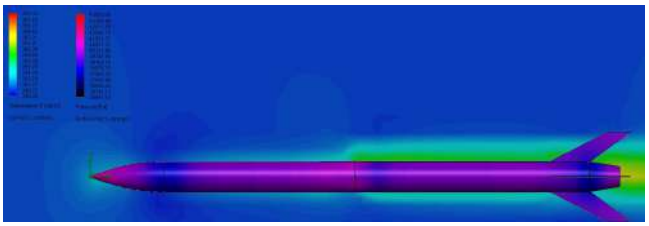

(b) Temperature and pressure of flow around rocket.

that of sea level. In addition, density of air is also about 60% of the density at sea level. As a result, the drag coefficient of the rocket with airbrake fully deployed obtained from the CFD is significantly lower than values expected at 0.03. This value is significantly lower than the value of 2.5 reported in literature [3]. This CFD result could contain errors due to limited computational power; which will be investigated in the lead-up to the launch. For the moment, the higher value of 2.5 is assumed as it represents the maximum effect, and thus, protects the vehicle from over-estimating the effect of the airbrake and reducing its apogee unnecessarily.

Figure 2.31a and 2.31b show the velocity, temperature, and the pressure at the surface. The velocity decreases significantly at the airbrake as expected. It is interesting to note the change in pressure over the length of the rocket shown on the surface. The boundary layer is fully developed after the nose cone, and so it verifies the assumption of flat plate not applicable for the airbrake. While the temperature rises by 20°C towards the aft of the rocket, because the ambient temperature is so low, the actual temperature is well below the material limits.

2.6.2 In-Flight Abort/ Manual Recovery Initiation

With the robust two-way communication protocol implemented on the SRAD FC (see Section 2.7.2, DIII features a manual abort system. On top of developing a robust Finite State Machine at the core of the software architecture with capabilities to detect a range of off-nominal scenarios, the endeavour GSO (Ground Station Operator) has the capability to instruct Darwin III to prematurely eject the recovery system. The envisaged use-case for this system is to prevent loss of life or damage to property caused by the launch vehicle deviating from the expected trajectory. An alternative use-case for the Abort system is to manually initiate recovery events should the vehicle be seen to be descending in a ballistic trajectory.

The effect of prematurely ejecting the parachute is highly unpredictable and dependent on parameters such as altitude, airspeed and angle of attack, as well as factors which cannot be quantified, such as the parachute folding arrangement. These initial conditions make simulating the effect of the premature ejection an impossible task. As such, the activation of this manual abort system must be discussed in depth with EuRoC officials before it can be approved for use on launch day. While the GSO has the capability to do so, ultimate authority to terminate the flight rests with EuRoC officials, and as such the Chain of Command for requesting or instructing the abort option MUST be clarified in the days leading up to the flight. If this is not clarified, or if for any reason the EuRoC officials demand it, these capabilities will be revoked at the software level from Sirius-GS, the Ground Station operating system.

The ground station features a touch-screen and mouse/keyboard input for interaction with the graphical user interface. Below the main touchscreen, there are two physical buttons. If, when the system is armed and a take-off has been detected, an endeavour Team Member (visually or otherwise) deems the use of the

system necessary, they will loudly exclaim "AUTHORISATION TO ABORT". If an authorised EuRoC official approves the request , the GSO presses both buttons simultaneously for 3 seconds. At this instant, due to the unpredictable consequences of the abort, the Range Safety Officer (RSO) may announce "RED FLAG" status and the public must retreat to a secure location. Upon the pressing of the buttons an encoded abort message will be broadcast on the frequency assigned by EuRoC officials. The SRAD flight computer will process the instruction and proceed to actuate both SRAD and COTS drogue ejection systems, followed by the COTS main release systems.

2.7 Special Subsystems

2.7.1 SRAD Avionics

A high-level view of the on-board avionics of Darwin III are given in Figure 2.32. There are 4 main systems. Figure 2.32 shows an overview of these systems and their integration. Their interactions are described below. All electrical schematics are presented in Appendix I.

1. Centralised Power Distribution
2. Main SRAD Avionics
3. COTS Avionics
4. Payload Avionics

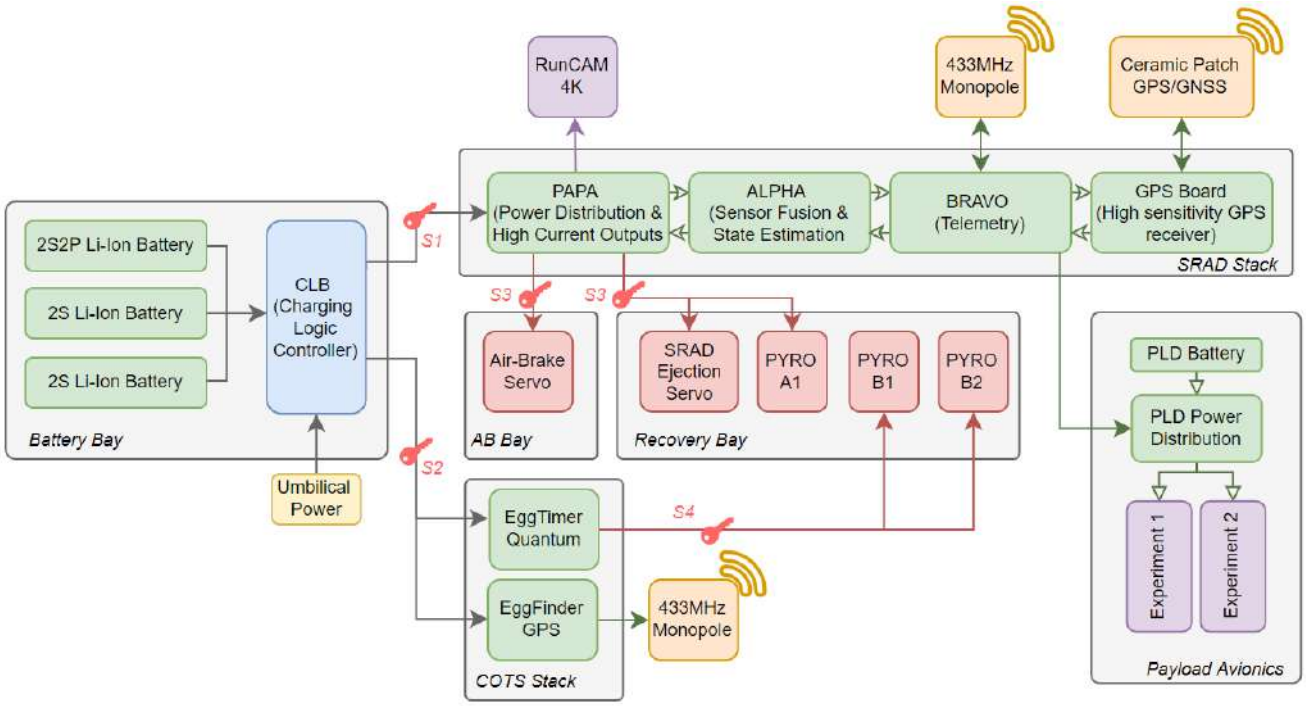

Figure 2.32: Darwin III Avionics Systems

Power Flow

At the launch pad, power is provided by a 60W (12V, 5A) DC power supply connected to a EuRoC provided generator and enters the Charging Logic Board (CLB). Three battery packs are also connected to the CLB which features a FET network that enables Alpha (SRAD flight computer master node) to switch the power source for the entire Avionics Bay from EXTERNAL to INTERNAL. Power is routed via independent harnesses to the Camera, SRAD Stack and COTS Stack. The payload cannot receive External Power due to its elevated position in the air-frame so to conserve power, it features a FET network on its Power Distribution Board which, which will keep the payload dormant until signalled from SRAD avionics stack (see Section 2.5.5). The aim of these systems is to prevent the usage of batteries on the pad. This approach was found to

be simpler, less intrusive in terms of EMI and safer to implement than charging circuits. Since Darwin III competes in the S9c category, its launch window is more likely to slip, and having the confidence to know that the vehicle does not require to be disassembled to replace depleted batteries simplifies launch-day operations.

The batteries are SRAD fabricated Li-Ion packs based on tbe LG MJ1 18650 cell, which offers a capacity of 3500mAh with nominal voltage of 3.7V. A 2S2P pack (7Ah, 7.4V nominal) powers the SRAD stack, while two 2S packs (3.5Ah, 7.4V nominal) packs power the COTS flight computers (EggFinder and Quantum Flight Computers from EggTimer Rocketry Inc.) and the RunCam Split 4K compact camera respectively. As mandated by the EuRoC DT&EG, they feature cell-balancing circuits and are under- and over- voltage protected through dedicated Battery Management Systems (BMS), and reverse polarity and reverse current protected through ideal diodes.

Safety Switches

Among the most significant lessons learnt from EuRoC '21 mission, is to include a greater number of clearly lablled, accessible hardware switches. The switches selected from DIII are Schurter 0033.4601, which actuate with a 90 degree twist of a screwdriver, meaning they can be accessed through small, 5mm perforations in the avionics bay tube section. The perforations double as pressure equalisation ports to ensure the flight computer barometers obtain accurate pressure readings. The switches enable systems to be enabled and armed sequentially while maintaining personnel safety as the highest priority. In Figure 2.32, the 4 safety interlock switches are visible. S1 and S2 enable power to the SRAD Stack and COTS stack respectively, while S3 and S4 disconnect the Recovery Bay high current outputs of SRAD stack and COTS stack respectively. This configuration keeps the COTS and SRAD systems completely parallel and independent, meaning a failure via vibration or excessive load of any one switch will not cause mission failure.

The SRAD Stack

The SRAD Stack is composed of three main boards (Papa, Alpha, Bravo) and one satellite board (GPS Board). Papa is fed power from the Power Routing Board (either 12V from the umbilical or 8.4V when power is internal) and it steps it down to 6V (to actuate the Air-Brake and Recovery servo-motors) and 5V (for powering Alpha and Bravo). The power conversions are carried out by buck converter units based on the MP2307DN-LF IC commercialised Monolithic Power Systems. Special care was given to the hardware layout and routing of the critical traces on the PCB to minimise voltage ripple and electro-magnetic interference (EMI). Laboratory tests were conducted with the bucks loaded to 2A, producing a voltage ripple below 50mV (peak to peak). For additional protection, the Bucks are shielded via a 25x30mm tin insulator cover. Papa also features numerous high-current outputs to other peripherals - in total these are:

- 3x Servo Outputs (6V, 3A max each, 3A max total)
- 2x Pyro Outputs (8.4V, 800mA continuous, 3A 10ms peak)
- 1x Digital Out (5V, 800mA continuous, used to switch power on for camera)

Alpha is stacked above Papa and receives regulated 5V. The vertical interconnect enables control signals from Alpha to control the gates of the high power output MosFETs on Papa. Alpha is a comparatively less complex board, mostly focused on safety- and flight-critical computation. Twin redundant barometers (MS5611 modules by TE MEAS, Switzerland) and accelerometers (LIS331HH by STMicroelectronics, Switzerland) provide inertial, temperature and absolute pressure readings which are fed into a Kalman Filter running on a Teensy 4.1 development board. Specifications for the sensors are provided in Table 2.10 and 2.11. Teensy 4.1 uses sensor inputs to estimate the current state of the vehicle (including heading, velocity and altitude). This data is used to identify transitions between the stages of the mission as defined in Section A.1.

Bravo, located atop of Alpha, handles all RF and telemetry tasks. Alpha and Bravo are connected via a UART link. Upon receiving GPS coordinates from the GPS board, Bravo packages it up with vehicle status received from Alpha into a structured EWDL packet (Endeavour Wireless Direct Link, see Section 2.7.2). The packet is transmitted to ground via a 433MHz link transmitting at 20 dB (100mW). Frequency and power were selected based on market availability and frequency spectrum regulations to allow for rapid, legal testing.

Table 2.10: LIS331HH Specifications.

Parameter	Specification
Axes	3 Axes, X,Y¡,Z
Range	Adjustable, Set to 24g
Resolution	16bit
Interface	SPI, I2C

Table 2.11: MS5611 Specifications.

Parameter	Specification
Range	10mbar - 1200mbar
Range Equivalent	30km to -1.5km ALS
Resolution	24bit
Resolution Equivalent	0.1m
Interface	SPI, I2C

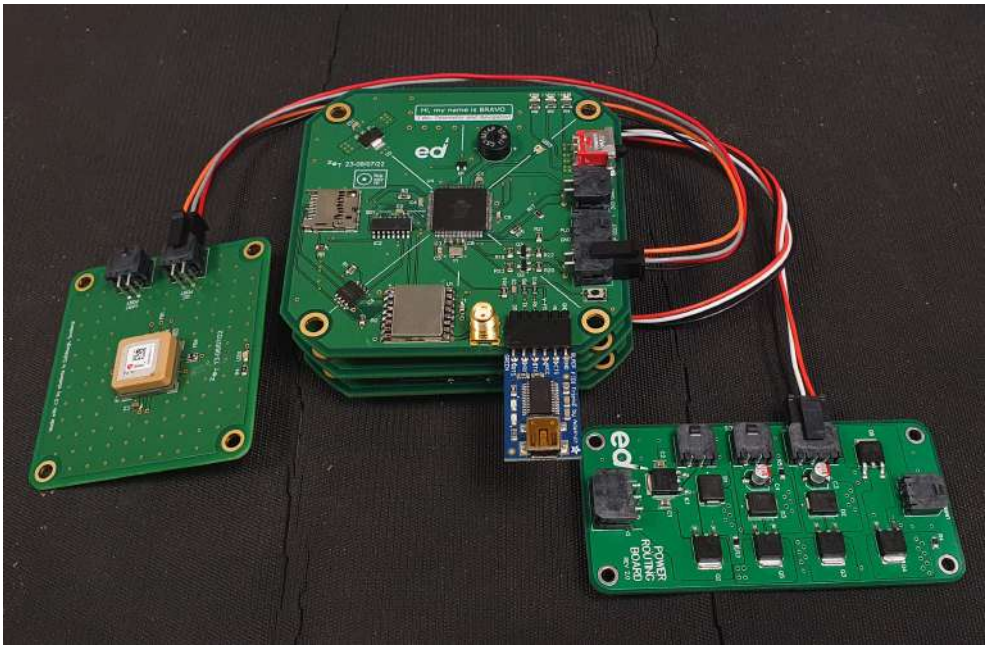

Figure 2.33: Full set of SRAD avionics aboard DIII

The set of fully populated SRAD boards is shown in Figure 2.33

2.7.2 Ground Station and the Endeavour Wireless Direct Link



Endeavour Wireless Direct Link (eWDL) is a reliable, addressed, half-duplex radio messaging system developed for Darwin III and future endeavour Launch Vehicles. eWDL is implemented on both the Ground Station and on Bravo, the telemetry computer onboard Darwin III. eWDL ensures reliability by enforcing a two-way handshake protocol (also known as "pairing"). This entails the rocket broadcasting a pairing signature (the magic value `ED 00 ED 00 4C 68 30 17`) along with a randomly generated integer, known as the rocket's RDID (reliable datagram ID). Upon receipt, a candidate Ground Station responds with an acknowledgement consisting of the rocket's RDID and its own RDID, another randomly generated integer.

At this point, both ground station and rocket have knowledge of each other's RDIDs and addressed (non-broadcast) communication may commence. To acknowledge this, the rocket sends a "syn-ack" (synchronise

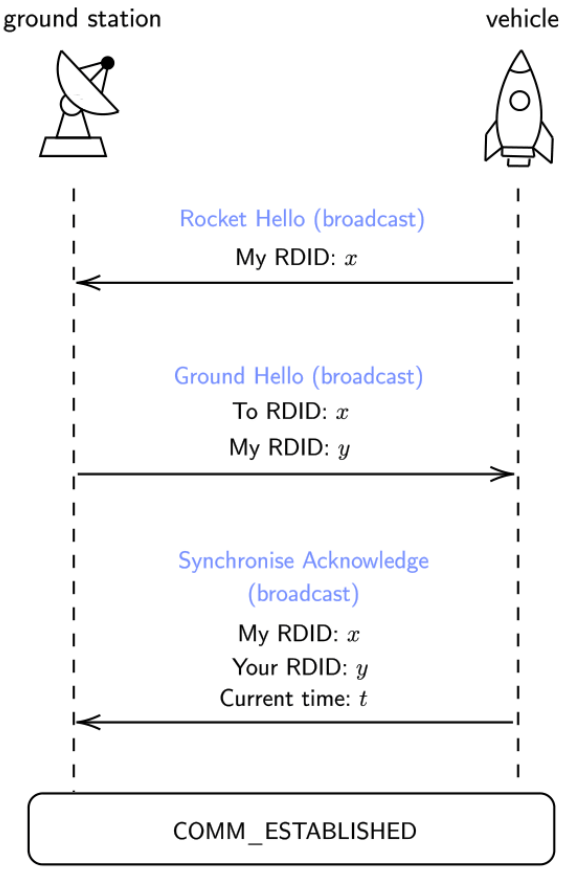

Figure 2.34: Simplified Model for a transaction on eWDL.

acknowledgement) packet which marks the end of the handshake process.

To prevent frame collision, a protocol similar to slotted ALOHA is implemented. The Ground Station is constantly listening as a default and may only transmit when it receives a special Transmit Window (TWND) frame from the rocket (where the rocket would already be listening for a response). A simplified diagram showing the protocol is shown in Figure 2.34.

Multiple redundancy mechanisms are in place, such as RSSI monitoring, automatic enforced message acknowledgements (and retries for no-acknowledgement), and automatic reconnection when it is deemed the connection is no longer alive.

The Ground Station is a Raspberry Pi 4B single-board computer with 3 GB on-board memory. It is a Raspbian 64-bit machine based on the Linux kernel.

3 — Mission Concept of Operations Overview

This section will focus purely on launch-day CONOPs. The mission phases will be delineated starting from Final Assembly and terminating with its recovery. Transitions between stages will be similarly defined. These are informed by Open Rocket simulations, as this is the trajectory simulation tool preferred by EuRoC. A comparison between the results produced by RASAero II (generally considered more accurate for supersonic flight) and OpenRocket can be seen in Figure 3.1. Simulations are conducted with a 85 degree, 12m launch rail and 2m/s of wind perpendicular to the rail inclination plane.

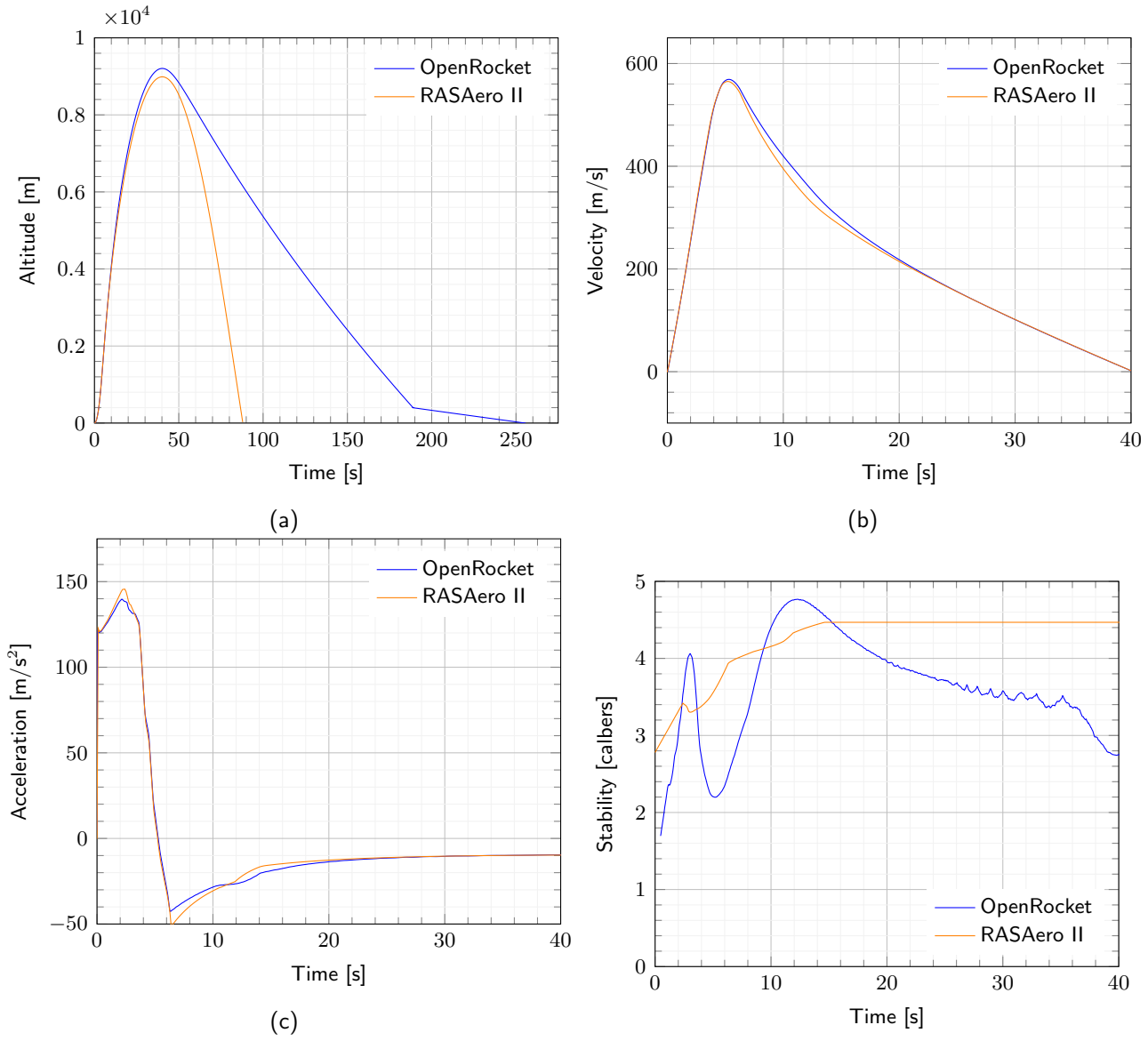

Figure 3.1: OpenRocket and RASAero II: (a) altitude, (b) velocity, (c) acceleration and (d) stability over duration of flight. RASAero II lacks recovery system, hence the discrepancy following apogee.

The key trajectory milestones as calculated by both simulation programs are summarised in Table 3.1, alongside time elapsed since ignition. The main flight events, as predicted by the OpenRocket Simulation, are collected in Table 3.2, together with the flight phases that are initiated and terminated by their detection.

Table 3.1: Main trajectory data-points for a nominal Darwin III mission, including time elapsed from ignition.

Parameter [unit]	OpenRocket	RASAeroII
Apogee [m]	9205.6	8979.7
Time to Apogee [s]	40.2	42.6
Time to Landing [s]	256	n/a
Stability (Off Rail) [cals]	1.75 (0.5s)	2.9 (0.5s)
Maximum Acceleration [ms^{-2}]	140 (2.1s)	145.6 (2.4s)
Maximum Velocity [ms^{-1}]	569.1 (5.3s)	564.9 (5.4s)

Table 3.2: Main flight events for a nominal Darwin III mission (leftmost and rightmost column) together with the main flight phases they delimitate.

Event	Time Elapsed	Marks starts of	Phase ends if
Ignition	t+0.00	Boosting Phase	Motor Burn-out
Motor Burn-out	t+ 6.34	Coasting Phase	Apogee Detected
Drogue Ejection	t+40.21	Drogue Descent	450m Altitude Detected
Main Release	t+188.36	Main Descent	Touchdown Detected
Enter Beacon Mode	t+255.76	Beacon Phase	Located by recovery teams
Recovered	n/a	Packing phase	PFR

A more granular view of the logic governing the transition between states, especially the handling of anomalies, airbrake actuation and potential loop-backs is given in Figure 3.2. This FSM is organised into States (Sx), with Events [Ex] causing transitions from one to the next. The Eventsare classed as follows:

- Manual Events (MEx) are triggered by team members via physical or software interfaces such as hardware switches or commands sent over the air via the Ground Station.
- Anomalous Events (AEx) are triggered by the SRAD avionics if the behaviours of the LV deviates from the simulated one, detecting CATO's or jammed/shredded recovery systems.
- Nominal Events (Ex) are triggered by the detection of the nominal transitions between flight stages as described in Table 3.2, or by processes within the SRAD avionics (successful initiation of sensors).

Complete definitions of all Events and States is available in Appendix A Section A.1.

In order to better understand the influence of wind speed on the overall trajectory of the rocket, a simple sensitivity analysis was carried out in OpenRocket for a range of wind speeds, ranging from 0 to 9 m/s, the results of which are presented in Figure 3.3. From this it can be seen that, whilst not having a major impact on the predicted apogee, increasing wind speed does have significant effect on the rocket's drift during descent. Note, the results shown here are for an upwind launch, and therefore should the rocket be launched downwind the results would be reversed, and the rocket would drift further East of launch during its descent.

A diagram depicting the division of responsibility among subsystems, and the tasks carried out by each sub-team during flight is given in Figure 3.4. A detailed description of Recovery CONOPs is available in Section 2.4.2, while detailed task-by-task breakdowns of the launch-day operations, including both Assembly and Launch operations, is available in Section E.

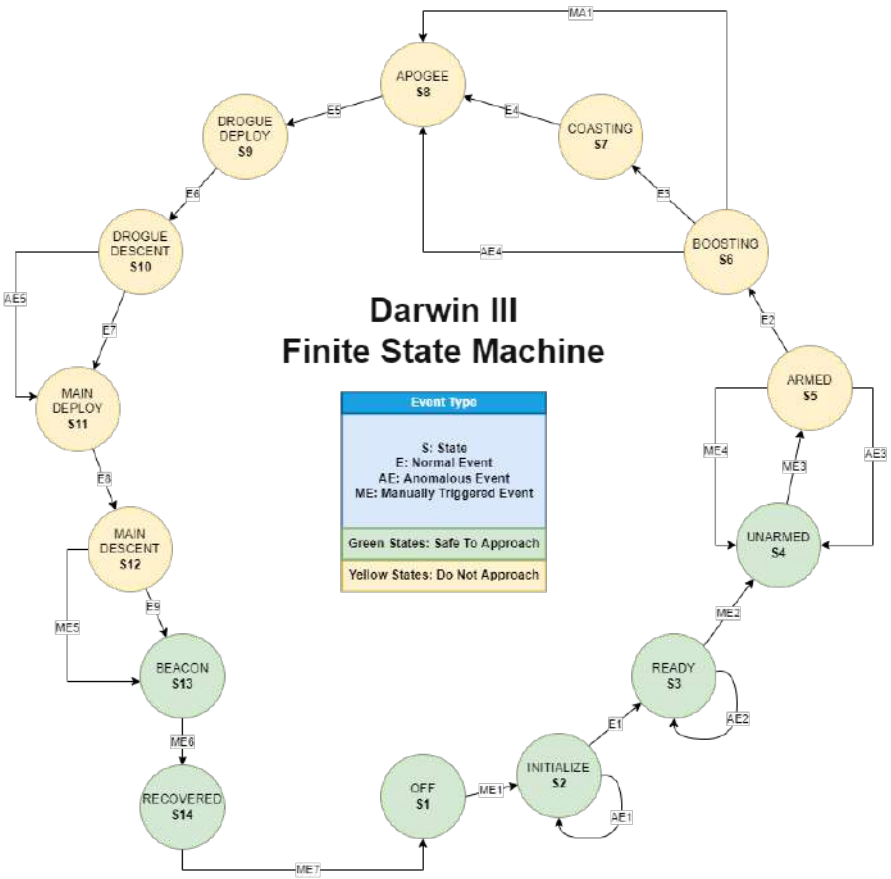

Figure 3.2: Finite State Machine used to organise every flight stage for nominal and off-nominal Darwin III missions.

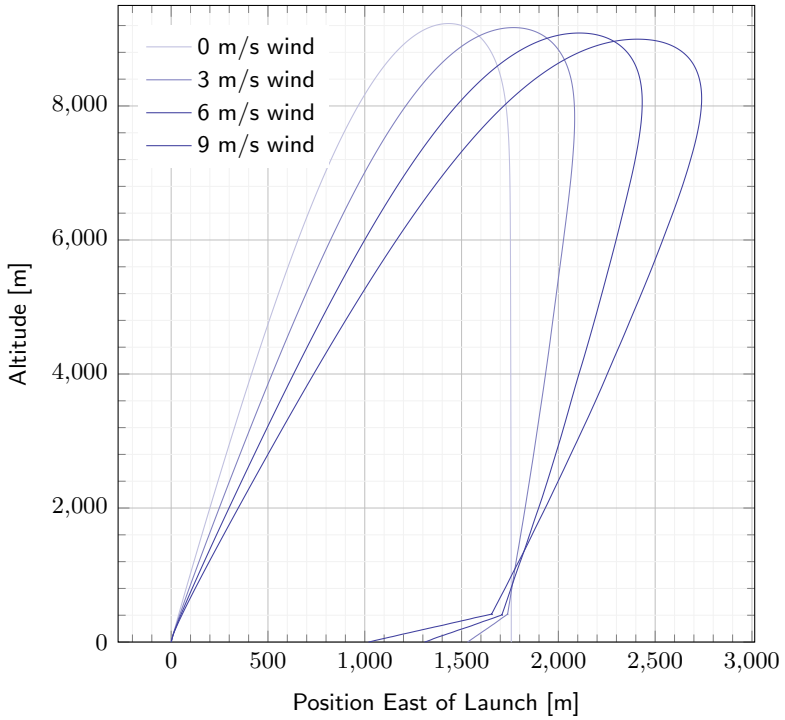

Figure 3.3: OpenRocket wind sensitivity analysis.

	T-3h	T-1.5h	T-1h	T-5min	T-2.5m	T=0	T+6.5s	X<t<40s	T+40s	T+40s	T+188s	T+255s	T+30m	T+60m
	Assembly	LRR	Final Prep and Pad Setup	Pad Armed	GO\ NO-GO	Ignition & Lift Off	Boost	Coast/ AB phase	Apogee	Drogue Deploy	Main Deploy	Touch down	Recovery Ops	Disassembly
Pass Test	**Complete Assembly Procedures**	**LRR Pass**	**Complete Pad Procedure**	**Ack from SRAD FC**	**All systems GO**	**Motor Ignition**	**Motor Burn ends**	**Zero Vertical Velocity**	**Descent begins**	**Nosecone Ejected**	**Main Chute released**	**Zero Vertical Velocity**	**Vehicle and/or debris collected**	**Vehicle disassembled / stored**
Avionics	Confirm Switches on off pos.	-	Switch on SRAD FC. When at the pad arm it + EggTimer	Runs pyro continuity check, acquired GPS	Initiates high-res data collection + camera	Detect lift-off	Record / transmit data	Actuate Airbrakes if necessary	Record/ transmit data/ **Eject NC**	Record/ transmit Apogee Altitude	Record/ transmit data/ **Release Main**	Begin transferring data from Flash to SD	All switches off	Recover, clone and store SD Cards
Payload	Confirm Switches on off pos.	-	Switch on Payload	-	Initiates data collection + camera	Record data	Record data	Record data	Record data	Record data	Record data	Record data	-	Recover, clone and store SD Cards
Recovery	Connect all linkages, fold chutes, NO BP	-	Insert BP & CO2, check lines	-	-	Members track rocket visually	-	-	-	Drogue chute released, 28m/s descent	Main chute released, 6m/s descent	Record last known location, landing site heading	Carefully approach vehicle, disarm, transport	Fold and Store
Structure	Secure main shoulder bolts	-	Torque bolts to prescribed amount	-	-	Members tracked rocket visually	-	-	-	Nosecone separation, shear pin breakage	Snatch force on recovery bulkhead	-	-	Neutralise energetics, disassemble and prepare vehicle for transport
Ground Station	IDLE	-	Health check of all sensors/ peripherals	Receives updates from SRAD FC	Triggers PLD, SRAD FC	Plot position, save location	-	-	Announce Apogee	Announce Chute Release	Announce Main Release	Communicate last known location	Deploy handheld recovery terminals	Pack and store ground station
Launch Pad Team	IDLE	-	Carry to pad, slide onto rail guide, insert igniter, set GSE	Standby at Launch Control	-	-	-	-	-	-	-	-	Clear GSE	Store GSE
Radio Team	Radio Checks, charge batteries	-	One member at pad, other at Launch control	-	-	-	-	-	-	-	-	-	-	Store Radios and Charge

Figure 3.4: Global CONOPs diagram

4 — Conclusions and Outlook

The design and manufacture of Darwin III has been a wide ranging technical project, with hundreds of pieces of hardware and thousands of line of code designed and implemented by dozens of undergraduate students. Each of these parts has been infused with the experiences of EuRoC '21, building on our efforts to present a much more robust launch vehicle by building on top of successful designs and manufacturing methods, while rethinking systems and processes that cracked under pressure.

Among the systems that have seen the greatest improvement we count:

- Redesigned Air-Brakes with smooth deployment and simple assembly on the field,
- SRAD Avionics with upgraded telemetry capabilities, a robust form factor with a compact and reliable cable harnesses,
- Completely SRAD deployment system for repeatable testing and increased reliability of the recovery system,
- A capable Ground Station with a rich GUI, instant online data archiving and globally accessible, live telemetry.
- The endeavour Wireless Direct Link (eWDL), a half-duplex, robust telemetry architecture to connect our Avionics and Ground Station.
- Two scientifically rigorous of Physics experiments housed within a fully independent 2U CubeSat.

Despite the technical achievements, endeavour remains a young team, and there were countless obstacles and lessons learnt. The main issues we faced this year were related to workshop space and access to funds. The team had to leave its workshop due to University regeneration works. While kitchen tables and backyards can yield good results for some assembly tasks, this also increases the complexity required to complete the more detail-oriented ones. Reduced access to high-performance simulation machines limited our access to CFD simulations, reducing our confidence in the Drag Coefficient values. As the University transitioned its procurement systems, the team lost access to a significant portion of our funds during a capital-intensive period of the year, when components must be purchased, competition fees paid and accommodation and transport secured. The team banded together, and thanks to the generosity of our Industrial Partners, and the flexibility of our members and of the University staff, Darwin III was successfully completed.

On the technical side, the DII program highlighted some improvements to our processes that could vastly streamline operations. The team should move to hold in-person meetings as the standard, with virtual meetings being the exception - this would foster a greater camaraderie, sense of responsibility and community, leading improved talent retention across the length of the program. Despite the team being small, thus not used to dealing with formalities and documentation, a more robust System's Engineering approach should be undertaken: careful definitions of interfaces, minimum viable deliverables and personal technical responsibilities would eliminate the operational inefficiencies that often slowed down or delayed testing campaigns. Among the technical improvements planned for next year, we aim to develop and refine customised, 6-DOF simulation suites, extending SRAD deployment system capability to include the Main Chute Ejection and creating a more modular and repairable Fin Retention system.

Through all the highs and lows, the 2021-2022 endeavour Team is proud to present Darwin III, and cannot wait to learn a whole new set of lessons at the 2022 European Rocketry Challenge.

Bibliography

[1] M. DINULOVIĆ, B. RAŠUO, and B. KRSTIĆ, "The analysis of laminate lay-up effect on the flutter speed of composite stabilizers," in *30th Congress of the International Council of the Aeronautical Sciences, ICAS*, 2016.

[2] D. B. Pengra, *Cosmic ray counting*, 2021. [Online]. Available: http://courses.washington.edu/phys433/muon_counting/counting_telescope.pdf.

[3] A. R. Vick, *An Investigation of the Drag Characteristics of Speed Brakes for Mach Numbers from 0.20 to 1.30*. National Advisory Committee for Aeronautics, 1958.

[4] S. N. Axani, *The physics behind the cosmicwatch desktop muon detectors*, 2019. DOI: 10.48550/ARXIV.1908.00146. [Online]. Available: https://arxiv.org/abs/1908.00146.

[5] J. Forshaw and G. Smith, *Dynamics and Relativity*, ser. Manchester Physics Series. Wiley, 2014, ISBN: 9781118933299. [Online]. Available: https://books.google.co.uk/books?id=5TaiAwAAQBAJ.

[6] L. Liu and P. Solis, *The speed and lifetime of cosmic ray muons*, Nov. 2007.

[7] M. Naagar and S. Chalia, "Comparative study of slosh suppression devices and techniques for liquid and hybrid rocket propellant tanks," vol. 5, p. 1693, May 2017.

[8] H. Yang and J. Peugeot, "Propellant sloshing parameter extraction from computational-fluid-dynamics analysis," *Journal of Spacecraft and Rockets*, vol. 51, pp. 908–916, May 2014. DOI: 10.2514/1.A32608.

A — System Data

Table A.1: Structural system data of Darwin II.

Parameter	Value	Units
Length	2,890	mm
Vehicle & payload mass with propellant	34,333	g
Propellant mass	10.93	kg
Payload mass	2.2	kg
Number of stages	1	-
Inner diameter	152	mm
Outer diameter	156	mm
Number of fins	4	-
Fin span	150	mm
Fin root length	210	mm
Fin tip length	120	mm
Target apogee	9000	m
Maximum velocity	572	m/s
Maximum acceleration	140	m/s^2
Flight duration	260	s
Motor burn time	6.4	s
Time from launch to apogee	40	s

Table A.2: Recovery system data of Darwin III.

Parameter	Value	Units
Coefficient of drag	1.6	-
Diameter	24	inch
Mass of CO_2 separation charge: SRAD	33	g
Mass of CO_2 separation charge: COTS	33	g
Mass of black powder used	0.24	g
Deployment altitude	9000	m
Descent rate	30	m/s
Chute coefficient of drag	2.2	-
Diameter	96	inch
Mass of CO_2 separation charge	0	g
Mass of black powder used	0.2	g
Chute deployment altitude	500	m
Chute descent rate	6	m/s

Table A.3: Telemetry system data of Darwin II.

Assembly	Parameter	Value	Units
SRAD Flight Computer	Power duration	10	hours
	Communication frequency	433	MHz
	Output power (max.)	100	mW
	Communication range (w/ Yagi RX)	20000	m
SRAD Ground Station	Power duration	Mains	n/a
	Transceiver sensitivity (max.)	-120	dBm
	Communication range (uni-directional)	20000	m
	Communication range (omni-directional)	3000	m

A.1 State and Event Definitions

Table A.4: Definition of Events

ID	Definition
ME1	Main SRAD Avionics switch turned ON
ME2	Ground Station signal received to set up components and run tests
ME3	Ground Station signal received to enter ARMED state
ME4	Ground Station signal received to return to UNARMED state
ME5	Ground Station signal received to enter the BEACON state
ME6	Ground Station signal received to enter the Recovered state
ME7	Main SRAD Avionics switch turned OFF
MA1	Ground Station signal has been received to enter the apogee state (Manual abort event)
AE1	Flight computer boot error
AE2	One or more software tests did not pass
AE3	No continuity to pyrotechnics
AE4	Too much time passed since entering Boosting state (Redundancy trigger)
AE5	Too much time passed since entering the Drogue Descent state (Redundancy trigger)
E1	Ground Station connection to ground station established
E2	Rocket launch has been detected (acceleration greater than threshold)
E3	Coasting has been detected (acceleration $\approx$ constant)
E4	Apogee has been detected
E5	Apogee reached
E6	Drogue chute has been deployed
E7	Altitude reaches lower than a set altitude threshold
E8	Main chute has been deployed
E9	Landing detected

A.1.1 Actions during each state

Initial activities are activities that will happen ONCE, just when the specified state is entered.

Loop activities are activities that will happen in a LOOP, while the flight computer is in the specified state.

- ❏ S1: OFF
  - ❏ Flight computer is off, and is not being powered. Nothing happens
- ❏ S2: INITIALISE
  - ❏ Initial activities
    - ❏ Check battery voltage

- ❏ RETURN AE1 if battery voltage is too low
- ❏ Initialize all peripheral interfaces (e.g. UART communication, sensors, etc)
- ❏ Loop activities
  - ❏ Attempt to confirm successful radio signal exchange with ground station
    - ❏ RETURN E1 if communication with the ground station is working

❏ S3: READY
- ❏ Initial activities
  - ❏ Nothing
- ❏ Loop activities
  - ❏ Check if the ground station sends a radio signal to start tests
    - ❏ Once the signal is received from the ground station, run all tests except the pyrotechnics test
    - ❏ Return AE2 if anything goes wrong during testing of peripherals
    - ❏ Return ME2 if all tests pass successfully (except pyrotechnics test)

❏ S4: UNARMED
- ❏ Initial activities
  - ❏ Nothing
- ❏ Loop activities
  - ❏ Check if the ground station sends a radio signal to arm the rocket
    - ❏ If the signal is received from the ground station
    - ❏ Return ME3

❏ S5: ARMED
- ❏ Initial activities
  - ❏ Run pyrotechnics test
    - ❏ Return AE3 if PyroTest fails
  - ❏ Start the runcam
- ❏ Loop activities
  - ❏ Take sensor measurements and check if acceleration reaches higher than a set acceleration threshold
    - ❏ If acceleration greater than acceleration threshold
    - ❏ Return E2
  - ❏ Check if the ground station sends a radio signal to disarm the rocket
    - ❏ If the signal is received from the ground station
    - ❏ Return ME4

❏ S6: BOOSTING
- ❏ Initial activities
  - ❏ Set a variable in flight state to log the takeoff time
  - ❏ Broadcast takeoff radio signal to ground station
- ❏ Loop activities
  - ❏ Take sensor measurements and check if acceleration is approximately constant
    - ❏ If acceleration is approximately constant
    - ❏ Return E3
  - ❏ Check if time in boosting state greater than threshold time
    - ❏ If time in boosting state greater than threshold time
    - ❏ Return AE4
  - ❏ Check for ground station radio signals to manually abort the flight

- ❏ Abort signal is received from the ground station
- ❏ Return MA1

❏ S7: COASTING
- ❏ Initial activities
  - ❏ Broadcast coasting signal to ground station
- ❏ Loop activities
  - ❏ Take sensor measurements and check if AT LEAST 2 of the following 3 conditions are TRUE. If AT LEAST 2 of these 3 conditions are TRUE, return E4:
    - ❏ Downwards velocity is increasing
    - ❏ Altitude is dropping
    - ❏ Pressure is increasing

❏ S8: APOGEE
- ❏ Initial activities
  - ❏ Log apogee time
  - ❏ Broadcast apogee signal to ground station
  - ❏ Return E5 (no conditions, just return it)
- ❏ Loop activities
  - ❏ Nothing

❏ S9: DROGUE DEPLOY
- ❏ Initial activities
  - ❏ Deploy the drogue parachute
  - ❏ Broadcast drogue deploy signal to ground station
  - ❏ Return E6 (no conditions, just return it)
- ❏ Loop activities
  - ❏ Nothing

❏ S10: DROGUE DESCENT
- ❏ Initial activities
  - ❏ Broadcast drogue descent signal to ground station
- ❏ Loop activities
  - ❏ Take sensor measurements and check if altitude less than threshold altitude
    - ❏ If altitude less than threshold altitude
    - ❏ Return E7
  - ❏ Check if time in drogue descent state greater than threshold time
    - ❏ If time in drogue descent state greater than threshold time
    - ❏ Return AE5

❏ S11: MAIN DEPLOY
- ❏ Initial activities
  - ❏ Deploy the main parachute
  - ❏ Broadcast main deploy signal to ground station
  - ❏ Return E8 (no conditions, just return it)
- ❏ Loop activities
  - ❏ Nothing

❏ S12: MAIN DESCENT
- ❏ Initial activities
  - ❏ Broadcast main descent signal to ground station
  - ❏ Dump all sensor readings saved in memory to the SD card

- ❏ Loop activities
  - ❏ Take sensor measurements and check if they all stop changing more than a certain small percentage (the values would stop changing when the rocket hits the ground). Check if the change is less than a certain threshold percentage over a 3 second span for altitude, and acceleration
    - ❏ Return E9
  - ❏ Check for ground station radio signals to manually enter the Beacon state
    - ❏ If signal is received from the ground station to enter Beacon state
    - ❏ Return ME5
  - ❏ Read GPS coordinate data from Bravo
  - ❏ Broadcast GPS coordinates with radio signals every x seconds (make time configurable)
- ❏ S13: BEACON
  - ❏ Initial activities
    - ❏ Log the time of ground impact
    - ❏ Broadcast beacon signal to ground station
    - ❏ Dump all sensor readings saved in the memory to the SD card (again)
  - ❏ Loop activities¨
    - ❏ Read GPS coordinate data from Bravo
    - ❏ Broadcast GPS coordinates with radio signals every 10 seconds
    - ❏ Check for ground station radio signals to manually enter the Recovered state
      - ❏ If signal is received from the ground station to enter the Recovered state
      - ❏ Return ME6
- ❏ S14: RECOVERED
  - ❏ Initial activities
    - ❏ Broadcast recovered signal to ground station
  - ❏ Loop activities

B — Detailed Test Reports

B.1 Preliminary Ejection Mechanism Viability

Responsible Engineers:	Blessy Ananth, Thomas Stott, Alex Stevenson
Date of Test:	14/07/22
Location of test:	Private garden
Equipment used:	Darwin II Upper Body, SRAD Ejection Mechanism, 33g CO2 Canister
Test Description:	A breadboard analogue of the SRAD flight computer circuitry, inclusive of voltage conversion and micro-controller, shall actuate an SPT high torque servo-motor. The aim is to validate the SRAD mechanism, specifically choose the geometry of the Piercing Head (D3-406A vs D3-406B) and the choice of servo-motor. This preliminary test was conducted using the Darwin II upper body, as the Darwin III upper body was still in the manufacturing stage at the time. The mass was adjusted accordingly by adding sufficient ballast to compensate for the heavier 2U CubeSat present on Darwin III.
Test Result:	Test Successful: (i) Nosecone with analogue mass ejected, (ii) D3-4-6A piercing element geometry selected due to greater piercing effectiveness, (iii) servo-motor choice validated



Figure B.1: Results from SRAD ejection system tests using DII upper body

B.2 Recovery Test - SRAD Ejection powered by SRAD Flight Computer

Responsible Engineers:	Alex Stevenson, Thomas Stott, Ann Lee, Joseph Azrak
Date of Test:	10/09/22
Location of test:	Private garden
Equipment used:	Darwin III Upper Body, SRAD Electronics, SRAD Ejection Mechanism, 33g CO2 Canister
Test Description:	The SRAD system was tested using the cutter and servo that were validated using the earlier DII test. The SRAD avionics and ground station were used to activate the recovery system.
Test Result:	The SRAD system performed similarly to the COTS RAPTOR test. The nosecone was ejected far from the recovery bay and dragged the drogue parachute out and was prevented from going further by the Tender Descenders set up below the recovery separator plate.



Figure B.2: Results from SRAD ejection system tests using $\mathrm{DII}_{upperbody}$

B.3 Recovery Test - COTS Ejection system with external power supply

Responsible Engineers:	Alex Stevenson, Thomas Stott, Ann Lee, Joseph Azrak
Date of Test:	10/09/22
Location of test:	Private garden
Equipment used:	Darwin III Upper Body, Raptor Ejection Mechanism, 33g CO2 Canister
Test Description:	The COTS RAPTOR system was tested using a 33g CO_2 cartridge to test the back up ejection system for the rocket. An e-match was set off using an external power supply, which activated the RAPTOR ejection kit.
Test Result:	The RAPTOR behaved as expected, ejecting the nosecone clear from the recovery bay and deploying the drogue parachute. It was stopped from going further by the Tender Descenders below the separator plate.



Figure B.3: Results from COTS ejection system tests using DIII upper body

B.4 Recovery Test - COTS Ejection powered by SRAD Flight Computer

Responsible Engineers:	Alex Stevenson, Ann Lee, Joseph Azrak
Date of Test:	11/09/2022
Location of test:	Private garden
Equipment used:	Darwin III Upper Body, COTS Ejection Mechanism, SRAD Electronics, 24g CO2 Canister
Test Description:	This test will perform a COTS ejection powered by the SRAD flight computers. It is expected to perform the same as the COTS ejection system using external power supply as it uses all the same ejection equipment but a different method of setting off an e-match.
Test Result:	The COTS ejection system worked the same as the COTS ejection using the power supply to set off the e-match. Although a smaller cartridge was used for the test, it performed nominally.



Figure B.4: Results from COTS ejection system tests using DIII upper body, activated by the SRAD avionics

B.5 Recovery Test - COTS Ejection powered by COTS Flight Computer

Responsible Engineers:	Alex Stevenson, Thomas Stott, Ann Lee, Joseph Azrak
Date of Test:	TBD
Location of test:	Private garden
Equipment used:	Darwin III Upper Body, COTS Ejection Mechanism, COTS Electronics, 33g CO2 Canister
Test Description:	This test will perform a COTS ejection powered by the COTS flight computers. It is expected to perform the same as the COTS ejection system using external power supply as it uses all the same ejection equipment but a different method of setting off an e-match.
Test Result:	Due to delays in shipping of the EggTimer Quantum Flight Computer, this test will be conducted after the submission deadline for this Technical Report. Results will be promptly communicated to EuRoC officials and available for viewing online and during jury visits at the event.



Thomas Stott
Team Lead



Ann Lee
Operations Lead



Alex Stevenson
Recovery Lead

B.6 Recovery Test - COTS Main Release powered by COTS Flight Computer

Responsible Engineers:	Alex Stevenson, Thomas Stott, Ann Lee, Joseph Azrak
Date of Test:	TBD
Location of test:	Private garden
Equipment used:	COTS Main release Mechanism, COTS Electronics, Tender Descender
Test Description:	This test will perform a COTS main release powered by the COTS flight computers. An analogous weight will be hung from the Tender Descender parallel set up and the Tender Descenders will be activated, dropping the weight.
Test Result:	Due to delays in shipping of the EggTimer Quantum Flight Computer, this test will be conducted after the submission deadline for this Technical Report. Results will be promptly communicated to EuRoC officials and available for viewing online and during jury visits at the event.



Thomas Stott
Team Lead



Ann Lee
Operations Lead



Alex Stevenson
Recovery Lead

B.7 Recovery Test - COTS main release powered by SRAD Flight Computer

Responsible Engineers:	Alex Stevenson, Ann Lee, Joseph Azrak
Date of Test:	11/09/2022
Location of test:	Private garden
Equipment used:	COTS main release Mechanism, SRAD Electronics, Tender Descender
Test Description:	This test will perform a COTS main release powered by the SRAD flight computers. An analogous weight will be hung from the Tender Descender parallel set up and the Tender Descenders will be activated, dropping the weight.
Test Result:	The Tender Descenders acted as expected, with the activation of the Tender Descender releasing the quicklinks, allowing the quicklink to pass through the recovery ring, dropping the weight of 24kg. It shows that the parallel system works as expected and the Tender Descenders will work while under load.



Figure B.5: Results from COTS main release system test using analogous weight.

Thomas Stott
Team Lead

Ann Lee
Operations Lead

Alex Stevenson
Recovery Lead

B.8 Payload Muon Detector Test

Responsible Engineers:	Jo Shepton
Date of Test:	16/08/2022
Location of test:	Fleeming Jenkin Electrical Teaching Laboratory
Equipment used:	Arduino 1.8.13 Software
Test Description:	Power was supplied to both Arduino Nanos through the serial port of the left Arduino Nano. The test was left running for 30 minutes. The serial monitor output was observed as well as the data saved on both SD cards to evaluated the number of muon detected met the expected muon count at sea level.
Test Result:	Muon Count of detector A = 0.226 muons per second. Muon Count of detector B = 0.231 muons per second. These are both close to the expected count of 0.224 muons per second at sea level with special relativity taken into account. This proves the detector is functioning correctly though further tests will be performed to verify this.

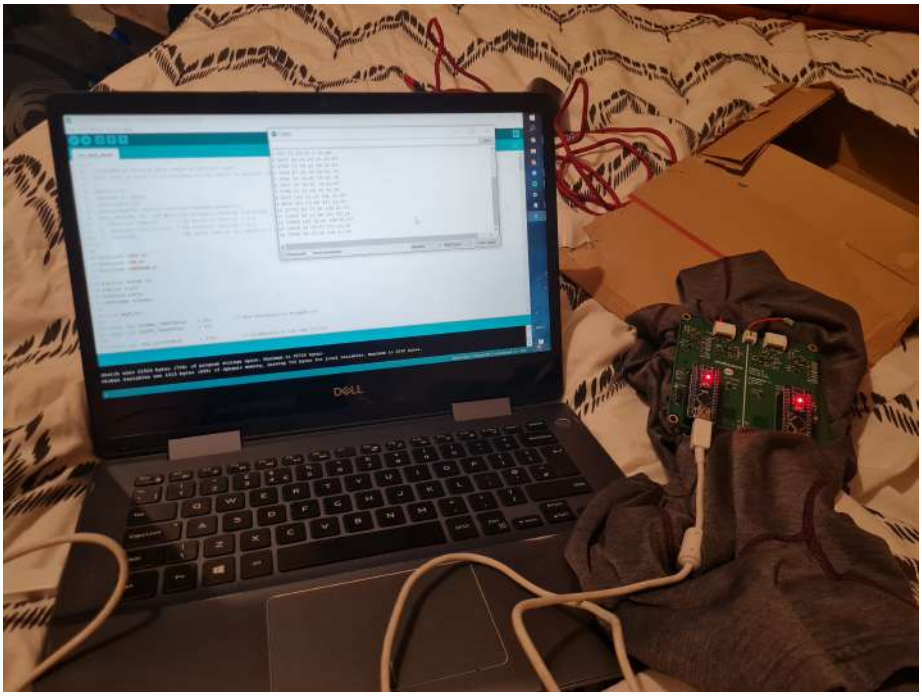

Figure B.6: Muon Detector Testing

B.9 Payload Muon Detector Altitude Test

Responsible Engineers:	Jo Shepton
Date of Test:	18/07/2022
Location of test:	Ben Macdui, Cairngorm
Equipment used:	CosmicWatch Muon Detector, Laptop
Test Description:	The muon detector was taken up Ben Macdui (Scotland's second highest mountain) in a backpack. At the summit (1318m), a laptop was connected to one of the muon detectors for 30 minutes to provide power and muon rate readings were taken
Test Result:	The muon rate at that altitude was found to be 0.713 muons per second. Based on this value, if special relativity is taken into account, the expected rate at 42m (altitude of usual testing laboratory), there should be 81% of the muons detected at 1318m (i.e a rate of 0.508 muons per second). However, at an altitude of 42m and a similar temperature (approximately $16°C$, tests show that the muon detector detects 36% of muons found at a higher altitude (rate of 0.26 muons per second). While this is closer to the literature value for muon rate at sea level, it indicates a lack of efficiency in the muon detector. This is most likely caused by light coming into the scintillators, along with imperfect cable connections which have now been fixed. This test, despite confirming that the muon detector is not perfect, is considered successful as the muon detectors detected a change in muon rate at a higher altitude.

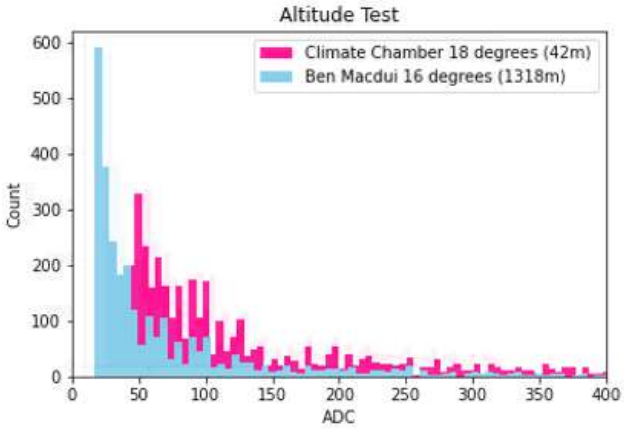

(a) Muon detector altitude test results indicating more muons present on Ben Macdui



(b) Results being collected at the summit of Ben Macdui

B.10 Payload Muon Detector Climate Chamber Tests

Responsible Engineers:	Jo Shepton
Date of Test:	26/07/2022
Location of test:	James Clerk Maxwell Building (School of Physics and Astronomy)
Equipment used:	CosmicWatch Muon Detector, laptop, climate chamber
Test Description:	The muon detector was placed in a the climate chamber and the temperature was varied form $-10°C$ to $+30°C$ and the muon rate was recorded
Test Result:	As expected, the muon rate increased at higher temperatures, however not by as much as literature values would suggest it should have. SiPM noise is often very thermally governed, and so the increase in temperature would have created more dark currents, i.e where electrons in the SiPM chip are displaced due to the energy from heat, hence registering a false signal to the Arduino. This test data will be used as a template to help correlate the muon rate found during flight to the temperature

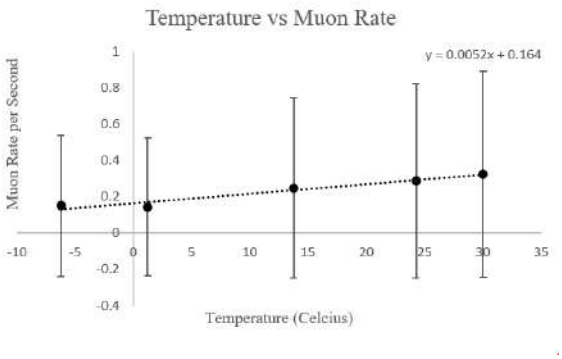

(a) Muon Detector rate vs temperature

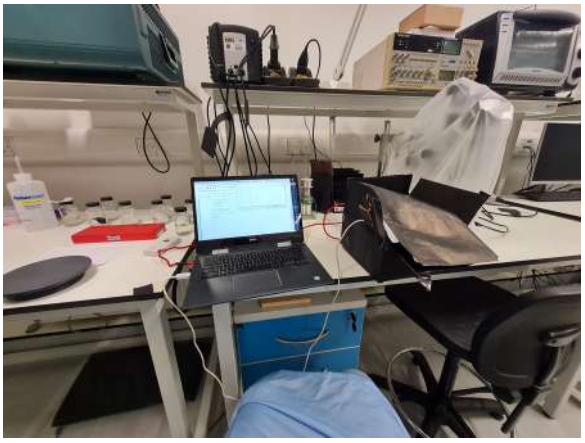

(b) Environment where climate chamber tests were performed

B.11 Payload Muon Detector Hodoscope Test

Responsible Engineers:	Jo Shepton
Date of Test:	06/08/2022
Location of test:	James Clerk Maxwell Building (School of Physics and Astronomy)
Equipment used:	CosmicWatch Muon Detector, laptop, two PMT (photomultiplier tube) muon detectors, high voltage power supply, external discriminator and LHC Buser software
Test Description:	The CosmicWatch muon detector was placed between two scintillator bats attached to PMTs. The muon detector was then connected to an oscilloscope, which was set to trigger only when a signal was registered in both of the PMT muon detectors. This reduces the noise associated with the SiPM chips. The signal was then discriminated externally (i.e not on the CosmicWatch) and this was in turn given to the LHC Buser software, which would save the signal display as a binary file. Each trigger event takes up 1024 bits, and the python code written for this task finds the maximum coordinate to determine the peak voltage associated with each signal. This is then calculated as an ADC in order to find the correct threshold. The baseline of noise was subtracted from each event, then the average ADC was found
Test Result:	The average ADC with the subtracted noise is around 50ADC, which is in agreement with CosmicWatch's suggestion for a threshold value. The threshold was then set for all ongoing tests, which means the Arduino only saves signals with an ADC larger than 50 to the SD card. The rest is deemed to be noise.



Figure B.9: Oscilloscope showing the CosmicWatch detector signal (blue) being triggered by the two PMT detectors' signal (yellow). The blue signal shows a characteristic curve indicating it is a muon, and the size of the signal shows it is not background noise

B.12 Payload Power Board Electrical Load Test

Responsible Engineers:	Virginia Cangelosi, Phil Henrich
Date of Test:	01/09/2022
Location of test:	Fleeming Jenkin Electrical Teaching Laboratory
Equipment used:	Keysight EDU 36311A Triple Output Programmable DC Pwr Supply, Arcol HS50 12Ohm Power Resistor 50W
Test Description:	8.5V was supplied to the Power PCB feeding 5V to two 12Ohm power resistors in parallel. The power board was left running for half an hour to monitor the ability of the board to supply high current over long periods of time.
Test Result:	All components remained at a stable temperature and a stable 5V was supplied to the resistor. This confirms the ability of the power board to power high loads and ensures it operates safely.

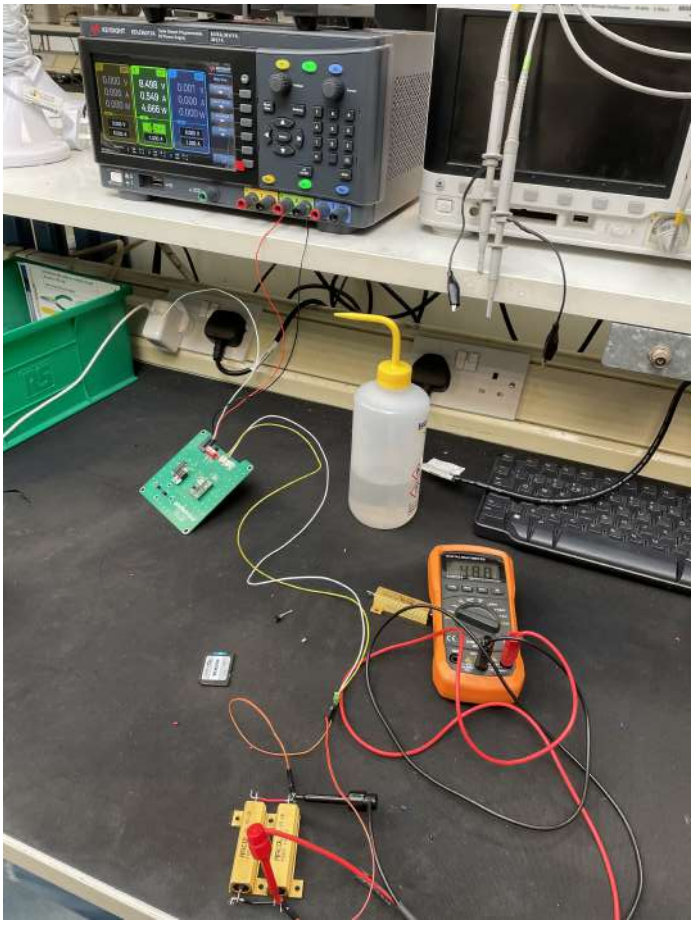

Figure B.10: Power Load Testing

B.13 Payload Power Draw Test

Responsible Engineers:	Virginia Cangelosi, Phil Henrich
Date of Test:	02/09/2022
Location of test:	Fleeming Jenkin Electrical Teaching Laboratory
Equipment used:	Keysight EDU 36311A Triple Output Programmable DC Pwr Supply
Test Description:	7.6V was supplied to the Power PCB feeding 5V to both the Arduino and Slosh PCBs. The peak power consumption whilst the camera was recording and illumination LEDs was measured.
Test Result:	Payload Peak Power draw: 2.92W. This is low enough to remain powered by the chosen LiPo batteries for 6 hours. Both experiments ran correctly obtaining sensible muon counts of 0.31 and 0.29 muons per second and clear camera footage.

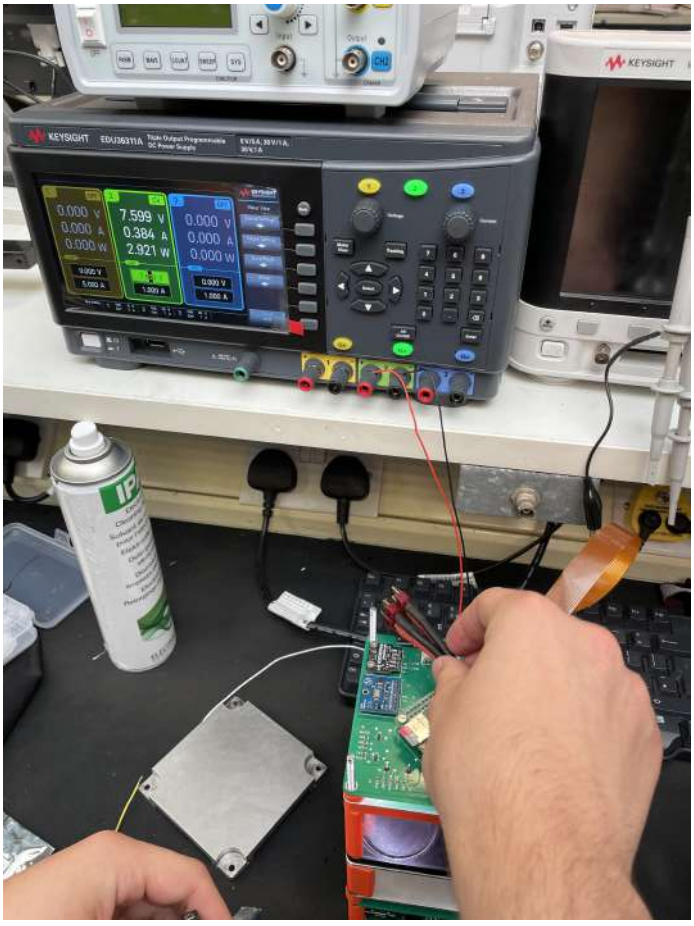

Figure B.11: Power Consumption Testing

B.14 Payload Power Board Electrical Switch Test

Responsible Engineers:	Virginia Cangelosi, Phil Henrich
Date of Test:	03/09/2022
Location of test:	Fleeming Jenkin Electrical Teaching Laboratory
Equipment used:	Keysight EDU 36311A Triple Output Programmable DC Pwr Supply
Test Description:	8.4V was supplied to the full electrical subsystem (the Power PCB supplying 5V to both experiments). 3.3V was supplied to the input of the electrical switch simulating the avionics board. The test verifies the ability of the switch to isolate power from the experiments drawing minimal current.
Test Result:	Current draw when the switch is open (3.3V supplied to the switch input) = 0.000A. The negligible current draw proves the circuty is not drawing power from the batteries when the switch is closed and visual inspection of all LEDs and microcontrollers being off proves that the system is "off".

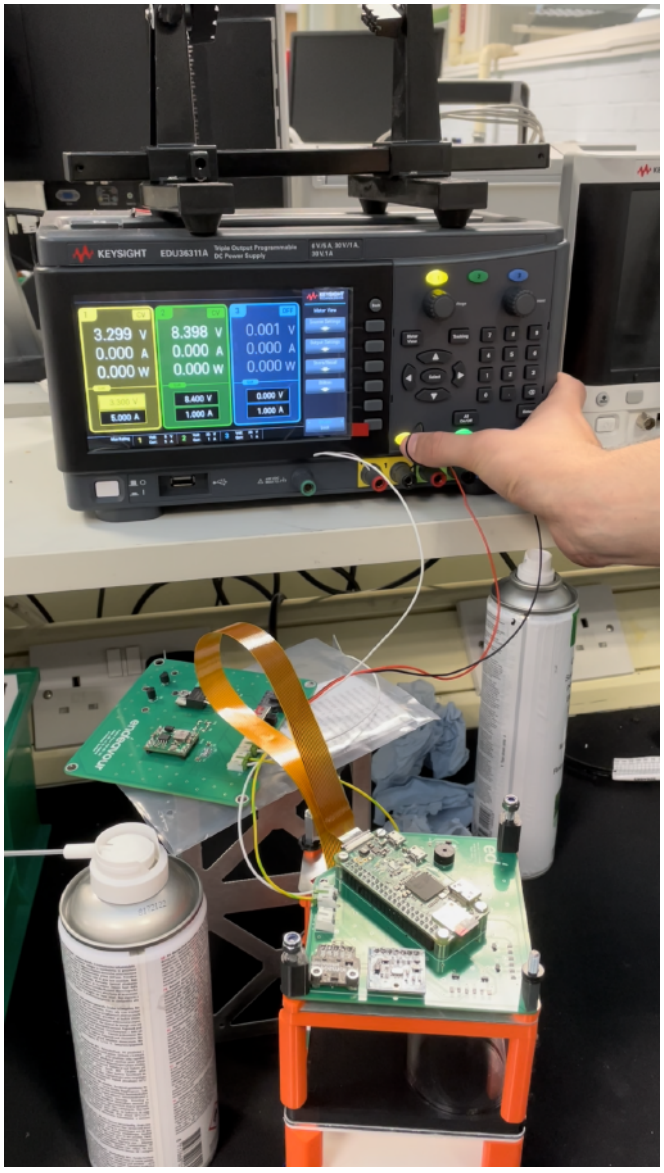

Figure B.12: Power Electrical Switch Testing

B.15 Payload Launch Load Test

Responsible Engineers:	Jo Shepton, Fergus Wilson
Date of Test:	05/09/2022
Location of test:	Fleeming Jenkin Electrical Teaching Laboratory
Equipment used:	Beam Masses
Test Description:	10kg of mass was placed on the forward payload bulkhead to simulate the downward force at lift off. All spacers in the payload successfully took 125% the launch load, proving that the spacers are strong enough for the axial load.
Test Result:	The high infill spacers support the 125% of the launch load comfortably



B.16 Integrated Test of Avionics Stack and Ground Station

See Section B.4,B.5, B.6, and B.7 for proof of functionality in recovery.

Responsible Engineers:	Jospeph Azrak, Thomas Stott, Blessy Ananth, Alberto Progida, Jo Shepton, Daniel Soulam Holler
Date of Test:	18/07/2022
Location of test:	Braid Hill to Arthur's Seat
Equipment used:	Full SRAD Stack, SRAD Ground Station
Test Description:	SRAD avionics bay and SRAD ground station were positioned 3.4km apart (longest LOS distance possible in Edinburgh). The full eWDL pipeline with call and response, including acknowledgement was assessed and RSSI recorded. See Figure B.13 and B.14 for testing pictures.
Test Result:	RSSI of -81dBi was significantly greater than predicted by the Friss Free Space eqn. adjusted with 30dB of miscellaneous losses. This value for loss was proven to be highly conservative, showing that the transmitter power should provide sufficient range, provided humidity conditions are not worse than Edinburgh (highly unlikely based on historical weather patterns).

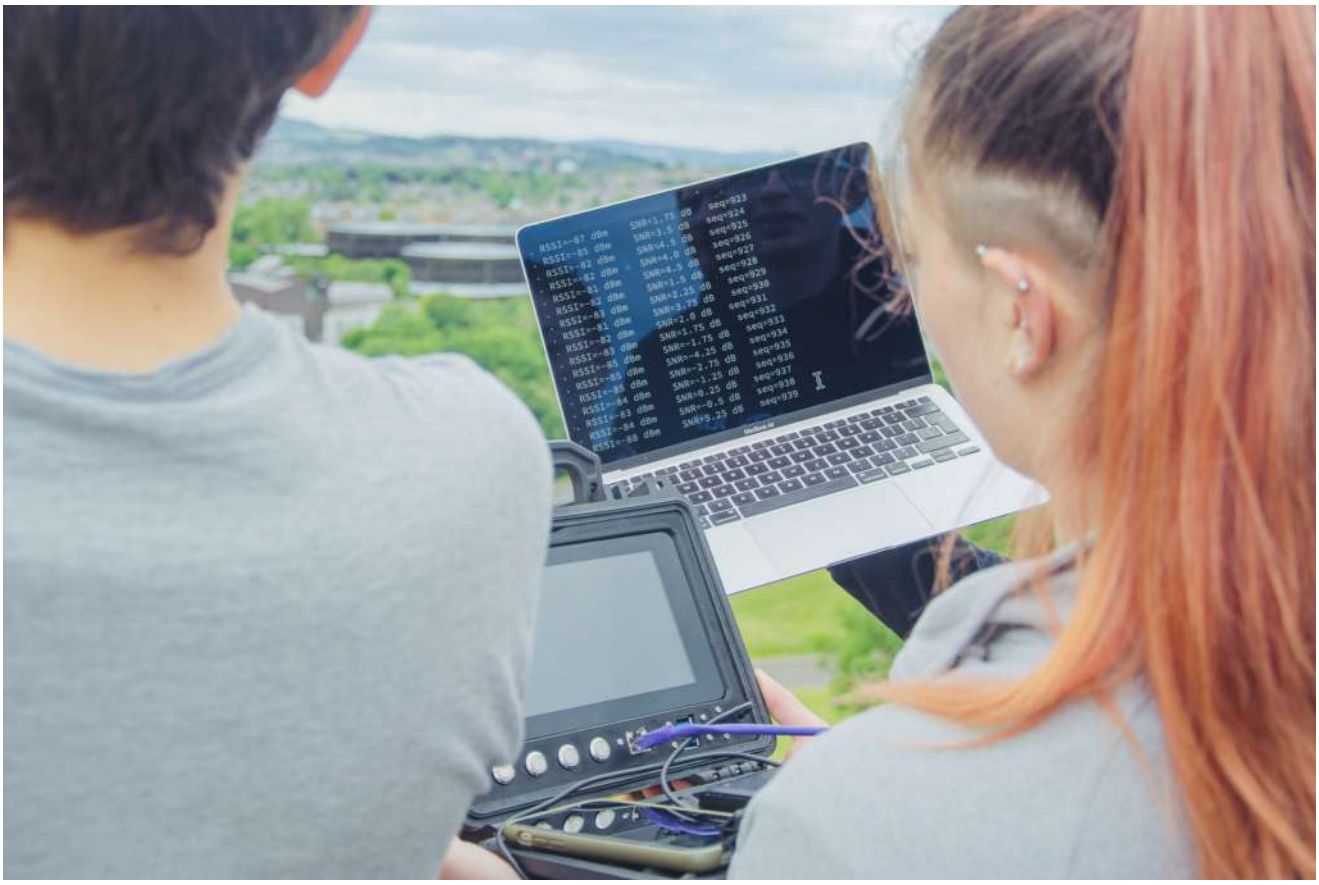

Figure B.13: Data transmission screen.



Figure B.14: Ground station test.

B.17 SRAD propulsion system testing

THIS PAGE INTENTIONALLY LEFT BLANK

B.18 SRAD pressure vessel testing

THIS PAGE INTENTIONALLY LEFT BLANK

C — Hazard Analysis Report

C.1 Motor assembly - explosives handling

Hazards	Loss of life, sight or hearing, Severe burns, Wounds from sharp ejecta.
Probability	LOW
Severity	VERY HIGH
Criticality	HIGH
Mitigation Strategy	While using a COTS motor mitigates most of the hazards from transport, mixing and chemical reactions associated with grain preparation and casting, it is still important to take precaution when assembling the motor itself, integrating to the rocket, and transporting the assembled and loaded rocket in the launch area. To ensure safe assembly, the supplier-provided instructions and notes will be read by all members. The members that will be handling the motor will be from the structures team that have designed the motor assembly and has familiarised themselves with the motor checklist and instructions and notes from the supplier. The **PROP1 Checklist** will provide detailed steps for assembly and disassembly of the motor and the motor integration. In case of an off-nominal situation, the members will only approach the rocket if they are explicitly told that it is cleared to do so by the RSO and Bombeiros. During rocket recovery, separate containers for the motor components will be prepared to ensure that the combustion byproducts do not contaminate other components.

C.2 Recovery System Stored Energy Devices

Hazards	Loss of sight or hearing, Intermediate burns, Wounds from sharp ejecta.
Probability	MEDIUM
Severity	VERY HIGH
Criticality	VERY HIGH
Mitigation Strategy	While our recovery system uses minimal amount of black powder, it is still present. In EuRoC and other competitions, energetics have been known to inadvertently be actuated, either by software bugs or unpredictable environmental factors. The handling of black powder will be minimised and will only be introduced to the system by the Lead Recovery Engineer, who has experience with arming and loading our previous launch vehicles. A buddy will assist them with the REC1 checklist during recovery integration. CO_2 canisters, which is the key to our separation, is less sensitive to external conditions but has potential to be dangerous since it is a compressed gas which can cause damage if the casing is damaged and the gas is ejected in a way that was not designed to. Additionally, all energetics are isolated by physical switched until the vehicle is on the launch-pad, meaning that any bug in the deployment software logic cannot cause any casualties. The risk arises not only from the black powder in itself, but to the ejected parts of the launch vehicle, such as the sharp nosecone and stabilising fin tips. Additionally to being protected with a soft cap until the positioning on the launch-pad, there will be strict enforcement of assembly procedures to **reduce to zero** the amount of time team members will spend in line with any sharp points.

C.3 Avionics and Payload Lithium Battery Packs

Hazards	Fire Hazard.
Probability	MEDIUM
Severity	HIGH
Criticality	HIGH
Mitigation Strategy	Li-ion and Li-Po battery packs are sensitive to conditions of over and undervoltage, and may swell, emit fumes and catch fire if in conditions of overcurrent or overvoltage. Care will be taken to label every single battery and keep track of their charge history before assembling them into launch vehicle. High quality charging equipment will be used for their charging and specialised boxes will be used for their transport.

D — Risk assessment

The following risk assessment was undertaken to identify and mitigate several risks spanning human resources to logistics, but focused on launch-day operations. It follows a Failure Mode and Effect Criticality Analysis approach with a scale of 1-3 reserved for the PROBABILITY of a risk taking place and a separate 1-3 scale for the SEVERITY associated with its consequences. The product of the probability and severity scores yields a CRITICALITY score, which indicated which risks and hazards must be addressed via specific mitigation strategies. In the following the scales are defined in ascending order - 1 is the lowest and 3 (for severity and probability) or 9 (criticality) being the highest - and colour-coded accordingly.

This remainder page has been intentionally left blank for formatting reasons.

Table D.1: FMECA (Failure Mode and Effect Criticality Analysis for the Darwin III Mission

RISK ID	PHASE	RISK	CAUSES	PRB.	SEV.	CRI.	MITIGATION
R_PC_01	PRE-COMP	Failure to complete all R&D or Manufacturing tasks	(i) Miscommunication (ii) Poor planning (iii) Lack of transparency	2	3	6	Group discussions at start of program to define expectations of internal communication expectations and documentation standards
R_PC_02	PRE-COMP	Damage of test equipment or test hardware	Missing or incomplete Risk Assesments (RA), Safe Systems of Work (SSOW) or COSHH documentation	2	2	4	Compilation of RA, COSHH, SSOW for all maufacturing or testing activites conducted in a laboratory
R_PC_03	PRE-COMP	Injury during operation of manufacturing/ testing equipment	Time pressure to complete assembly or incomplete RAs, SSOWs or COSHH documentation	2	3	6	Only members related to the development of a subsystem shall be involved in manufacturing/testing it.
R_PC_04	PRE-COMP	Early termination of budget	Poor budget planning at R&D phase and/or unexpected obstacles during assembly	1	2	2	Set up emergency fund, report every single expenditure to finance manager promptly, monthly reports to track expenses.
R_PC_05	PRE-COMP	Key member not able to participate in competition	Ill health, financial reasons, personal reasons	1	3	3	Divide responsibilities among Sub-Team Leads, choose two Technical Leads so team is not reliant on any one member.
R_PC_06	PRE-COMP	Lack of justification /understanding of design decisions in final report	Incomplete documentation generated throughout R&D process	2	1	2	Group discussions at start of program to define expectations of internal communication expectations and documentation standards
R_PC_07	PRE-COMP	Design CP does not match Simulation CP	Incomplete or Inaccurate definition of LV within commercial rocket simulator programs	1	3	3	Hand calculation using Barrowman method

Table D.2: FMECA (Failure Mode and Effect Criticality Analysis for the Darwin III Mission

RISK ID	PHASE	RISK	CAUSES	PRB.	SEV.	CRI.	MITIGATION
R_PC_08	PRE-COMP	Design CM does not match Simulation CM	Incomplete or Inaccurate definition of LV within commercial rocket simulator programs	2	3	6	Weekly tracking of subsystem masses: all machined/manufactured components weighed and reported at weekly Team Leads meeting. Allow for ballast masses to be added on competition day depending on wind conditions.
R_PC_09	PRE-COMP	Injury from handling sharp components (Fins, Nosecone tip)	Incorrect handling due to time pressure or unclear procedures/responsibilities	2	2	4	Sharp components shall be covered with protective layers of Polystyrene and handled with care
R_SH_01	SHIPPING	Delays in preparation of final vehicle for shipping	Insufficient preparation of Crate Design, delayed purchase of timber	2	3	6	Shipping date defined 6 months in advance. Crate based on succesful design from last year. Timber purchasing and crate assembly to be conducted in advance.
R_SH_02	SHIPPING	Delays at customs	Incomplete Import/export documentation	3	3	9	Given delays in previous edition of competition, where 11 days were allowed for shipping, 25 days will be accounted for this year the shipping date set well in advance for the 16/09/22
R_LD_02	LAUNCH DAY	Part/cable assembled/plugged in incorrectly during final assembly	Unclear procedures/responsibilities or environmental factors (dust, rain, wind)	3	3	9	Team shall present itself to launch site at 9am, or 4.5hrs before the allotted launch window in case of an early launch to reduce time pressure. Team members shall practice the assembly and disassembly of their subsystem extensively. Buddy system on all critical connections. All critical wiring kept as fixed as possible to reduce assembly operations on launch day. Use of compressed air to clean all mating surfaces and electrical connections

Table D.3: FMECA (Failure Mode and Effect Criticality Analysis for the Darwin III Mission

RISK ID	PHASE	RISK	CAUSES	PRB.	SEV.	CRI.	MITIGATION
R_LD_03	LAUNCH DAY	Chaos due to key member feeling indisposed/unavailabl on launch day	Incomplete training of the whole team, weak procedures lacking redundancy, unclear chain of command	2	2	4	Team members to practice the assembly and disassembly of their subsystem extensively. Clarify chain of command. Review of launch day procedures and launch day schedule in days leading up to launch window and on morning briefing session.
R_LD_04	LAUNCH DAY	Clash between members during final assembly	Time/emotional pressure, Unclear chain of command, insufficient launch-day preparations	1	2	2	Team-building excercises and activities to be conducted throughout the academic year to ensure friendly and trusting bonds between team-mates. Launch day briefing to finalise operations and schedule.
R_LD_05	LAUNCH DAY	Premature activation of stored energy devices	Incorrectly assembled avionics or disregard for switching order as defined by procedures.	1	3	3	Buddy system on all critical wiring on stored energy actuation outputs, and on switching operations. Clearly labelled switches on AVBAY canopy. Securely fastnede LV and all team members standing clear of nosecone during avionics power-up in case wrong switch is flicked.
R_LD_06	FLIGHT - PAD	Injury during planned arming of stored energy devices on Pad	Members switching on energetics while too close to launch vehicle	2	3	6	All but one members to keep safety distance (6m) from pad when energetics are given power. Maintain maximum attention and avoid use of stepladder to maintain agility in case of premature nosecone ejection.
R_LD_07	FLIGHT - ON PAD	Exhausted batteries on the pad	Umbilical (external power system) failure.	1	3	3	Extensive umbuilical system testing in a variety of environmental conditions, especially heat (¡50C).

Table D.4: FMECA (Failure Mode and Effect Criticality Analysis for the Darwin III Mission

RISK ID	PHASE	RISK	CAUSES	PRB.	SEV.	CRI.	MITIGATION
R_LD_08	FLIGHT - ON PAD	Poor telemetry link to Ground Station from Launch Pad	Unexpected electro-magnetic interference	2	3	6	Yagi antenna handler to attempt different angles, and GSO (Ground Station Operator) to request RSO to approach Launch Pad to middle distance bunker to attempt to regain connection to launch vehicle.
R_LD_09	FLIGHT - IGNIT	Misfire	Improperly posistioned igniter, Incorrect motor assembly	2	1	2	Ensure correct interpretation of Cesaroni Technologies assembly and ignition instructions.
R_LD_10	FLIGHT - IGNIT	Injury/Damage to Hearing	Team members too close to launch pad	1	3	3	If GSO and buddy are stationed at middle distance bunker, they must wear ear protection.
R_LD_11	FLIGHT - BOOST	CATO (propusion-related catastrophic accident at take-off)	Improperly posistioned igniter, Incorrect motor assembly	3	3	9	Ensure correct interpretation of Cesaroni Technologies assembly and ignition instructions. In depth study of assembly instructions and procedures ahead of actual assembly. For any mishap during assembly, notify supporting EuRoC official before going ahead.
R_LD_12	FLIGHT - BOOST	Motor underperforms, leading to lower apogee	Expected variability in manufacturing process	1	2	2	No action possible
R_LD_13	FLIGHT - BOOST	Motor overperforms, exceeding airspace limitation	Expected variability in manufacturing process	1	3	3	Inclusion of Air-Brakes system to refulate Apogee.
R_LD_14	FLIGHT - BOOST	Structural failure of LV during ascent	Improper setup of simulations, incorrect manufacturing of components, low Safety Factors, insufficient Quality Control	1	3	3	Follow standard design practices. Impose safety factor of at least 3 on all structural components during R&D phase. Meticulous Quality Control machined components

Table D.5: FMECA (Failure Mode and Effect Criticality Analysis for the Darwin III Mission

RISK ID	PHASE	RISK	CAUSES	PRB.	SEV.	CRI.	MITIGATION
R_LD_15	FLIGHT - BOOST-ING	Fin Failure	Improper setup of fin simulation leading to poor geometry/thickness choice	2	3	6	Adding to FinSim FoS of 1.5, thickness is to be further increased by tip-to-tip CFRP layup
R_LD_16	FLIGHT - COAST	Actuation of air-brakes while travelling above 200m/s	Error in computer logic, high rate of spin causes centrifugal forces to pull out the Air-Brake blades	1	3	3	Servo-motor holding torque passively prevents blades from being spun out. Mach-timer sinche launch detect to overrides any altitude estimations made by Kalman Filter to precent anomalies in sensor readings from anticipating Air-Brake deployment
R_LD_17	FLIGHT - COAST	Loss of signal to ground station	Insufficeintly fast manual tracking with Yagi antenna	3	2	6	Yagi Antenna Handler shall train the movement by attempting to track other launches taking place ahead of DIII.
R_LD_18	FLIGHT - COAST	Abrupt change of direction/heading	See causes for Structural failure, Fin Failure, CATO, premature Air-Brake actuation.	2	3	6	Communicate instantly to RSO, reach Tribuna. If approved by RSO and mission control, attempt manual Abort once public is safely located under the Tribuna.
R_LD_19	FLIGHT - REC. EVENT 1	Premature or Delayed actuation of ejection mechanisms	Error in SRAD FC logic, or in the programming of COTS FCs	1	3	3	Use of two dissimilar, cross-strapped deployent devices, attempts to correct for each system's weaknesses. Buddy system when programming deployment criteria on both systems.
R_LD_20	FLIGHT - REC. EVENT 1	Failure of BOTH ejecection systems	Excessively tight fit of Nosecone Coupler (D3-606) with Recovery Bay Tube (D3-405)	1	3	3	Buddy system to confirm telescoping motion of coupler is effortless. Ground test of ejection system. No launch until telemetry confirms continuity on all four deployment channels.

Table D.6: FMECA (Failure Mode and Effect Criticality Analysis for the Darwin III Mission

RISK ID	PHASE	RISK	CAUSES	PRB.	SEV.	CRI.	MITIGATION
R_LD_21	FLIGHT - REC. EVENT 1	Failure of EITHER SRAD or COTS systems	Incorrect wiring, failure to ignite black powder	2	2	4	Use of two dissimilar, cross-strapped deployent devices, attempts to correct for each system's weaknesses. No launch until telemetry confirms continuity on all four deployment channels.
R_LD_22	FLIGHT - REC. EVENT 1	Jamming of SRAD system	Incorrect assembly, lack of attention to procedures, lack of dry teflon grease.	1	1	1	Buddy system when assembling mechanism, careful attention to assembly procedure. Confirmation of dry lubricant.
R_LD_23	FLIGHT - DRG DSCNT	Shredded drogue	Greater windspeed than predicted at apogee, delayed apogee detection causes high vertical velocity	2	2	4	Drogue specified for opening speed up to 50m/s
R_LD_24	FLIGHT - DRG DSCNT	Recovery hardware failure	Imperfection in manufacturing of hardware, snags or tears on the lines during packing, greater forces than expected	2	3	6	Meticulous quality control of Recovery Hardware. All hardware with safety factor of at least 2 with respect to the nominal worst case scenario
R_LD_25	FLIGHT - DRG DSCNT	Structural failure of LV during descent	Greater snatch forces than predicted	1	3	3	Follow standard design practices where possible. Impose safety factor of at least 3 on all structural components during R&D phase. Meticulous Quality Control of incoming machined components (on CMM when available)
R_LD_26	FLIGHT - REC. EVENT 2	Premature or Delayed actuation of release mechanisms	Faulty detection of 500m altitude	1	2	2	Hard coded timer based on simulated trajectory shall measuring elapsed time from apogee to force ejection of parachute in case of barometer malfunction

Table D.7: FMECA (Failure Mode and Effect Criticality Analysis for the Darwin III Mission

RISK ID	PHASE	RISK	CAUSES	PRB.	SEV.	CRI.	MITIGATION
R_LD_27	FLIGHT - RECOVERY EVENT 2	Failed actuation of BOTH release mechanisms	Incorrect wiring, failure to ignite black powder	1	2	2	Use of two dissimilar, cross-strapped deployent devices, attempts to correct for each system's weaknesses. Buddy system when programming deployment criteria on both systems.
R_LD_28	FLIGHT - MAIN DESCENT	Higher descent speed than predicted	Damaged main chute	1	2	2	Drogue specified for opening speed up to 60m/s
R_LD_29	FLIGHT - MAIN DESCENT	Shredded main	Tangle leading to fins or lines applying excessive wear on Nylon canopy	1	3	3	Use parachute bag to reduce wear on RipStop Nylon canopy.
R_LD_30	FLIGHT - NOMINAL RECOVERY	Injury or burns during recovery operations	Handling of motor or sharp fin leading/trailing edge	1	3	3	Handling of Lower Body to be exclusively left to on-site Bombeiros.
R_LD_31	FLIGHT - OFF-NOMINAL RECOVERY	Fire hazard	Handling of damaged Lithium batteries	1	3	3	Handling of Lower Body to be exclusively left to on-site Bombeiros.
R_LD_32	FLIGHT - OFF-NOMINAL RECOVERY	Injury or burns during collection of flight remains	Handling of motor, damaged Lithium batteries or fractured CFRP shards	2	3	6	Handling of burned remains to be exclusively left to on-site Bombeiros, and if approved for team-members, only while wearing protective gloves.

E — Checklists

E.1 Shipping Checklist

Procedure ID:	LOG1
Responsible Engineers:	Operations Lead, Ann Lee.
Date:	16/09/2022
Location:	King's Buildings, Edinburgh
Equipment used:	Crate Assembly & Shipping Carnet DHL Shipping Forms DHL Air Waybill Tools and other Support Equipment Bubble Wrap Disassembled Darwin III LV
Procedure Aim:	Orderly and tidy packaging of the items chosen for shipping, including the Launch Vehicle and all spare parts, tools, marketing materials and documentation

- Preparation
  - ❏ **[1.1]** In the two days leading up to shipping date, all spare parts are collected and laid out on the workbenches of the Hudson Bear MakerSpace.
  - ❏ **[1.2]** Using the shipping carnet approved by DHL and the Portuguese Customs, Responsible engineer to tick off every item.
  - ❏ **[1.3]** Supporting team members can be dispatched to locate any missing items.
- Inspection of Structural Integrity of Crate
- Final Documentation Check
- Launch Vehicle Packing
  - ❏ **[2.1]** Darwin III LV is disassembled into its 4 sectors: Lower Body (without Motor Bulkhead D3-111), Avionics Bay (including Motor Bulkhead), Recovery Body Tube, Payload Bay.
  - ❏ **[2.2]** Sharp edges (Fins and Nosecone Tip) protected with 3D printed covers taped in place.
  - ❏ **[2.3]** Lower Body is wrapped in bubble wrap and laid within support braces. Special attention and additional protective material given to the portions of tubing in contact with the support braces.
  - ❏ **[2.4]** The Avionics Bay, Recovery bay and Nosecone are also laid in the crate, spaced by specially designed wooden spacers to prevent knocking during shipping.
- Tools and Spare parts' Packing: Once again, running through the Shipping Carnet, remaining spare parts, fasteners and tools are added to the crate. A concise list is presented below.
  - ❏ **[3.1]** Hand tool kit
  - ❏ **[3.2]** Power tool kit
  - ❏ **[3.3]** Soldering kit
  - ❏ **[3.4]** Craft Knife, Rugged Scissor
  - ❏ **[3.5]** Dremel set
  - ❏ **[3.6]** Electrical adapters
  - ❏ **[3.7]** Metrology Kit (Calipers and rulers)
  - ❏ **[3.8]** Steel-toed safety boots, goggles, binocular
  - ❏ **[3.9]** Yagi Antenna

- ❏ **[3.10]** HDMI Monitor
- ❏ **[3.11]** Promotional Banner

E.2 Edinburgh departure checklist

Procedure ID:	LOG2
Responsible Engineers:	Technical Lead - Zsolt Csonka
Date:	08/10/2022
Location of test:	King's Buildings, Edinburgh
Procedure Aim:	Collect final components that were kept in Edinburgh for final validation tests ahead of the competition, pack them in hand luggage ahead of departure

- Avionics
  - ❑ **[1.1]** In the two days leading up to shipping date, all spare parts are collected and laid out on the workbenches of the Hudson Bear MakerSpace.
  - ❑ **[1.2]** Using the shipping carnet approved by DHL and the Portuguese Customs, Responsible engineer to tick off every item.
  - ❑ **[1.3]** Supporting team members can be dispatched to locate any missing items.
- Avionics Packing
  - ❑ **2.1** Complete Stack
  - ❑ **2.2** Fastener Stack
  - ❑ **2.3** Ground Station Pelican Case
  - ❑ **2.4** Wire Harness Set
  - ❑ **2.5** Battery Packs and Charger Sets
  - ❑ **2.6** Replacement (spare) Stack
- Payload Packing
  - ❑ **3.1** Complete PCB Stack
  - ❑ **3.2** Fastener Set
  - ❑ **3.3** Wire Harness Set
  - ❑ **3.4** Battery Packs and Charger Sets
- Payload
  - ❑ **[4.1]** Printed copies of technical report
  - ❑ **[4.2]** Printed copies of Propulsion system handling procedure & checklist
  - ❑ **[4.3]** Printed copies of Recovery system assembly procedure & checklist
  - ❑ **[4.4]** Printed copies of Preflight checklist
  - ❑ **[4.5]** Printed copies of Countdown checklist
  - ❑ **[4.6]** Printed copies of Rocket recovery checklist

E.3 Propulsion System Handling & Integration Procedure

Procedure ID:	PROP1
Responsible Engineers:	Alberto Progida, Jo Shepton.
Date:	TBD
Location:	Santa Margarida Army Base, Portugal
Equipment used:	CTI 21062O3400-P Reload & CTI Pro98 6GXL Gen 2 Casing and Hardware CTI Pro98 Assembly Guide Vaseline Grease 2.5mm Hex Key Fully Integrated Darwin III LV
Procedure Aim:	Given the basic contents of the reload kit and the casing hardware, the responsible engineers shall assemble the motor as described by the CTI instructions set, with the support of Pyrotechnic Technicians and EuRoC technical volounteers

- Preparation
  - ❏ **[1.1]** Clear area of any source of ignition or explosives
  - ❏ **[1.2]** Inspect the components carefully before beginning assembly. DO NOT use any parts that appear damaged or faulty in any way.
  - ❏ **[1.3]** Follow Cesaroni Instruction sets. These are not reported onto this checklists to avoid transcription errors.
- Forward Closure and Smoke Grain Assembly
- Motor Assembly
  - ❏ **[2.1]** Grain Integration
  - ❏ **[2.2] [2.2]** Liner Integration
  - ❏ **[2.2]** Nozzle and Aft retaining Ring Integration
  - ❏ **[2.3]** Forward Closure and Forward retention ring Integration
- Final Integration with Darwin III
  - ❏ **[3.1]** Fully integrated Darwin III LV is rested horizontally on LV stand.
  - ❏ **[3.2]** the 4 bolts retaining the Darwin III Aft Cone (D3-101) are unscrewed from the Thrust Plate (D3-105) using a 2.5mm hex key, and stored nearby for use.
  - ❏ **[3.3]** All Electronics (SRAD & COTS) are de-activated.
  - ❏ **[3.4]** Motor is unpacked from protective enclosure where it has been stored since the grain, nozzle and closures integration procedures.
  - ❏ **[3.5]** Responsible Engineer and Buddy carefully lift the motor.
  - ❏ **[3.6]** The Thrust Ring (D3-102) is slid onto the Motor Reload, with the taper facing aft, until it contacts the Motor's Aft Lip.
  - ❏ **[3.7]** While maintaining motor horizontal and level with the LV Thrust Assembly, the motor is inserted into LV with its Forward Closure pointing in the same direction as the LV Nosecone Tip (+Z direction).
  - ❏ **[3.8]** As the motor is being slid in, special care must be taken to align it with the Centering Rings and Thrust Assembly, **avoiding any prying or wedging action**.
  - ❏ **[3.9]** When the forward closure is heard to come into contact the Motor Bulkhead (D3-111), spin in a clockwise direction in order to ensure engagement of the threaded forward closure with the Motor Bolt.
  - ❏ **[3.10] DO NOT** over tighten the motor onto the Motor Bolt, as it could shear off the machined features maintaining it secure.

- ❏ **[3.11]** **Lightly tug** on the Thrust ring in the -Z direction to ensure it is being positively retained.
- ❏ **[3.12]** **ENSURE** The Thrust ring makes good and full contact with the thrust assembly
- ❏ **[3.13]** If motor is loose when tugged, or if the Thrust Ring does not make good and full contact with the Thrust assembly, attempt to lightly tighten motor further and retry.
- ❏ **[3.14]** Conclude the procedure by fastening the Aft Cone using 4x M4x20mm bolts previously unscrewed.

E.4 Recovery checklist/procedure

Procedure ID:	REC1
Responsible Engineers:	Alex Stevenson, Fergus Wilson (TBD).
Date:	TBD
Location:	Santa Margarida Army Base, Portugal
Equipment used:	2x Tender Descender & 3x JTEK low-current Pyro Igniters 1x SPT High Torque Servo with SRAD mechanism 2x 33g CO2 canisters Raptor Kit Hardware 1x 96in Main Parachute 1x 24in Main Parachute 1x 10ft Nylon Shock Cord 1x 20ft Nylon Shock Cord 1x Kevlar Y-Harness (6ft) 1x Polycarbonate separator plate (aka Mezzanine) 1x M10 Eye Bolt & Nylock Nut 3x M6 Eye Bolt & Nylock Nut 6x 221 Wago Clip Connectors 4x M3 PA6 Nylon shear pins 1x 1.5cm wide roll of 3M 1900 Tape
Procedure Aim:	A procedure to check the entirety of recovery hardware is transported to the launch site and installed within the Darwin III recovery Bay

- Preparation
  - ❏ **[1.1]** Check all equipment is present, ticking off each as they are laid out.
  - ❏ **[1.2]** Ensure the pyrotechnic devices are loaded prior to recovery assembly. If not, load devices and return to step E.4.1.1.
  - ❏ **[1.3]** Inspect the shock cords and drogue parachute for tears, rips, or other damage. The main parachute will have been previously checked for damage and packed to save time in assembly and to protect it from potential damage.
- SRAD System Assembly
  - ❏ **[1.4]** Install SRAD ejection system: Insert the RAPTOR mount. Add servo mount and holder and bolt into place.
  - ❏ **[1.5]** Add in a CO2 cartridge and slowly thread puncture device until it butts up to the seal. Unthread the puncture device 0.75 turns and attach the servo to the end by using the servo coupler. Remove the CO2 cartridge.
  - ❏ **[1.6]** Connect the servo power cables to the avionics bay. Confirm before that the servo has no active power (S3 OFF).
- COTS Raptor System Assembly
  - ❏ **[2.1]** Install loaded RAPTOR following installation instructions on the RAPTOR kit.
  - ❏ **[2.2]** Connect the pyrotechnic lines to SRAD and COTS avionics following wiring convention that is at the end of this checklist.
  - ❏ **[2.3]** Confirm that there is no active power (S3, S4 OFF).
- Tender Descender and Final Hardware Assembly
  - ❏ **[3.1]** Install/confirm the M10 and M6 eyebolts using complementary nylock nuts.
  - ❏ **[3.2]** Attach 8mm quicklink to both eyebolts.
  - ❏ **[3.3]** Connect one Tender Descender to each eyebolt.
  - ❏ **[3.4]** Connect TDs to the avionics. Confirm that there is no active power.

- ❏ **[3.5]** Connect the M10 connected TD to the shared paracord line between the drogue and the main.
- ❏ **[3.6]** Attach the main shock cord to the M10 eyebolt.
- ❏ **[3.7]** Thread the other end of the main shock cord through the central opening on the separator plate and the shared paracord through the adjacent hole.
- ❏ **[3.8]** Slide separator plate down onto the separator plate holders and screw into place.
- ❏ **[3.9]** Slide the shared paracord through the main recovery ring.
- ❏ **[3.10]** Attach the second TD through the remaining separator plate hole.
- ❏ **[3.11]** Attach the drogue shock cord to the main recovery ring.
- ❏ **[3.12]** Bundle main shock cord using electrical tape method.
- ❏ **[3.13]** Attach the packed main parachute to the main shock cord and place into the recovery bay, ensuring the recovery ring is not trapped beneath but to the side of the bag.
- ❏ **[3.14]** Attach the top loop of the parachute bag to the main recovery ring using a paracord.
- ❏ **[3.15]** Attach the drogue parachute to the drogue shock cord.
- ❏ **[3.16]** Attach the Y-harness to the nosecone bulkhead eyebolts.
- ❏ **[3.17]** Attach the swivel of the Y-harness to the drogue parachute using a quicklink.
- ❏ **[3.18]** Fold drogue parachute and place above the main parachute bag.
- ❏ **[3.19]** Mount the CO2 cartridges.
- ❏ **[3.20]** Announce that stored energy devices and pyrotechnic devices have been loaded. From now onwards, DO NOT, under any circumstance, go downrange of the nosecone in the event of premature ejection actuation
- ❏ **[3.21]** Place on the nosecone
- ❏ **[3.22]** Screw in 4x M3 Nylon shear pins securing Nosecone to Recovery Bay Tube.
- ❏ **[3.23]** Cover all holes in aft end of Recovery Bay Tube with one continuous length of 3M 1900 Tape to prevent any leaks
- ❏ **[3.24]** Repeat step 3.23 for all holes in forward end of the Recovery Bay Tube.

Responsible Engineers:	COTS avionics lead and Flight director
Convention aim:	Introduce the tape convention of wiring harnesses between avionics bay and recovery bulkhead. Note: colour convention same for both sides.

- **Frog tape** on main bundle of wire - SRAD energetics
  - Plugs into SRV
  1. Pyro harness
     - Pink and blue: apogee
     - Grey and white: main
  2. Servo harness
     - Red, yellow, brown
- **Red tape** on main bundle of wire - COTS & Payload harness
  - Plugs into PLD SIDE
  1. Pyro harness
     - Pink and blue: main
     - Grey and white: apogee
  2. Payload harness
     - Yellow and green

E.5 Payload Assembly Procedure

Procedure ID:	PAY1
Responsible Engineers:	Jo Shepton, Virginia Cangelosi, Fergus Wison, Phil Henrich
Date:	TBD
Location of test:	Santa Margarida Army Base, Portugal
Equipment used:	Pliers
	M4 spanner Screwdriver with M3 and M2 heads available (marked with red tape in the box) Multimeter
Procedure Aim:	Assemble the payload from its semi-dismantled travel state to be flight ready.

- Ensure all components are laid out and the correct tools are gathered
- Assemble the bays separately then fully integrate
- **Battery bay assembly**
  - ❑ **[1.1]** Taking the bottom battery brace plate, friction fit the black spacers marked 'Battery' onto the extrusions. Using a small amount of epoxy, glue the spacers in this configuration.
  - ❑ **[1.2]** Place the batteries in the slots, taking care to put the cables at the bottom
  - ❑ **[1.3]** Using small zip ties and the holes in the brace cut for them,secure the charging cables, the connector unit and the female end of both batteries
  - ❑ **[1.4]** Place the top plate on, ensuring the extrusions align with the holes. Do not glue in case of emergency battery removal, instead friction fit.
- **Assemble the slosh bay**
  - ❑ **[2.1]** Take the slosh brace bottom plate (black) and apply a small layer of silicon in the circular inset.
  - ❑ **[2.2]**Push the 55mm acrylic tube into place using the silicon as a glue that also ensures the water tightness of the experiment. If needed, add a small layer on the outside, along with a little epoxy for stability during flight.
  - ❑ **[3.3]** Taking the triangular spacer, bolt on the camera using the M2 x 8mm bolts and 3 M2 plastic washers on each bolt. The washers act as spacers to ensure the camera remains parallel to the bottom slosh brace.
  - ❑ **[3.4]** Friction fit the extrusions from the slosh base plate to the camera spacer and epoxy
  - ❑ **[3.5]** Repeat friction fit and epoxy procedure with L-shaped orange brackets with 'Slosh' engraved on them. These two spacers go along the other diagonal than the camera spacer
  - ❑ **[3.6]** Align the final thinner spacer also engraved 'Slosh' with the extrusions in the corner opposite the camera spacer and epoxy into place
  - ❑ **[3.7]** Pour in a little of the propylene glycol and swirl to check the water tightness of the tube. If satisfied, fill 3/4 of the way up and add the reflective particulates and colour
  - ❑ **[3.8]** Silicon the frosted acrylic window into the slot cut in the top slosh brace. Ensure a watertight seal
  - ❑ **[3.9]** Place the top slosh brace on top of the acrylic tube and spacers,and epoxy/silicon into place when the fit has been found
- **Full Assembly**
  - ❑ **[4.1]** Gently slide on the Arduino PCB to the four rods, taking care not to stress the JST connections between it and the SiPM PCB. Only slide on around 15mm
  - ❑ **[4.2]** Screw on one 10mm spacer with an M4 nut in it's insert onto each of the four M4 rods until it sits just below the Arduino PCB

- ❏ **[4.3]** Slide on the SiPM PCB and adjust the stack until it sits about 25 mm up the rod
- ❏ **[4.4]** Slide on the scintillator bracket, ensuring the scintillators sit in the hole
- ❏ **[4.5]** Slide on the payload aft bulkhead (PLD-502).
- ❏ **[4.6]** On the aft side, slide on a washer and secure the rods with an M4 nylock. Ensure that when placed on a flat surface, the rods do not extend past the flat surface of the bulkhead. Tighten the 10mm torque spacer to secure this set up
- ❏ **[4.7]** Slide on four 20mm spacers to sit on top of the Arduino PCB
- ❏ **[4.8]** Slide on the power PCB
- ❏ **[4.9]** Connect the Arduino PCB to the Power PCB with the 3-pin JST
- ❏ **[4.10]** Add four 10mm spacers
- ❏ **[4.11]** Slide on one of the battery aluminium plates
- ❏ **[4.12]** Slide on the assembled battery bay with the batteries inside
- ❏ **[4.13]** Add the final battery aluminium plate
- ❏ **[4.14]** Slide on the assembled slosh bay
- ❏ **[4.15]** Slide on the aluminium top plate, ensuring the camera cable comes through the hole
- ❏ **[4.16]** Slide on the three 5mm spacers to the rods, leaving the rod the camera is attached to empty
- ❏ **[4.17]** Slide on the Slosh PCB and use two M3 x 12 bolts to secure it at the two holes with spacers glued underneath. These bolts screw into threaded inserts in the top of the slosh brace 3D printed part to minimise the movement of the PCB during flight.
- ❏ **[4.18]** Connect the Slosh PCB to the Power PCB using the 3-pin JST
- ❏ **[4.19]** Using a multimeter, test continuity and resistance between the positive and negative terminals on the Power PCB. If the resistance is above $1k\Omega$, then this is regarded as high and the system is working
- ❏ **[4.20]** Connect the batteries to the deans connector which connects them in parallel. The other end is connected to a 3-pin microfit molex
- ❏ **[4.21]** Connect the 3-pin molex to the Power PCB. The payload electronics are now able to receive power, so the mechanical switch will remain OFF until the rest of the system is built
- ❏ **[4.22]** On the rod which the camera is attached to, add the 15mm spacer. On the other rods, add the 7mm spacer (these are clearly marked with engravings of size to avoid confusion)
- ❏ **[4.23]** Add the payload forward bulkhead (PLD-503), along with washers and nylocks on every rod.
- ❏ **[4.24]** Tighten the nylocks on both ends of the payload to compress the spacers inside. Take care to work in the diagonals to avoid putting too much pressure on one side initially
- ❏ **[4.25]** Slot on the c-shaped shell and using eight M3 x 6 bolts, attach to the aft and forward bulkheads
- ❏ **[4.26]** Place the shell panel on the remaining side and bolt into place with four M3x6 bolts, ensuring the diagonal pattern is followed to avoid unnecessary unbalanced tension.
- ❏ **[4.27]** Switch the mechanical switch to arm the system

E.6 Pre-Flight Integration

Procedure ID:	PAD1
Responsible Engineers:	————————
Date:	Launch window date
Location of test:	Santa Margarida Army Base, Portugal
Equipment used:	Allen keys (M2, M2.5, M3)
	Avionics arming key
	Separation charges
	Ground station
	Fully assembled Nose Cone (including payload and connection to parachutes)
	Recovery Bay with parachutes loaded
	Recovery Bulkhead without separation charges
	Fully assembled Avionics bay & airbrake stack & Lower Body (including motor)
Procedure Aim:	Mount fully assembled rocket to launch rail and prepare for countdown.

INITIAL INTEGRATION - Assembly Tent

- ❏ **[1.1]** Assemble Lower Body, Avionics Bay and Recovery Bay as below:
  - ❏ **[1.1.1]** Lower Body to Avionics Bay: 6x M4x12 bolts
  - ❏ **[1.1.2]** Avionics Wiring Harness plugged into Recovery Bulkhead according to connection guide visible on aft end of bulkhead.
  - ❏ **[1.1.3]** Avionics Bay to Recovery Bulkhead: 3x M5 Shoulder Bolts (6mm shoulder, 12mm length)
- ❏ **[1.2]** Assemble the Payload according to PAY1 checklist
- ❏ **[1.3]** Before proceeding to Pyrotechnics Tent for FINAL MECHANICAL INTEGRATION, ensure avionics are configured as below.
  - ❏ **[1.3.1]** Ensure the SRAD and COTS FC is powered off
  - ❏ **[1.3.2]** Ensure the Payload Avionics are is powered off

FINAL INTEGRATION - Pyrotechnic Tent

- ❏ **[2.1]** Proceed with the Recovery Assembly procedure (including pyrotechnic device loading), as outlined by Procedure E (Code REC1)
- ❏ **[2.2]** Connect the Payload AUX Cable within the recovery bay
- ❏ **[2.3]** As per REC1, confirm Payload Y-Harness is connected to Payload Bulkhead Eye Bolt.
- ❏ **[2.4]** Use 4x Nylon Shear pins to secure the Payload Bulkhead to the Recovery Body tube
- ❏ **[2.5]** Install nosecone using 6x M4x12mm bolts
- ❏ **[2.5]** Perform LRR and obtain signatures for Flight Card from MCO, RSO and PO.
- ❏ **[2.6]** Remove nosecone
- ❏ **[2.7]** Clear of personnel ahead of nosecone.
- ❏ **[2.8]** Switch on Payload, wait 90s
- ❏ **[2.9]** Switch on COTS Avionics (Switch 1, first from the top, confirm by hearing 3 beeps in row)
- ❏ **[2.10]** Visually confirm payload LEDs are now off
- ❏ **[2.11]** Final check of all bolts and marking of rotational position.

AVIONICS CHECKOUT and PAD CHECKLIST

- ❏ **[3.1]** Confirm COTS Avionics are on by checking ground station
- ❏ **[3.2]** Await for signal from GSO that SRAD calibration and software tests are successfully completed

(three beeps in ascending order transition into one short beep every two seconds).

- ❏ **[3.3]** Confirm one walkie talkie is kept with Ann Lee at MCO,
- ❏ **[3.4]** Confirm one walkie talkie heads to Pad with Thomas Stott
- ❏ **[3.5]** Pad Team - THOMAS STOTT, ALBERTO PROGIDA, JOSPEPH AZRAK, MATUS KOMJATY, ZSOLT CSONKA, JASPER DAY - proceed to launch site.
  - ❏ **[3.5.1]** Alberto Progida and Zsolt Csonka carry vehicle on shoulder
  - ❏ **[3.5.2]** Thomas Stott to carry ladder
  - ❏ **[3.5.3]** Matus Komjaty to carry COTS GS, Jospeh Azrak to carry SRAD GS connected to the YAGI antenna, Jasper Day to carry YAGI antenna for SRAD GS.
- ❏ **[3.6] Confirm EggFinder TX is connected to EggFinder RX COTS GS**
- ❏ **[3.7] Confirm Quantum is responding via Wi-FI web-app**

Proceed to pad

- ❏ **[4.1]** Ensure charged walkie-talkie radio is taken to pad, and one is kept in Launch Control
- ❏ **[4.2]** Walk to pad (at least 3 people carrying Darwin III).
- ❏ **[4.3]** Install stopper for rail guides.
- ❏ **[4.4]** Mount rocket on rail guide at horizontal position
- ❏ **[4.5]** Install Umbilical Holder using 2x M8x70 T-NUTS and 2x M8 Flanged Nuts.
- ❏ **[4.6]** Raise to predetermined launch angle (TBD on day)
- ❏ **[4.7]** Final confirmation of avionics1 health
  - ❏ **[4.7.1] Confirm Continuity on Eggtimer Quantum**
  - ❏ **[4.7.2] Pending approval of LCO arm COTS avionics, SRAD avionics**
  - ❏ **[4.7.3] Confirm continuity on COTS Avionics**
  - ❏ **[4.7.4] Confirm continuity on SRAD Avionics**
  - ❏ **[4.7.5] Flight Controller instructs GSO to Switch to Umbilical Power**
  - ❏ **[4.7.6] GSO confirms switch by confirming PSU Voltage increases from 8.4V to 12V. Beeps increase frequency to once a second.**
- ❏ **[4.9]** Let PO install motor igniter.
- ❏ **[4.10]** Leave Launch Pad

SRAD BEEP GLOSSARY Three single tone beeps in quick succession, once: Avionics has been turned on
Three beeps in ascending tone, once: connection to SRAD GS succcessful
Short beep every two seconds: Vehicle is unarmed and on internal power
Short beep every second: vehicle is unamerd and on external power
Five fast beeps, once: vehicle is recording at high speed and is armed.

tpage

E.7 Countdown checklist

Procedure ID:	PAD2
Responsible Engineers:	Thomas Stott, Alberto Progida, Ann Lee, Joseph Azrak, Matus Komjaty
Date:	Launch window date
Location of test:	MCO, Santa Margarida Army Base, Portugal
Equipment used:	Ground Station, Yagi Antennas, Binoculars, Compass, Notepad
Procedure Aim:	Final preparations to initiate countdown.

- ❏ **[1.1]** Confirm Connection to COTS/SRAD ground stations
- ❏ **[1.2]** Prepare compass and SRAD GS yagi to point toward recovery bearing (to be noted on notepad)
- ❏ **[1.3]** Once launch is confirmed, await t-300s to broadcast "READY TO LAUNCH" datagram, disconnecting External Power, activating cameras and enabling high-frequency data-logging.
- ❏ **[1.4]** Attempt to maintain accurate tracking throughout flight, remaining composed until chute deployment is visually confirmed.
- ❏ **[1.4]** Record last received GPS reading from both COTS and SRAD GS

E.8 Rocket search and rescue checklist

Procedure ID:	PAD3
Responsible Engineers:	Thomas Stott, Alberto Progida, Alex Stevenson
Date:	Launch window date
Location of test:	Santa Margarida Army Base, Portugal
Equipment used:	Communication tools (walkie-talkie, phone) Ground station Container for black powder Container for separation charges Container for hardware Container for general trash
Procedure Aim:	Prepare for rocket recovery search.

- ❏ **[1.1]** Estimate location of rocket with visual bearing checks and ground station signal, and estimate possible duration of recovery search
- ❏ **[1.2]** Ensure all members are prepared to start recovery search and create a list of personnel and equipment
  - ❏ **[2.1]** Ensure communication tools are functional
  - ❏ **[2.2]** Ensure all members know the bearing of the rocket and can communicate with ground station
  - ❏ **[2.3]** Ensure all members are dressed appropriately for rough terrain
- ❏ **[3.0]** If rocket is found with no visible flames and/or smoke:
  - ❏ **[3.1]** Ensure that no smoke is coming off
  - ❏ **[3.2]** Carefully approach and ensure that no parts are warm to the touch and note sharp edges
  - ❏ **[3.3]** Carefully separate parts with exhausted separation charges if possible and store in separate containers for transportation
  - ❏ **[3.4]** Ensure all members are present and return to base
- ❏ **[4.0]** If rocket is found with visible flames and/or smoke, follow the instructions of military personnel and bombeiros

work preflight (change eggtimer switch, who goes where), preflight

E.9 Assembly Checklist

Procedure ID:	PAD1
Responsible Engineers:	Tom Stott, Alberto Progida, Zsolt Csonka
Date:	Launch window date
Location of test:	Santa Margarida Army Base, Portugal
Equipment used:	Allen keys (M2, M2.5, M3) Avionics arming key Separation charges Ground station Fully assembled Nose Cose (including payload and connection to parachutes) Recovery Bay with parachutes loaded Recovery Bulkhead without separation charges Fully assembled Avionics bay & airbrake stack & Lower Body (including motor)
Procedure Aim:	Mount fully assembled rocket to launch rail and prepare for countdown.

- Preparation
  - ❏ **[1.1]** Ensure the SRAD and COTS FC is powered off
  - ❏ **[1.1]** Ensure the Payload Avionics are is powered on
- Mechanical Assembly
  - ❏ **2.1** Insert COTS and SRAD separation charges and assemble Nose Cone, Recovery Bay & Recovery Bulkhead (REC1), Avionics Bay and assembly Motor (PROP1)
    - ❏ **2.1.1** Nose Cone to Payload Bulkhead: 4x M4 bolts
    - ❏ **2.1.2** Payload Bulkhead to Recovery Bay: 4x M3 shear pins
    - ❏ **2.1.3** Recovery Bay to Recovery Bulkhead: 5x M4 bolts
    - ❏ **2.1.4** Recovery Bulkhead to Avionics Bay and below: 3 M5 shoulder head socket screws
- Avionics configuration
  - ❏ **[3.1]** Await launch window confirmation from RSO
  - ❏ **[3.2]** Power on COTS and SRAD Avionics (Switches 1, 2 respectively)
  - ❏ **[3.3]** Await for signal from GSO that SRAD calibration and software tests are successfully completed
  - ❏ **[3.4]** Reconfigure RAD/COTS telemetry frequencies (if necessary)
- Proceed to pad
  - ❏ **[4.1]** Ensure charged walkie-talkie radio is taken to pad, and one is kept in Launch Control
  - ❏ **[4.1]** Walk to pad (at least 3 people carrying Darwin III.
  - ❏ **[4.1]** Mount rocket on rail guide at horizontal position
  - ❏ **[4.2]** Raise to predetermined launch angle (TBD on day)
  - ❏ **[4.3]** Final confirmation of vehicle health

F — Engineering Drawings

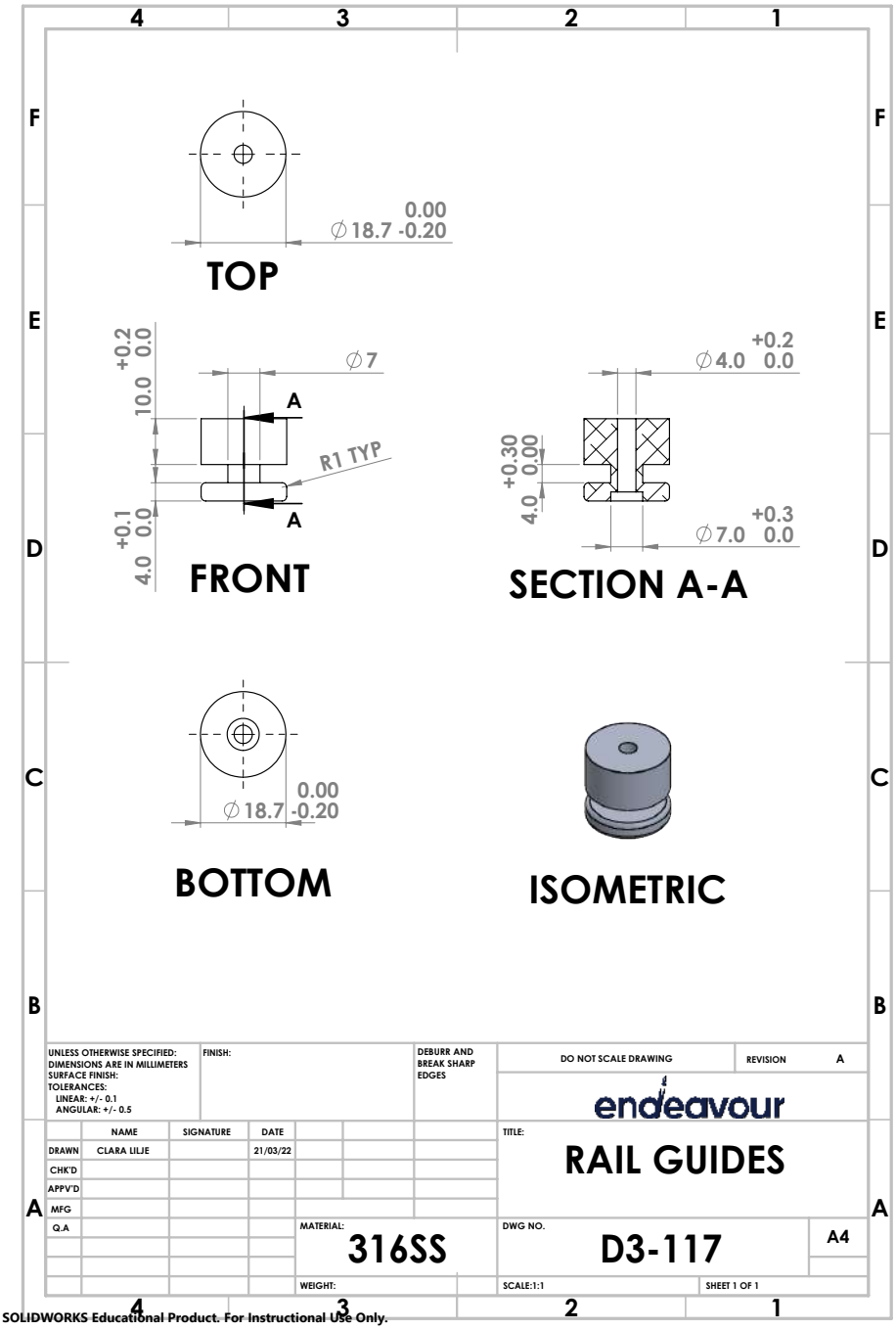

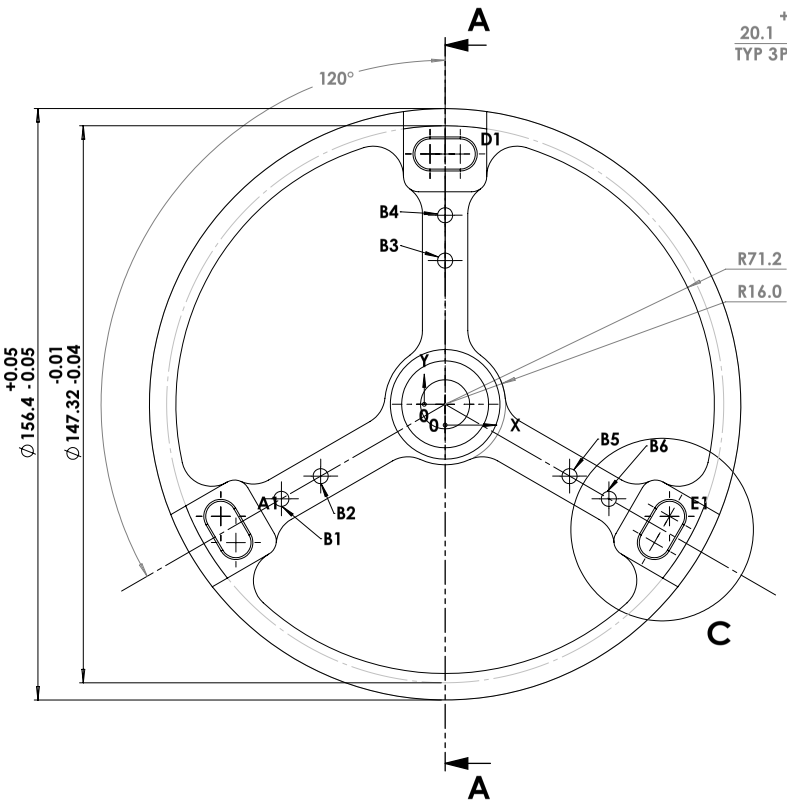

TOP VIEW

TAG	X LOC	Y LOC	SIZE
B1	-43.30	-25	M4x0.7 THRU
B2	-32.91	-19	
B3	0	38	
B4	0	50	
B5	32.91	-19	
B6	43.30	-25	
A1	-57.33	-33.10	8x16 SLOT Perpendicular to Radius
D1	0	66.20	
E1	57.33	-33.10	

HOLE TABLE

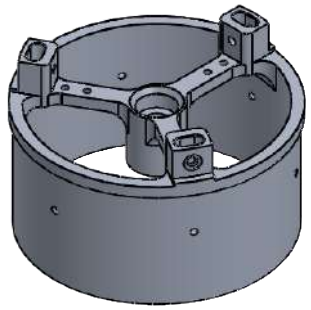

ISOMETRIC VIEW
SCALE 1:2

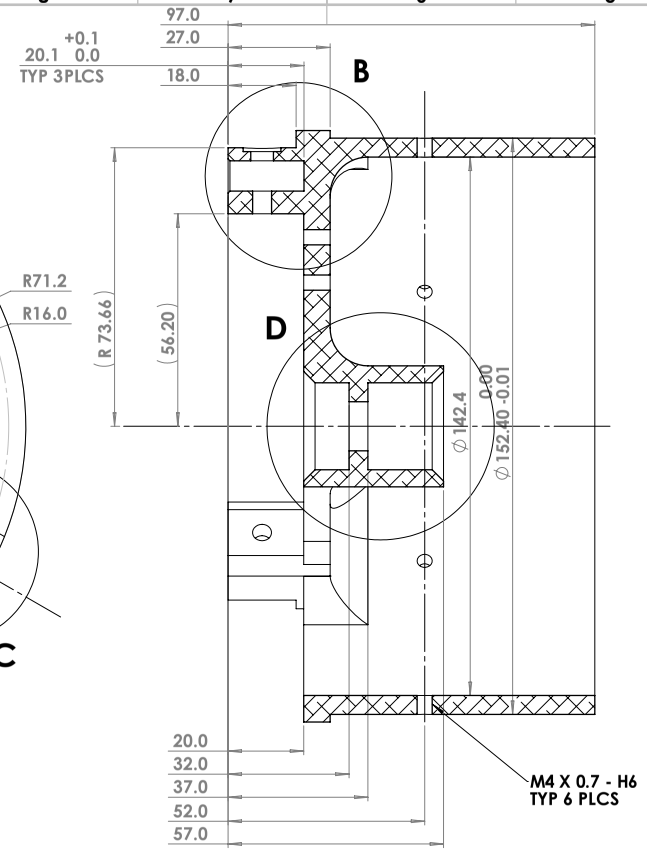

SECTION A-A
SCALE 1 : 1

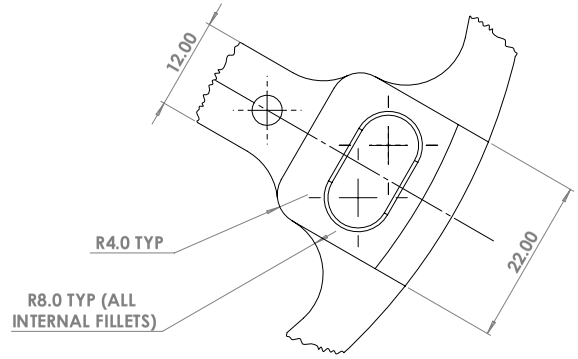

DETAIL C
SCALE 2 : 1

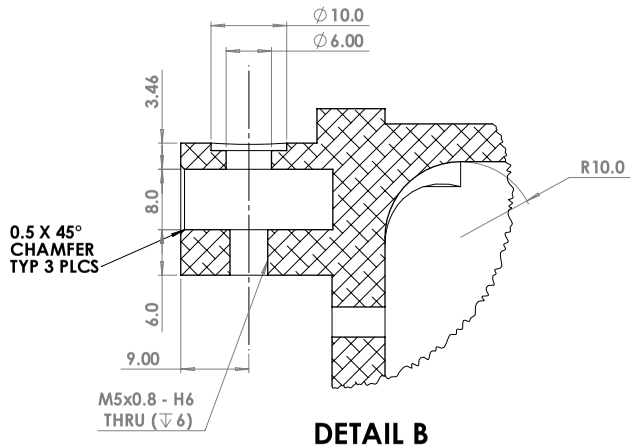

DETAIL B
SCALE 2 : 1

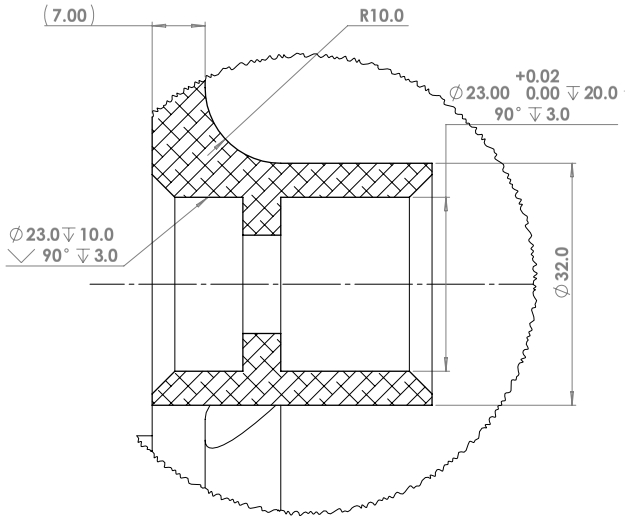

DETAIL D
SCALE 2 : 1

UNLESS OTHERWISE SPECIFIED: DIMENSIONS ARE IN MILLIMETERS SURFACE FINISH: TOLERANCES: LINEAR: +/- 0.1mm ANGULAR: +/- 0.5°		FINISH:		DEBURR AND BREAK SHARP EDGES		DO NOT SCALE DRAWING	REVISION A
	NAME	SIGNATURE	DATE			endeavour	
DRAWN	Alberto Progida		03/04			TITLE: MOTOR BULKHEAD	
CHK'D							
APPV'D							
MFG							
Q.A							
				MATERIAL: ALUMINIUM 7075-T6		DWG NO. D3-111	A2
				WEIGHT:		SCALE:1:1	SHEET 1 OF 1

SOLIDWORKS Educational Product. For Instructional Use Only.

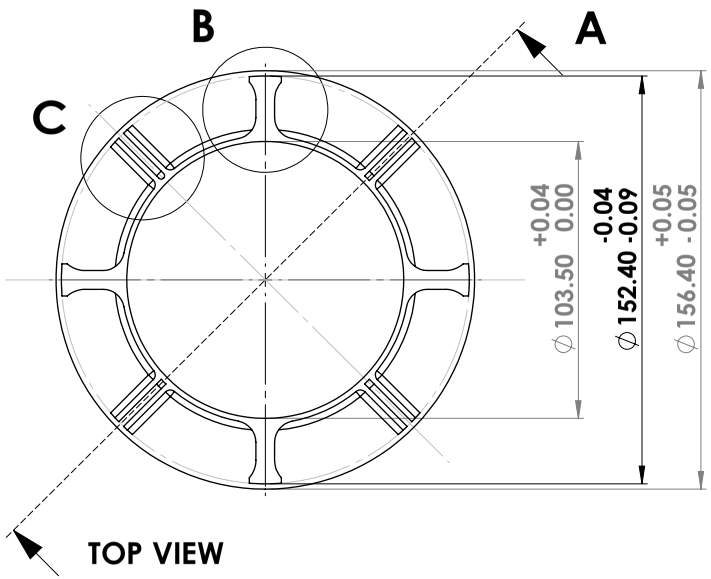

TOP VIEW

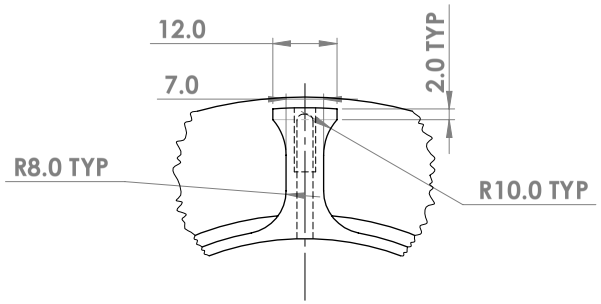

DETAIL B
SCALE 1 : 1

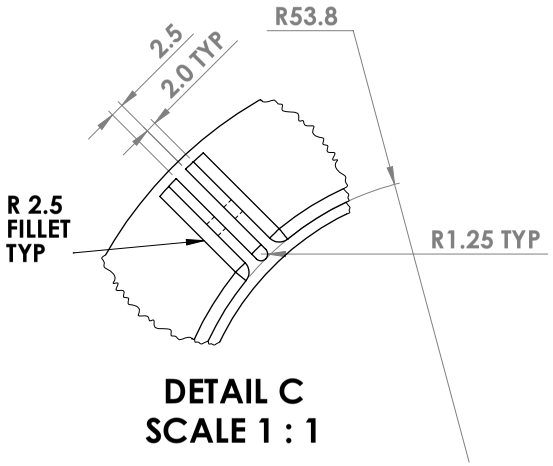

DETAIL C
SCALE 1 : 1

A

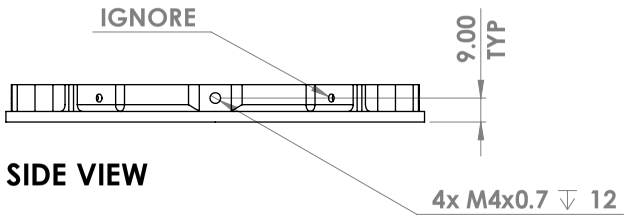

SIDE VIEW

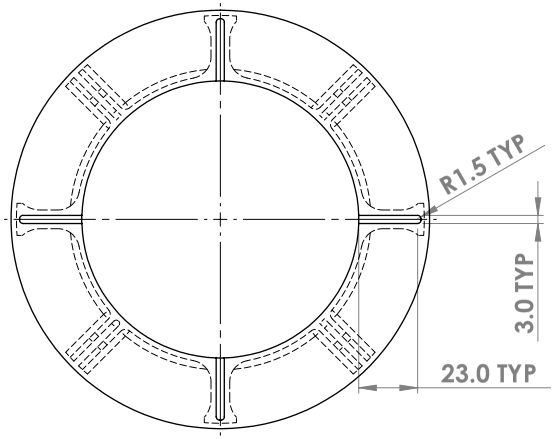

BOTTOM VIEW

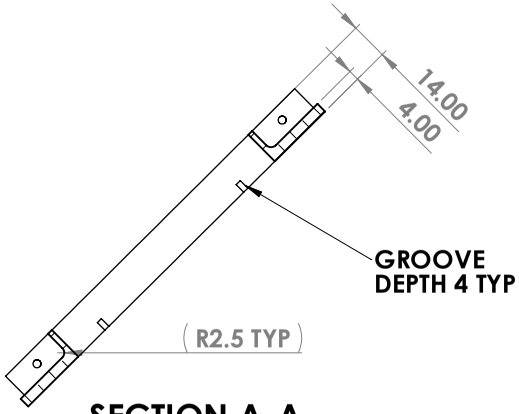

SECTION A-A

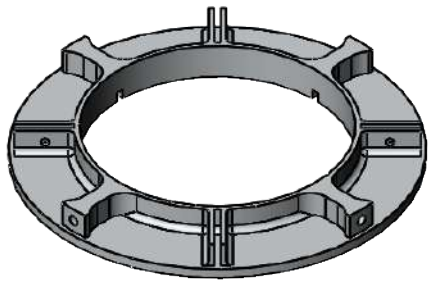

ISOMETRIC VIEW

UNLESS OTHERWISE SPECIFIED: DIMENSIONS ARE IN MILLIMETERS SURFACE FINISH: TOLERANCES: LINEAR: +/- 0.1 ANGULAR: +/- 0.5		FINISH:		DEBURR AND BREAK SHARP EDGES	DO NOT SCALE DRAWING	REVISION B
	NAME	SIGNATURE	DATE		endeavour	
DRAWN	ZSOLT CSONKA		02/03/22		TITLE:	
CHK'D	ALBERTO PROGIDA	A.P.	22/03/22		THRUST PLATE	
APPV'D	ZSOLT CSONKA		03/04/22			
MFG						
Q.A				MATERIAL: Aluminium 7075-T6	DWG NO. D3-105	A3
				WEIGHT:	SCALE:1:2	SHEET 1 OF 1

SOLIDWORKS Educational Product. For Instructional Use Only.

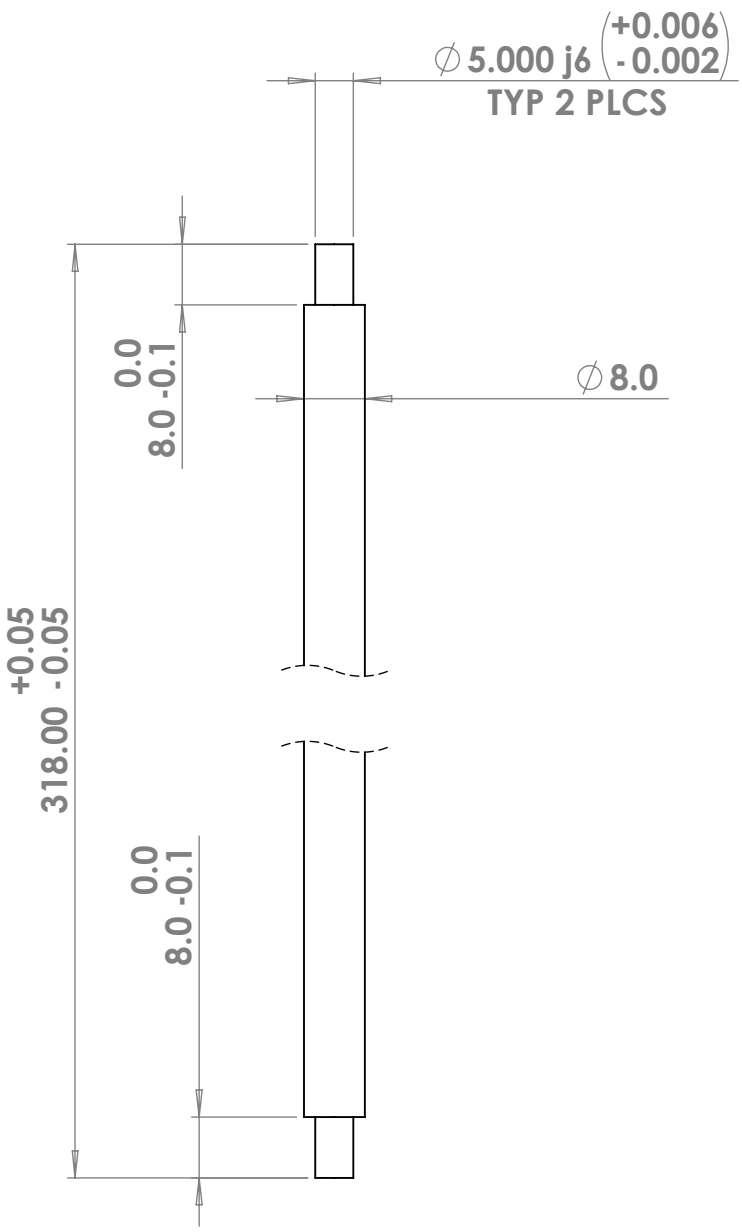

UNLESS OTHERWISE SPECIFIED: DIMENSIONS ARE IN MILLIMETERS SURFACE FINISH: TOLERANCES: LINEAR: +/- 0.1MM ANGULAR: +/- 0.5 DEG	FINISH: WELD-READY	DEBURR AND BREAK SHARP EDGES	DO NOT SCALE DRAWING	REVISION			
	NAME	SIGNATURE	DATE				TITLE: COMPRESSION ROD QUANTITY: 3
DRAWN	ZSOLT CSOKA		26/03				
CHK'D	ALBERTO PROGIDA		03/04				
APPV'D							
MFG							
Q.A				MATERIAL: 316L STAINLESS STEEL			DWG NO. D3-301
							A4
				WEIGHT:		SCALE:1:2	SHEET 1 OF 1

endeavour

SOLIDWORKS Educational Product. For Instructional Use Only.

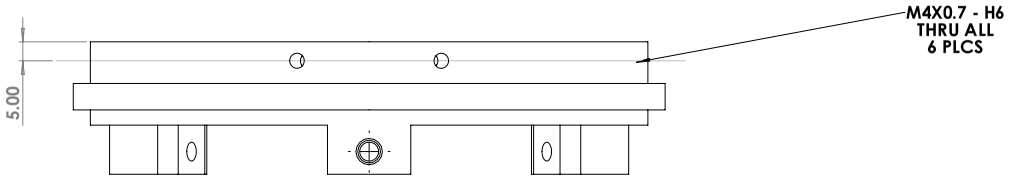

SIDE ELEVATION

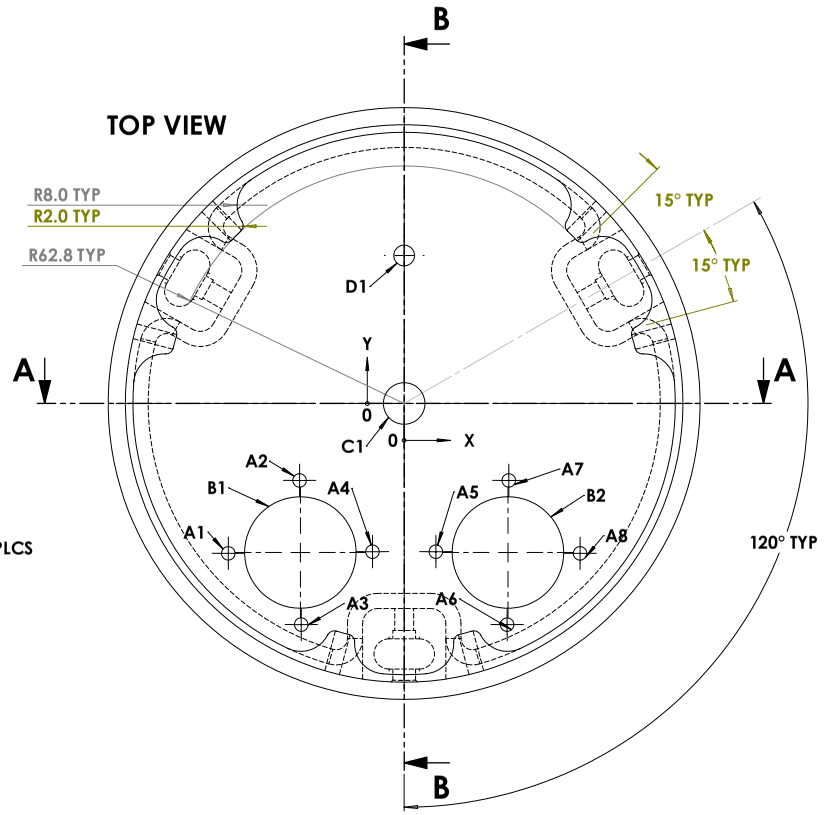

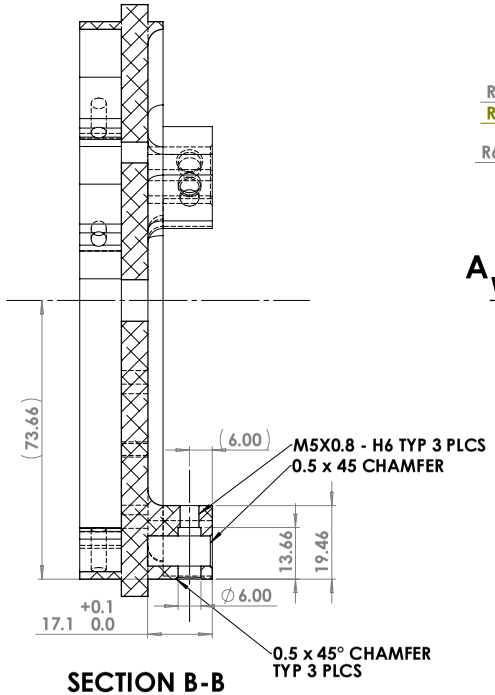

SECTION B-B
SCALE 1 : 1

HOLE TABLE
(TOP VIEW)

TAG	X LOC	Y LOC	SIZE
A1	-46.47	-39.60	∅3.58 THRU
A2	-27.64	-20.33	
A3	-27.21	-58.43	
A4	-8.37	-39.17	
A5	8.37	-39.17	
A6	27.21	-58.43	
A7	27.64	-20.33	
A8	46.47	-39.60	
B1	-27.42	-39.38	∅29.46 THRU
B2	27.42	-39.38	
C1	0	0	∅11.0 THRU
D1	0	39.10	∅5.5 THRU

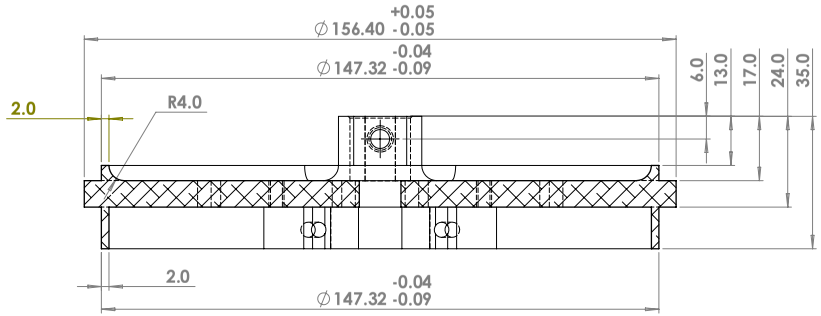

SECTION A-A
SCALE 1 : 1

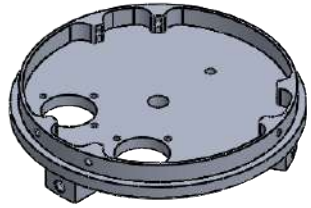

ISOMETRIC VIEW
SCALE 1:2

UNLESS OTHERWISE SPECIFIED:
DIMENSIONS ARE IN MILLIMETERS
SURFACE FINISH:
TOLERANCES:
LINEAR: +/- 0.1
ANGULAR: +/- 0.5°

FINISH:

DEBURR AND BREAK SHARP EDGES

DO NOT SCALE DRAWING

REVISION

endeavour

	NAME	SIGNATURE	DATE
DRAWN	Alberto Progida		23/03/22
CHK'D	ZSOLT CSONKA		04/04/22
APP'V'D			
MFG			
Q.A			

TITLE:
RECOVERY BULKHEAD

MATERIAL: ALUMINIUM 7075-T6

DWG NO. D3-401

A2

WEIGHT:

SCALE:1:1

SHEET 1 OF 2

SOLIDWORKS Educational Product. For Instructional Use Only.

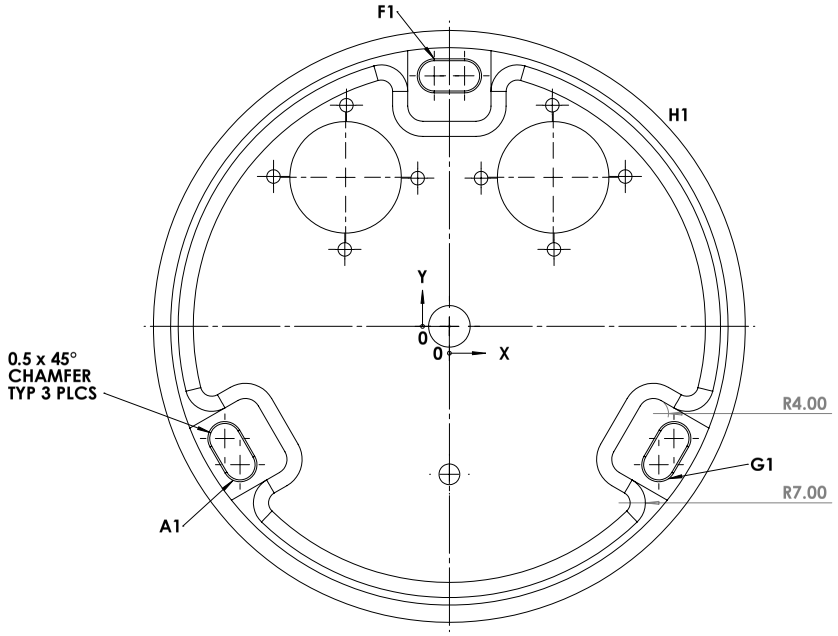

BOTTOM VIEW

HOLE TABLE
(BOTTOM VIEW)

TAG	X LOC	Y LOC	SIZE
A1	-57.33	-33.10	8 x 16 SLOT (Perpendicular to Radius)
F1	0	66.20	
G1	57.33	-33.10	
H1	0	0	∅147.32 THRU

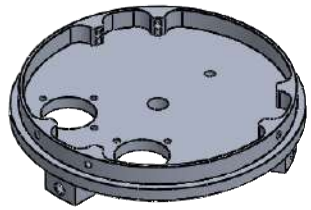

ISOMETRIC VIEW
SCALE 1:2

UNLESS OTHERWISE SPECIFIED: DIMENSIONS ARE IN MILLIMETERS SURFACE FINISH: TOLERANCES: LINEAR: +/- 0.1 ANGULAR: +/- 0.5 DEG		FINISH:		DEBURR AND BREAK SHARP EDGES		DO NOT SCALE DRAWING	REVISION A
	NAME	SIGNATURE	DATE			TITLE:	
DRAWN	ALBERTO PROGIDA		23/03/22			RECOVERY BULKHEAD	
CHK'D	ZSOLT CSONKA		04/04/22				
APP'V'D							
MFG							
Q.A				MATERIAL: ALUMINIUM 7075-T6		DWG NO. D3-401	A2
				WEIGHT:		SCALE:1:1	SHEET 2 OF 2

SOLIDWORKS Educational Product. For Instructional Use Only.

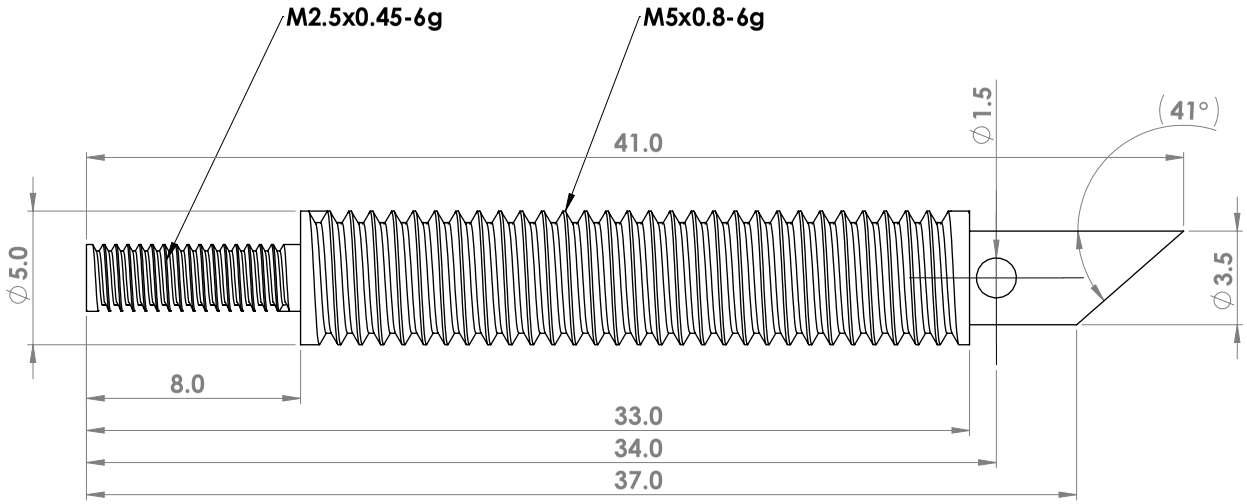

SIDE VIEW

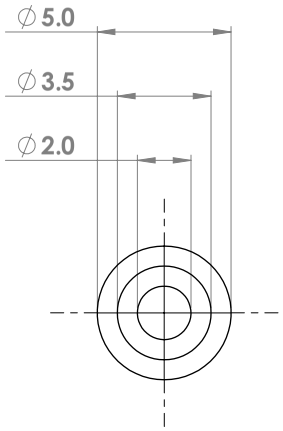

FRONT VIEW



ISOMETRIC VIEW

UNLESS OTHERWISE SPECIFIED: DIMENSIONS ARE IN MILLIMETERS SURFACE FINISH: TOLERANCES: LINEAR: +/- 0.1MM ANGULAR: +/- 0.5 DEG		FINISH:		DEBURR AND BREAK SHARP EDGES	DO NOT SCALE DRAWING	REVISION
	NAME	SIGNATURE	DATE		endeavour	
DRAWN	ALEX STEVENSON		01/04		TITLE: RECOVERY CUTTER	
CHK'D	ALBERTO PROGIDA		04/04			
APPV'D						
MFG						
Q.A				MATERIAL: 304 1020 steel STAINLESS STEEL	DWG NO. D3-406A	A3
				WEIGHT:	SCALE:5:1	SHEET 1 OF 1

SOLIDWORKS Educational Product. For Instructional Use Only.

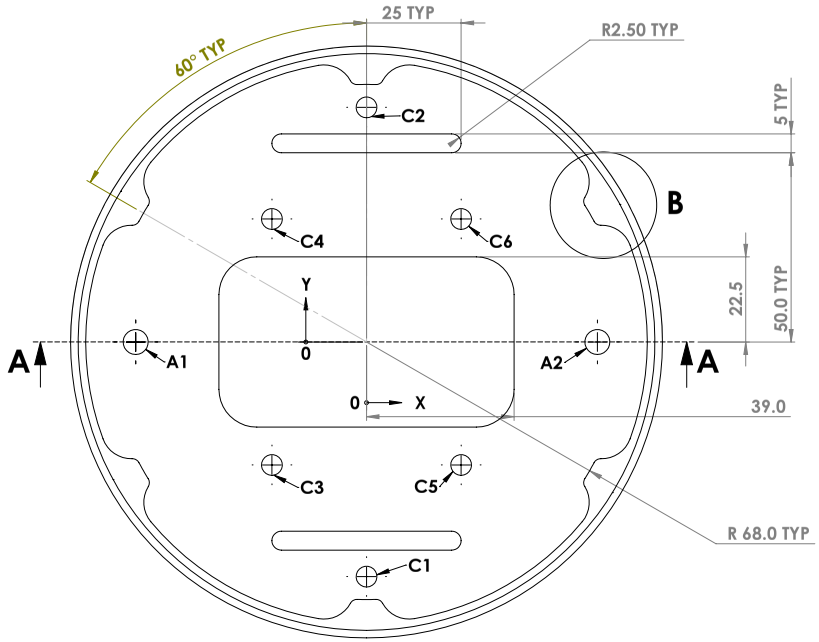

TOP VIEW

HOLE TABLE

TAG	X LOC	Y LOC	SIZE
A1	-61	0	∅6.60 THRU
A2	61	0	
C1	0	-62	∅5.50 THRU
C2	0	62	
C3	-25	-32.50	
C4	-25	32.50	
C5	25	-32.50	
C6	25	32.50	

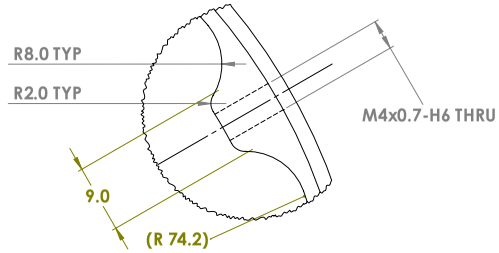

DETAIL B
SCALE 2 : 1

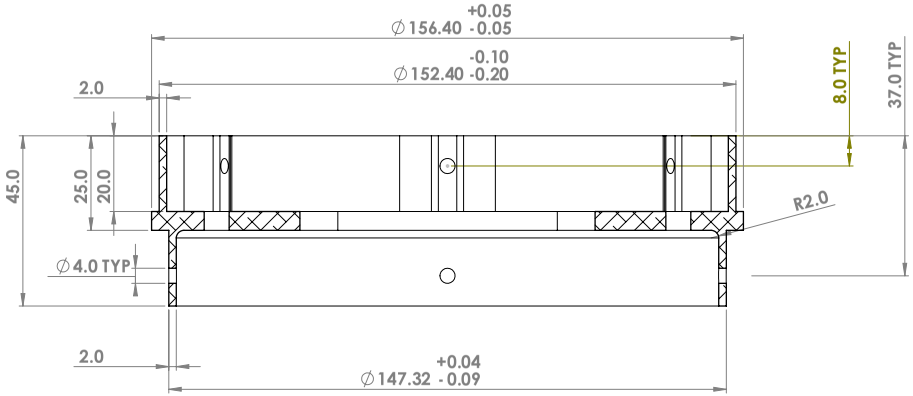

SECTION A-A

ISOMETRIC VIEW
SCALE 1:1.5

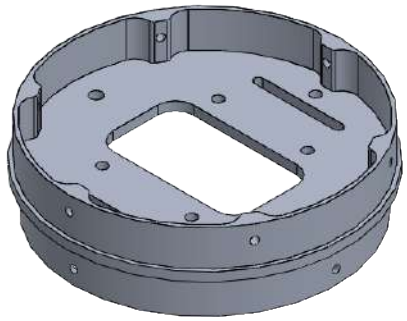

UNLESS OTHERWISE SPECIFIED: DIMENSIONS ARE IN MILLIMETERS SURFACE FINISH: TOLERANCES: LINEAR: +/- 0.1 ANGULAR: +/- 0.5°	FINISH:	DEBURR AND BREAK SHARP EDGES	DO NOT SCALE DRAWING / REVISION
	NAME / SIGNATURE / DATE		endeavour
DRAWN	ZSOLT CSONKA / 25/03		TITLE: PAYLOAD BULKHEAD
CHK'D	ALBERTO PROGIDA / 03/04		
APP'V'D			
MFG			
Q.A		MATERIAL: ALUMINIUM 7075-76	DWG NO. D3-501 / A2
		WEIGHT:	SCALE:1:1 / SHEET 1 OF 1

SOLIDWORKS Educational Product. For Instructional Use Only.

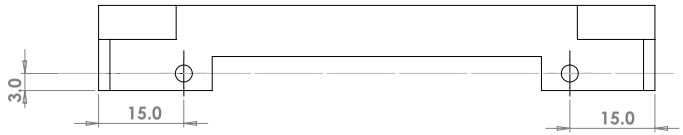

BACK ELEVATION

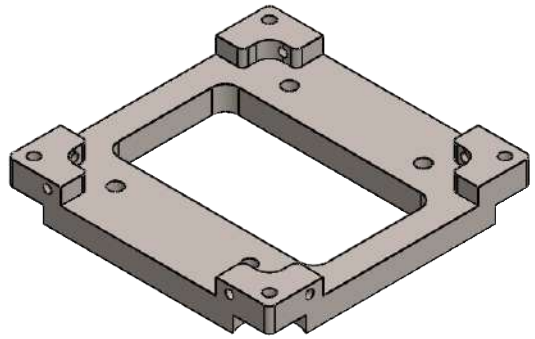

ISOMETRIC

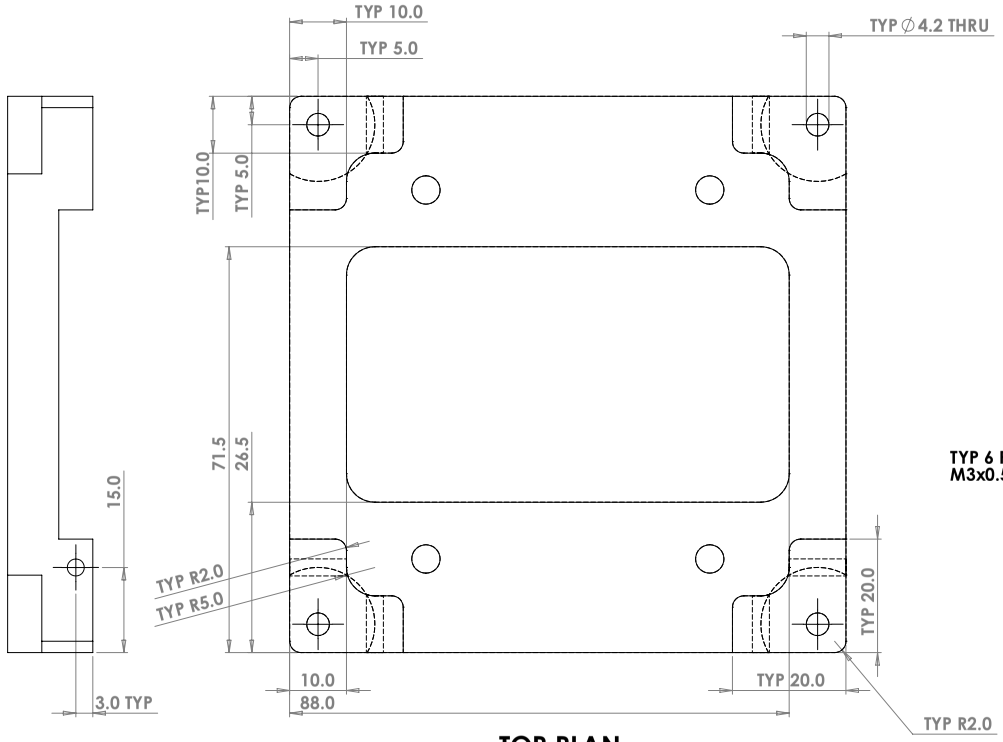

LEFT END ELEVATION

TOP PLAN

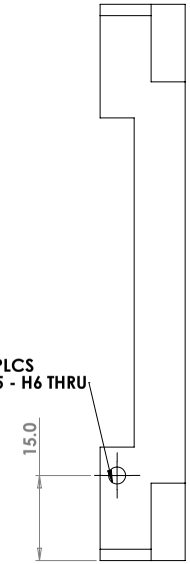

RIGHT END ELEVATION

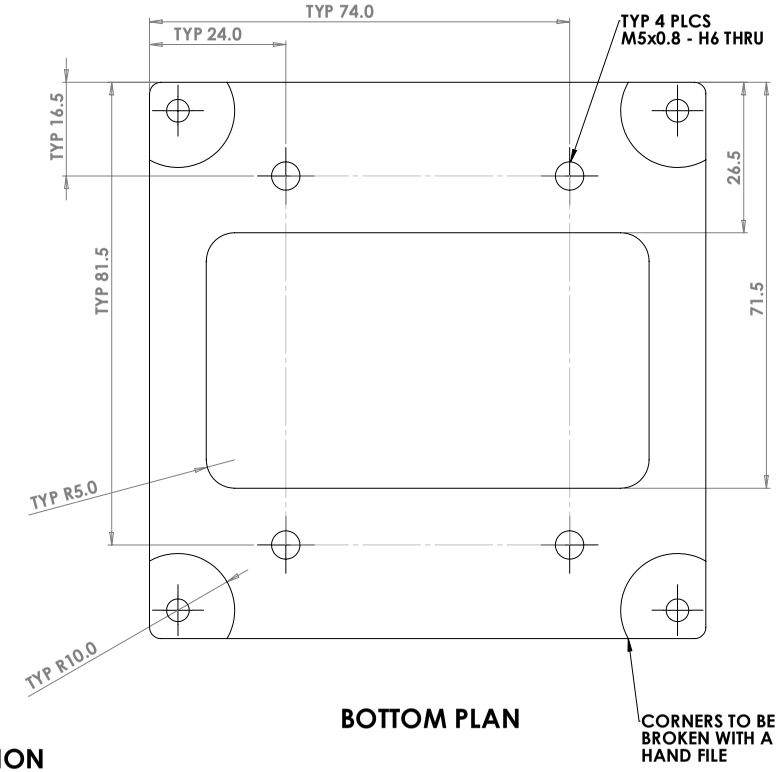

BOTTOM PLAN

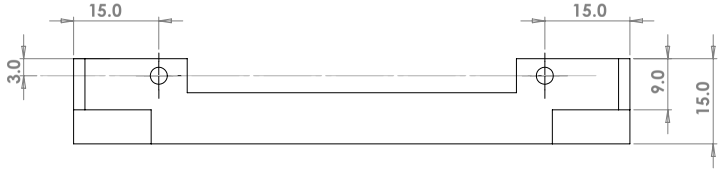

FRONT ELEVATION

REV	REASON FOR CHANGE
A	FIRST DRAFT. REVISED TO EASIER MANUFACTURE
B	CHANGE INTERNAL FILETS. CHANGE SQUARE INDENTS TO CIRCULAR FOR EASIER MANUFACTURE. REMOVED EXTRUDES AND INCREASED THICKNESS OF BULKHEAD

UNLESS OTHERWISE SPECIFIED:
DIMENSIONS ARE IN MILLIMETERS
SURFACE FINISH:
TOLERANCES:
LINEAR: +/- 0.1mm
ANGULAR: +/- 0.1 deg

FINISH:

DEBURR AND BREAK SHARP EDGES

DRAWING NOT TO SCALE | REVISION B

endeavour

	NAME	SIGNATURE	DATE
DRAWN	JO SHEPTON		22/03/22
CHK'D	Alberto Progida		02/04/22
APP'V'D			
MFG			
Q.A			

TITLE: PLD CUBESAT LOWER BULKHEAD

MATERIAL: 316L Stainless Steel

DWG NO. D3-502

A2

WEIGHT: 531.32g

SCALE:1:1.5

SHEET 1 OF 1

SOLIDWORKS Educational Product. For Instructional Use Only.

ISOMETRIC

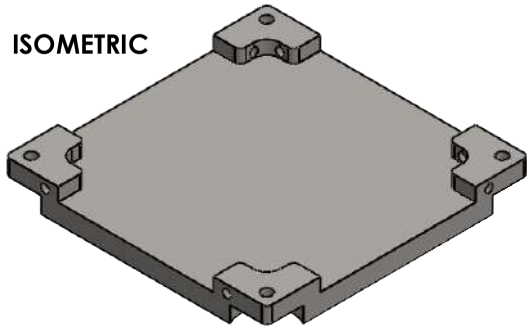

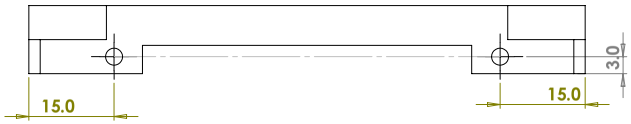

ELEVATION

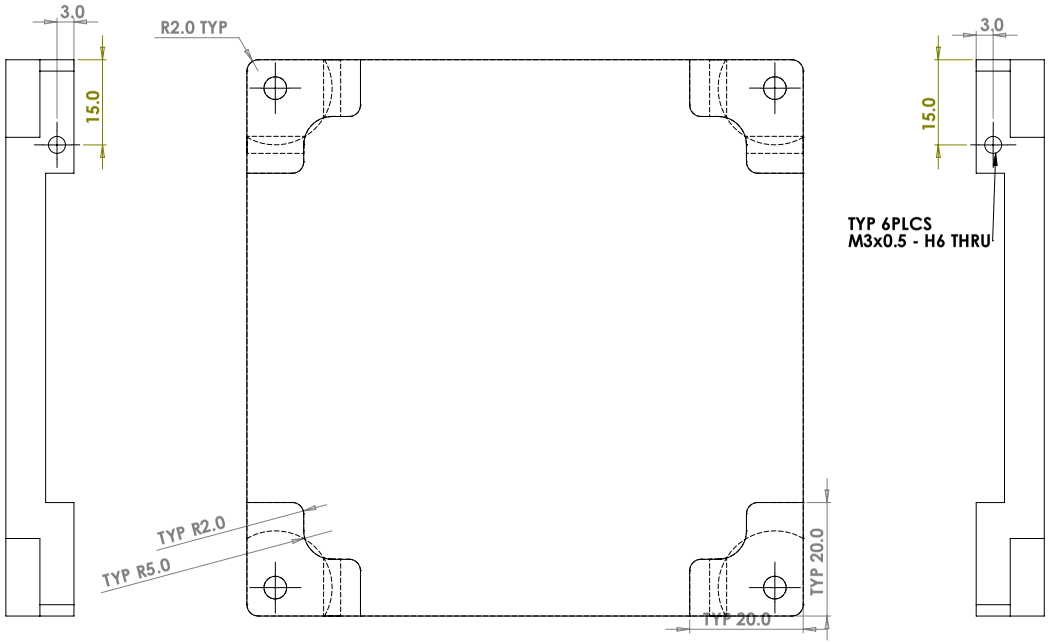

END ELEVATION

TOP PLAN

END ELEVATION

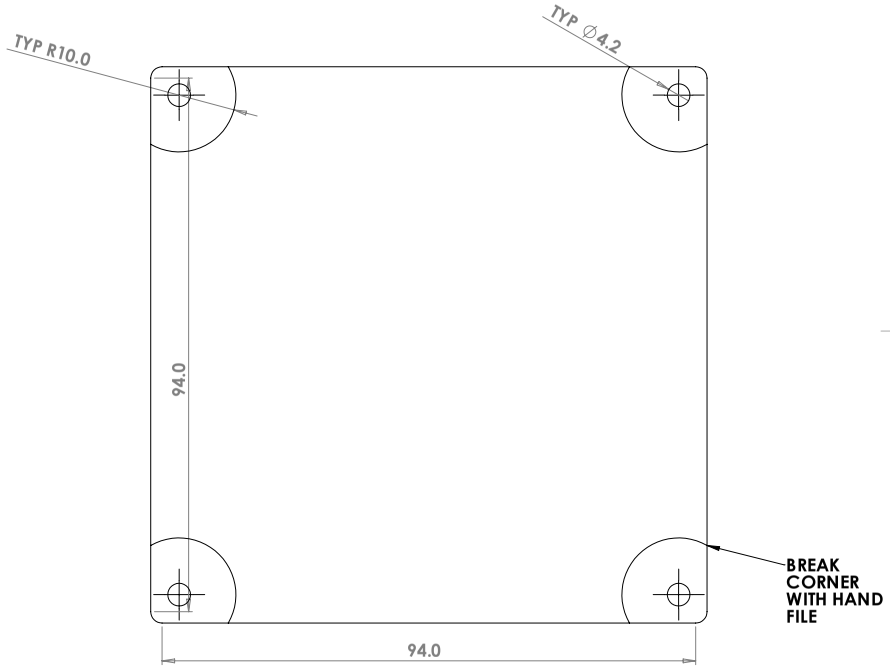

BOTTOM PLAN

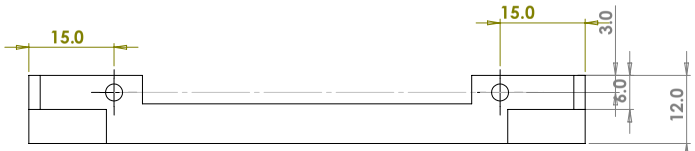

ELEVATION

REVISION	CHANGES
A	CHANGES MADE FROM A->B TO MANUFACTURE MORE EASILY
B	INNER FILETS INCREASED. SQUARE INDENTS MADE CIRULAR

UNLESS OTHERWISE SPECIFIED:
DIMENSIONS ARE IN MILLIMETERS
SURFACE FINISH:
TOLERANCES:
LINEAR: +/- 0.1 mm
ANGULAR: +/- 0.1 deg

FINISH:

DEBURR AND BREAK SHARP EDGES

DO NOT SCALE DRAWING | REVISION B

endeavour

	NAME	SIGNATURE	DATE
DRAWN	JO SHEPTON		22/3/22
CHK'D	Alberto Progida		02/04/22
APP'V'D			
MFG			
Q.A			

MATERIAL: 316L STAINLESS STEEL

WEIGHT: 536.24g

TITLE:

PLD CUBESAT UPPER BULKHEAD

DWG NO. D3-503

A2

SCALE: 1.5:1

SHEET 1 OF 1

SOLIDWORKS Educational Product. For Instructional Use Only.

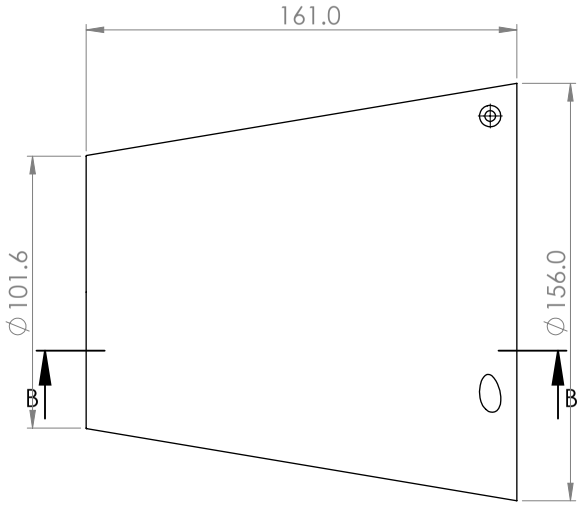

SIDE

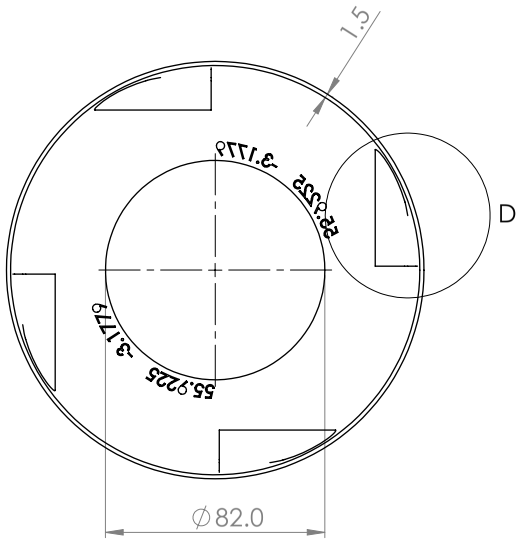

TOP

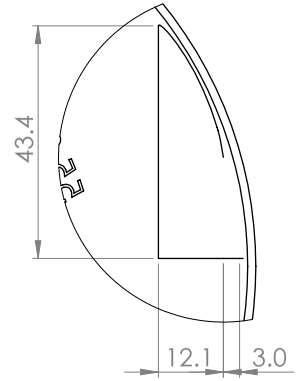

DETAIL D
SCALE 1 : 1

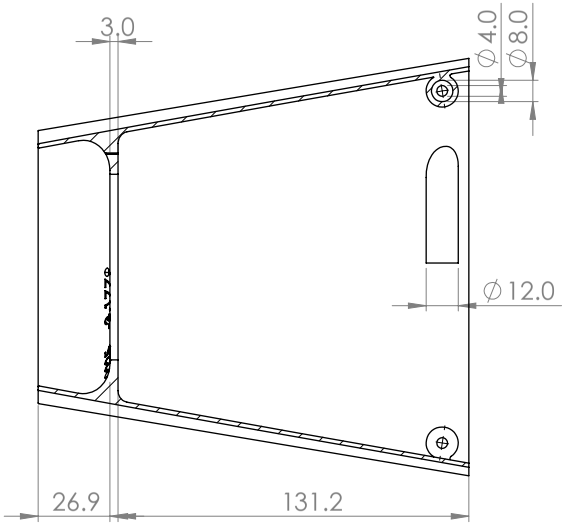

SECTION B-B



ISOMETRIC (SCALE 1:4)

UNLESS OTHERWISE SPECIFIED: DIMENSIONS ARE IN MILLIMETERS SURFACE FINISH: TOLERANCES: LINEAR: +/- 0.1 ANGULAR: +/- 0.5		FINISH:		DEBURR AND BREAK SHARP EDGES	DO NOT SCALE DRAWING	REVISION
	NAME	SIGNATURE	DATE		endeavour	
DRAWN	Clara Lilje		26/8/22		TITLE: AFT CONE	
CHK'D						
APPV'D						
MFG						
Q.A				MATERIAL: CARBON FIBRE	DWG NO. D3-101	A3
				WEIGHT:	SCALE:1:2	SHEET 1 OF 1

SOLIDWORKS Educational Product. For Instructional Use Only.

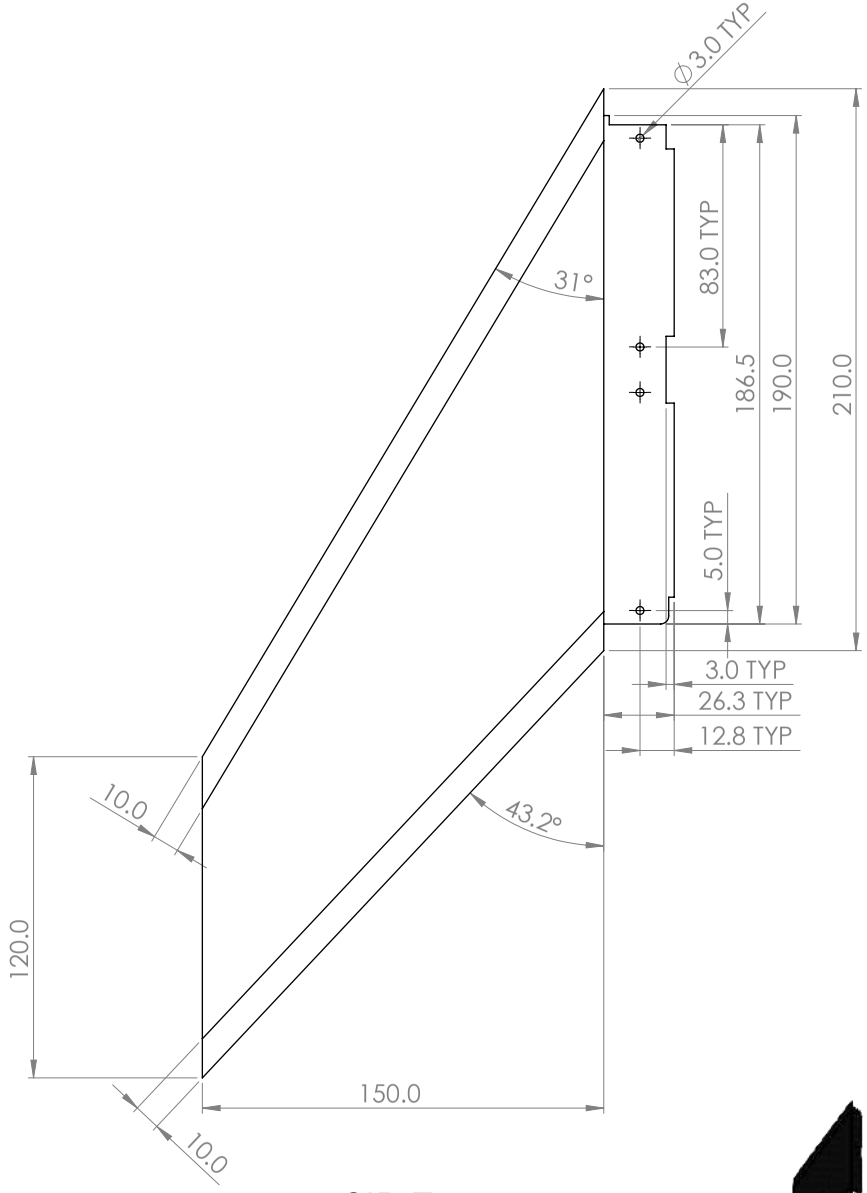

SIDE

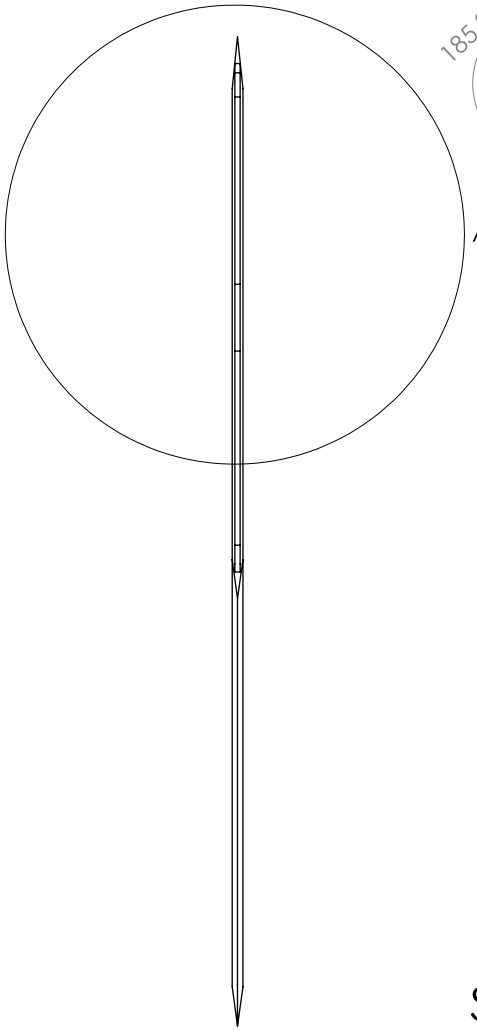

FRONT

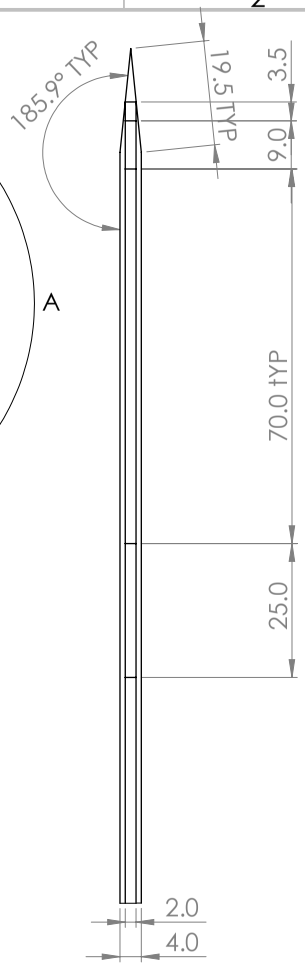

DETAIL A
SCALE 1 : 1

ISOMETRIC
SCALE 1:5

UNLESS OTHERWISE SPECIFIED: DIMENSIONS ARE IN MILLIMETERS SURFACE FINISH: TOLERANCES: LINEAR: +/- 0.1 ANGULAR: +/- 0.5		FINISH:		DEBURR AND BREAK SHARP EDGES		DO NOT SCALE DRAWING	REVISION B
	NAME	SIGNATURE	DATE			endeavour	
DRAWN	Clara Lilje		26/08/22			TITLE: FIN	
CHK'D							
APPV'D							
MFG							
Q.A				MATERIAL: Carbon Fibre		DWG NO. D3 - 106	A3
				WEIGHT:		SCALE:1:2	SHEET 1 OF 1

SOLIDWORKS Educational Product. For Instructional Use Only.

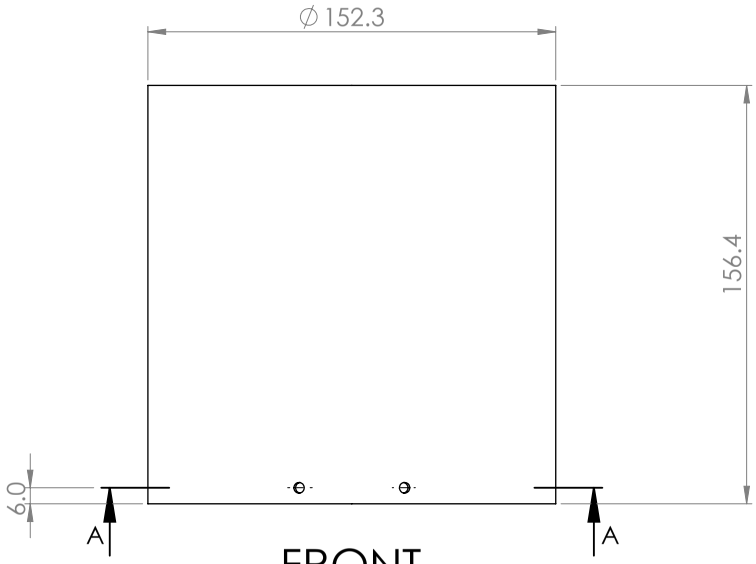

FRONT

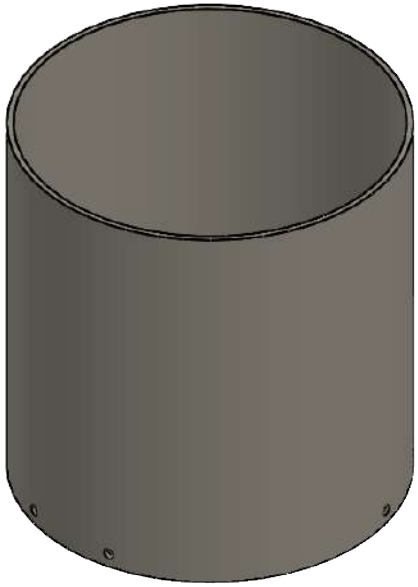

ISOMETRIC

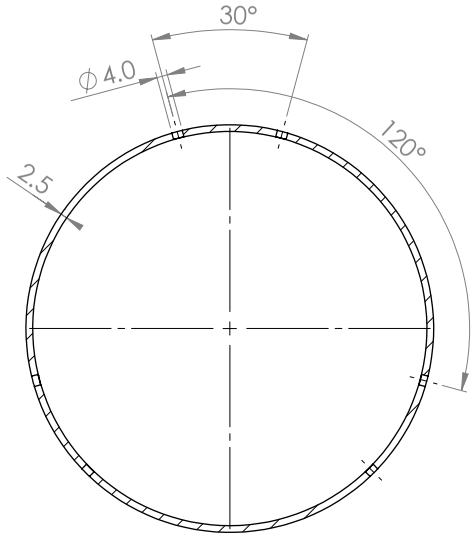

SECTION A-A

UNLESS OTHERWISE SPECIFIED: DIMENSIONS ARE IN MILLIMETERS SURFACE FINISH: TOLERANCES: LINEAR: +/- 0.1 ANGULAR: +/- 0.5		FINISH:		DEBURR AND BREAK SHARP EDGES	DO NOT SCALE DRAWING	REVISION
	NAME	SIGNATURE	DATE		endeavour	
DRAWN	Clara Lilje		26/8/22		TITLE: RECOVERY COUPLING TUBE	
CHK'D						
APPV'D						
MFG						
Q.A				MATERIAL: Glass Fibre	DWG NO. D3-402	A3
				WEIGHT:	SCALE:1:2	SHEET 1 OF 1

SOLIDWORKS Educational Product. For Instructional Use Only.

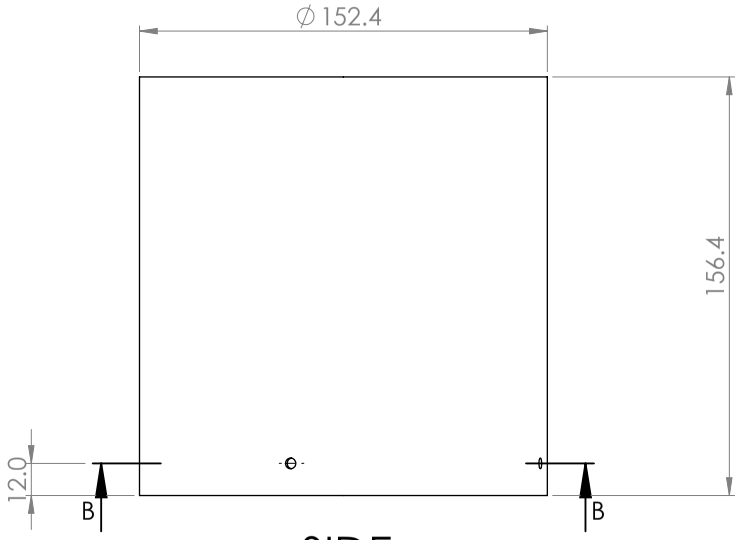

SIDE



ISOMETRIC

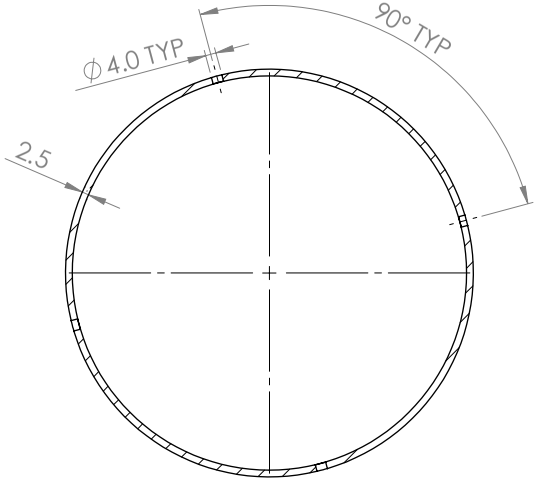

SECTION B-B

UNLESS OTHERWISE SPECIFIED: DIMENSIONS ARE IN MILLIMETERS SURFACE FINISH: TOLERANCES: LINEAR: +/- 0.1 ANGULAR: +/- 0.5		FINISH:		DEBURR AND BREAK SHARP EDGES		DO NOT SCALE DRAWING	REVISION
	NAME	SIGNATURE	DATE			endeavour	
DRAWN	Clara Lilje		26/08/22			TITLE: NOSE CONE COUPLING TUBE	
CHK'D							
APPV'D							
MFG							
Q.A				MATERIAL: GLASS FIBRE		DWG NO. D3-606	A3
				WEIGHT:		SCALE:1:2	SHEET 1 OF 1

SOLIDWORKS Educational Product. For Instructional Use Only.

G — Subsystem Details

G.1 Payload Scientific Background

G.1.1 CosmicWatch Muon Detector

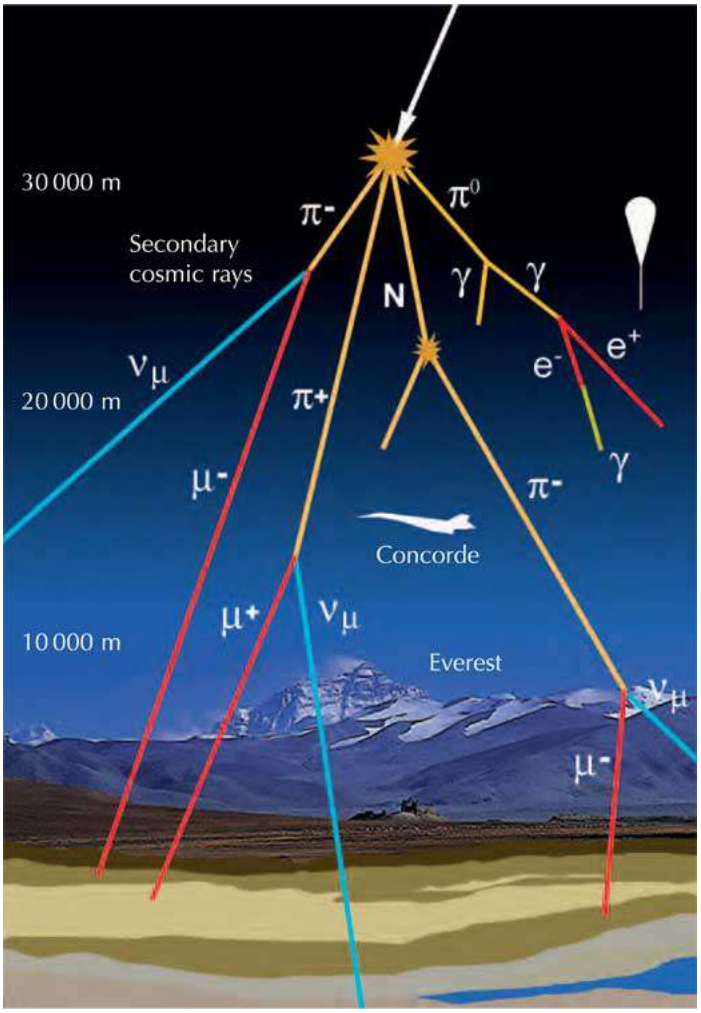

Figure G.1: Muons form in the upper atmosphere and continue down to the Earth's surface. Most other high energy particles decay before reaching the Earth's surface, making muons unique in this regard.

Muons are a result of an interaction between a cosmic ray and a particle nuclei in Earth's upper atmosphere. This results in the formation of a pion ($\pi^{+} or\ \pi^{0}$), which quickly decays into a muon ($\mu^{+} or\ \mu^{-}$) and a muon neutrino ($\nu^{+} or\ \nu^{-}$). Muons are very heavy leptons, with a mass 207 times that of an electron and travel at 0.98 times the speed of light (c). Muon decay follows the exponential decay law:

$$I(t) = I_0 e^{(-\frac{t}{\tau})}, \tag{G.1}$$

where τ is the mean muon lifetime, t is the travel time of the muon from a height with the Lorentz factor (see Equation G.2) taken into account ($t = \gamma\tau$) and I is the flux of muons. Due to their high velocity, muons are primarily used in physics to display Einstein's theory of special relativity. This theorum describes how objects moving at high velocity (at least $0.1c$) will experience time slower compared to a stationary observer. This time dilation effect is governed by the Lorentz factor and also corresponds directly to length contraction,

where objects moving very fast will appear shorter in order to keep the Lorentz factor difference between the moving and stationary reference frames intact. [4][5] The Lorentz factor is:

$$\gamma = \frac{1}{\sqrt{1 - v^2/c^2}}. \tag{G.2}$$

If special relativity is not taken into account, then the muons should travel an average distance of 655.5m. This is not the case, as there are muons detected on Earth, which is approximately 15000m from their point of generation, hence special relativity must be taken into account. In the case of Darwin III, the I_0 will be the muon flux measured at apogee which will be used to calculate the expected muon flux at sea level ($I(t)$). This will then be compared to a measurement taken at sea level to see the discrepancy and the potential reasons for the difference will be explored [6]

G.1.2 Slosh Experiment

Slosh dynamics are an important area of research for liquid rocket engines. Fuel continually moves in a tank, changing the centre of mass, leading to additional stresses and vibrations on the tank [7]. In addition to slosh due to lift off and manoeuvres, there are interesting effects on slosh dynamics during points of microgravity and zero gravity. This area of fluid dynamics has ignited a new section of engineering to design slosh suppressant devices for fuel tanks, such as baffles (a subsection of propellant management devices (PMD)) which affect the surface tension of the liquid and can reduce the slosh. Numerical simulations of these can be performed and compared to a video of fluid slosh in the same tank. In the case of Darwin III, the tank is vertical to simulate that of a rocket fuel tank. Computational fluid dynamic (CFD) simulations have been performed in several areas of industry to explore this effect, which is something we will replicate for this reduced size tank.

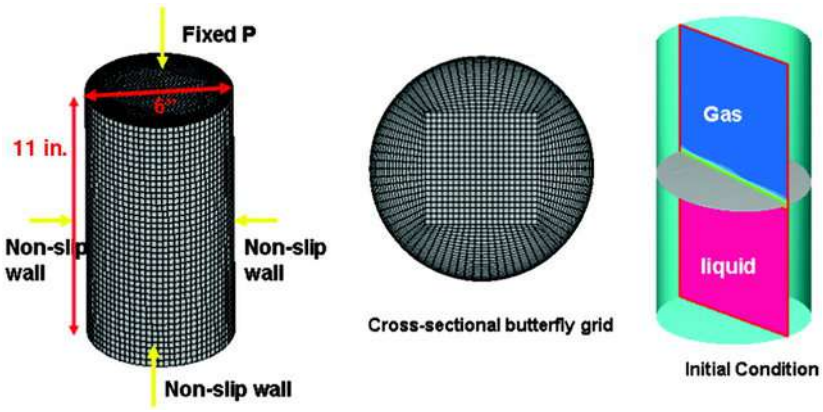

Figure G.2: A CFD simulation which was used as a baseline for slosh observation when looking into PMDs [8]."

H — Detailed Structural and Mechanical Calculations

H.1 Payload 15G Liftoff Load

Responsible Engineers:	Jo Shepton
Date of Test:	04/09/2022
Software Used:	Solidworks
Maximum Stress:	$1.151 \times 10^8 Nm^{-2}$
Material:	316L Stainless Steel
Material Yield Stress:	$3.564 \times 10^7 Nm^{-2}$
Factor of Safety :	3.23
Test Result:	The steel bulkhead has a suitable factor of safety under the expected maximum force of 15G at liftoff.

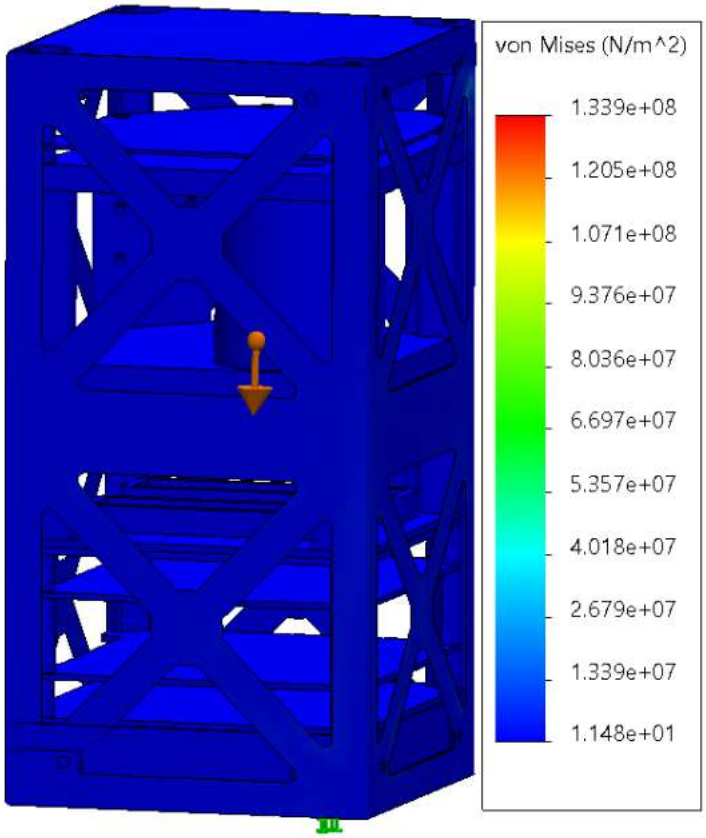

H.2 Payload 180N Parachute Shock Force

Responsible Engineers:	Jo Shepton
Date of Test:	05/09/2022
Software Used:	Solidworks
Maximum Stress:	$1.151 \times 10^8 Nm^{-2}$
Material:	316L Stainless Steel
Material Yield Stress:	$1.334 \times 10^7 Nm^{-2}$
Factor of Safety :	8.63
Test Result:	The steel aft bulkhead has a suitable factor of safety under the expected maximum force of 180N snatch force from parachute deployment at apogee. With a mass of 2.2kg and a velocity change of $24.4ms^{-1}$ in a maximum deployment time of 0.3 seconds, the force (calculated with $F = \frac{m\delta v}{t}$) acting upwards through the aft payload bulkhead is 178.93N.

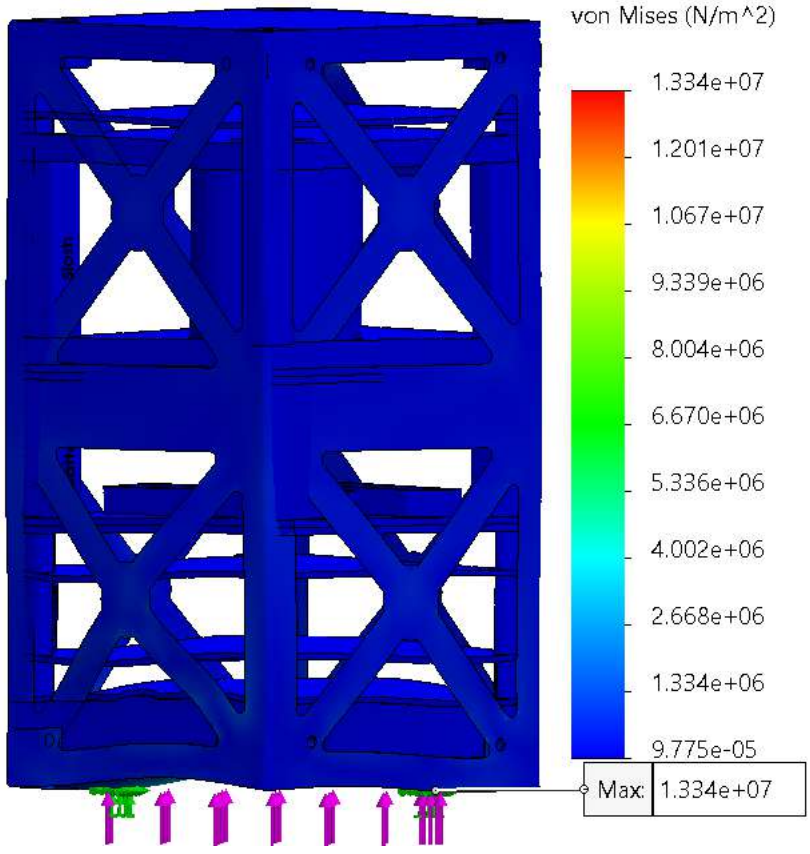

I — Detailed Electrical Schematics

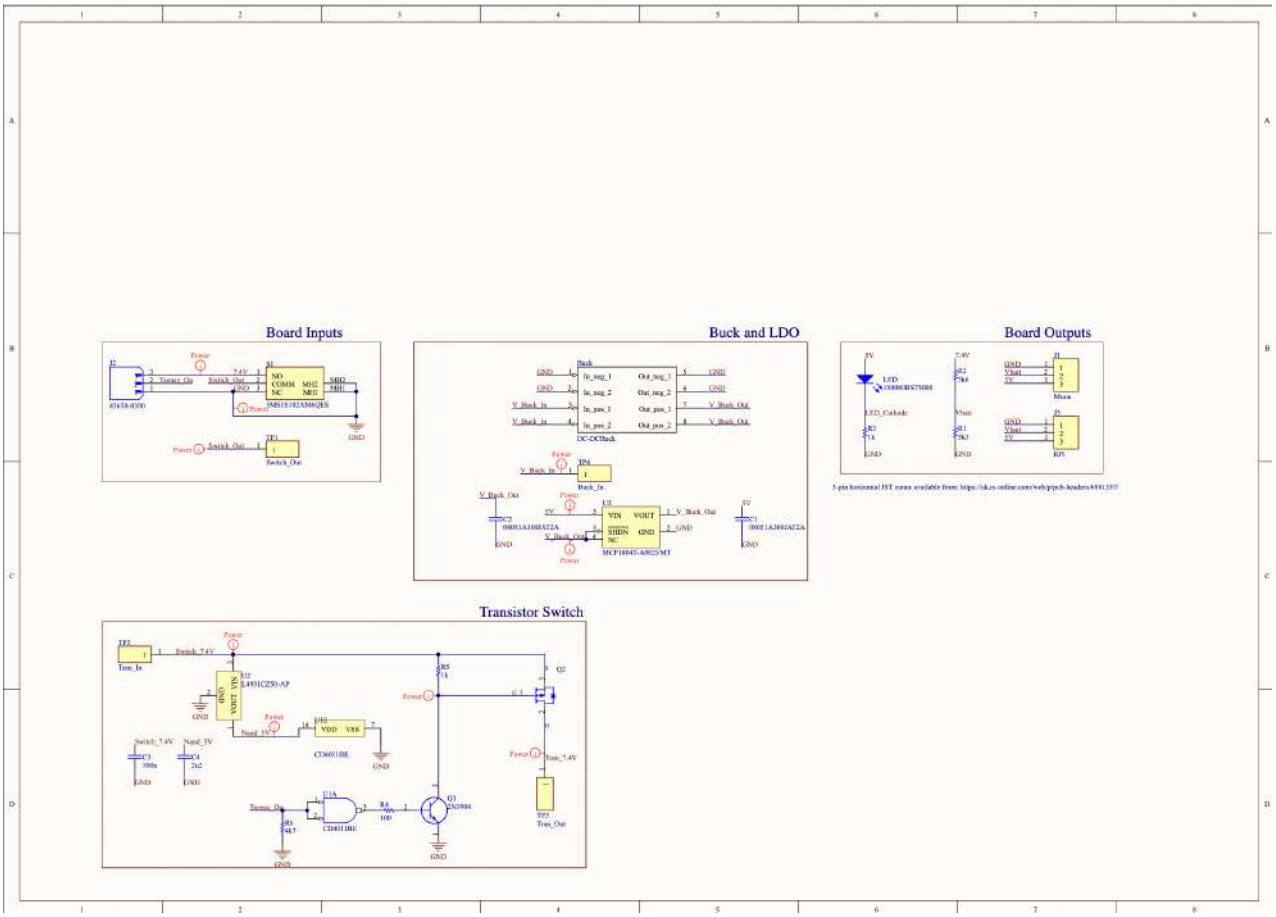

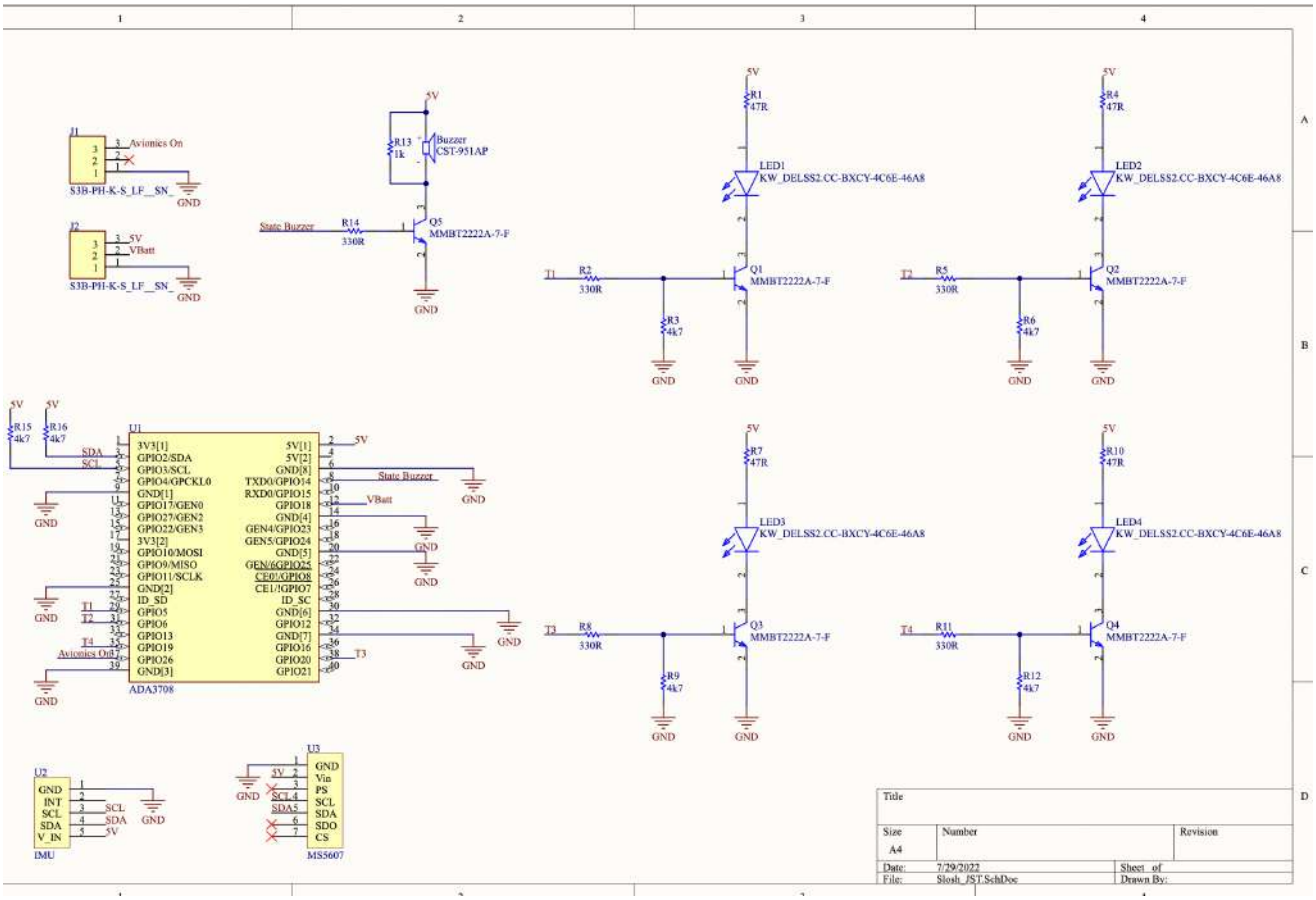
J1
Avionics On
S3B-PH-K-S_LF__SN_
GND
J2
5V
VBatt
S3B-PH-K-S_LF__SN_
GND
5V
R13
1k
Buzzer
CST-951AP
State Buzzer
R14
330R
Q5
MMBT2222A-7-F
GND
5V
R1
47R
LED1
KW_DELSS2.CC-BXCY-4C6E-46A8
T1
R2
330R
Q1
MMBT2222A-7-F
R3
4k7
GND
5V
R4
47R
LED2
KW_DELSS2.CC-BXCY-4C6E-46A8
T2
R5
330R
Q2
MMBT2222A-7-F
R6
4k7
GND
5V
R15
4k7
R16
4k7
SDA
SCL
U1
3V3[1]
GPIO2/SDA
GPIO3/SCL
GPIO4/GPCKL0
GND[1]
GPIO17/GEN0
GPIO27/GEN2
GPIO22/GEN3
3V3[2]
GPIO10/MOSI
GPIO9/MISO
GPIO11/SCLK
GND[2]
ID_SD
GPIO5
GPIO6
GPIO13
GPIO19
GPIO26
GND[3]
5V[1]
5V[2]
GND[8]
TXD0/GPIO14
RXD0/GPIO15
GPIO18
GND[4]
GEN4/GPIO23
GEN5/GPIO24
GND[5]
GEN6/GPIO25
CE0/GPIO8
CE1/GPIO7
ID_SC
GND[6]
GPIO12
GND[7]
GPIO16
GPIO20
GPIO21
ADA3708
State Buzzer
VBatt
Avionics On
T1
T2
T3
T4
GND
5V
R7
47R
LED3
KW_DELSS2.CC-BXCY-4C6E-46A8
T3
R8
330R
Q3
MMBT2222A-7-F
R9
4k7
GND
5V
R10
47R
LED4
KW_DELSS2.CC-BXCY-4C6E-46A8
T4
R11
330R
Q4
MMBT2222A-7-F
R12
4k7
GND
U2
GND
INT
SCL
SDA
V_IN
IMU
U3
GND
Vin
PS
SCL
SDA
SDO
CS
MS5607
Title
Size
A4
Number
Revision
Date:
7/29/2022
Sheet of
File:
Slosh_JST.SchDoc
Drawn By:

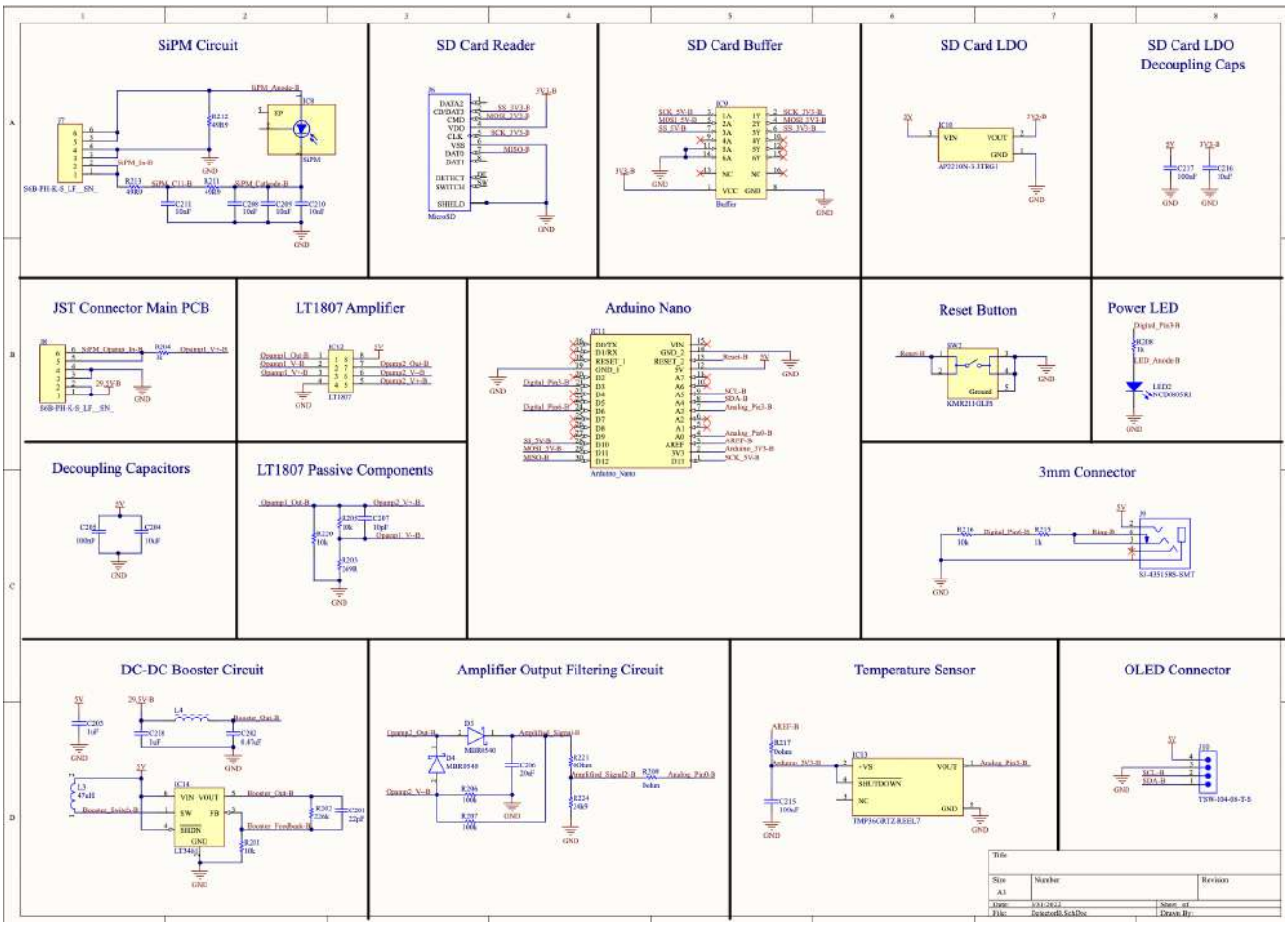
SiPM Circuit
SD Card Reader
SD Card Buffer
SD Card LDO
SD Card LDO Decoupling Caps
JST Connector Main PCB
LT1807 Amplifier
Arduino Nano
Reset Button
Power LED
Decoupling Capacitors
LT1807 Passive Components
3mm Connector
DC-DC Booster Circuit
Amplifier Output Filtering Circuit
Temperature Sensor
OLED Connector

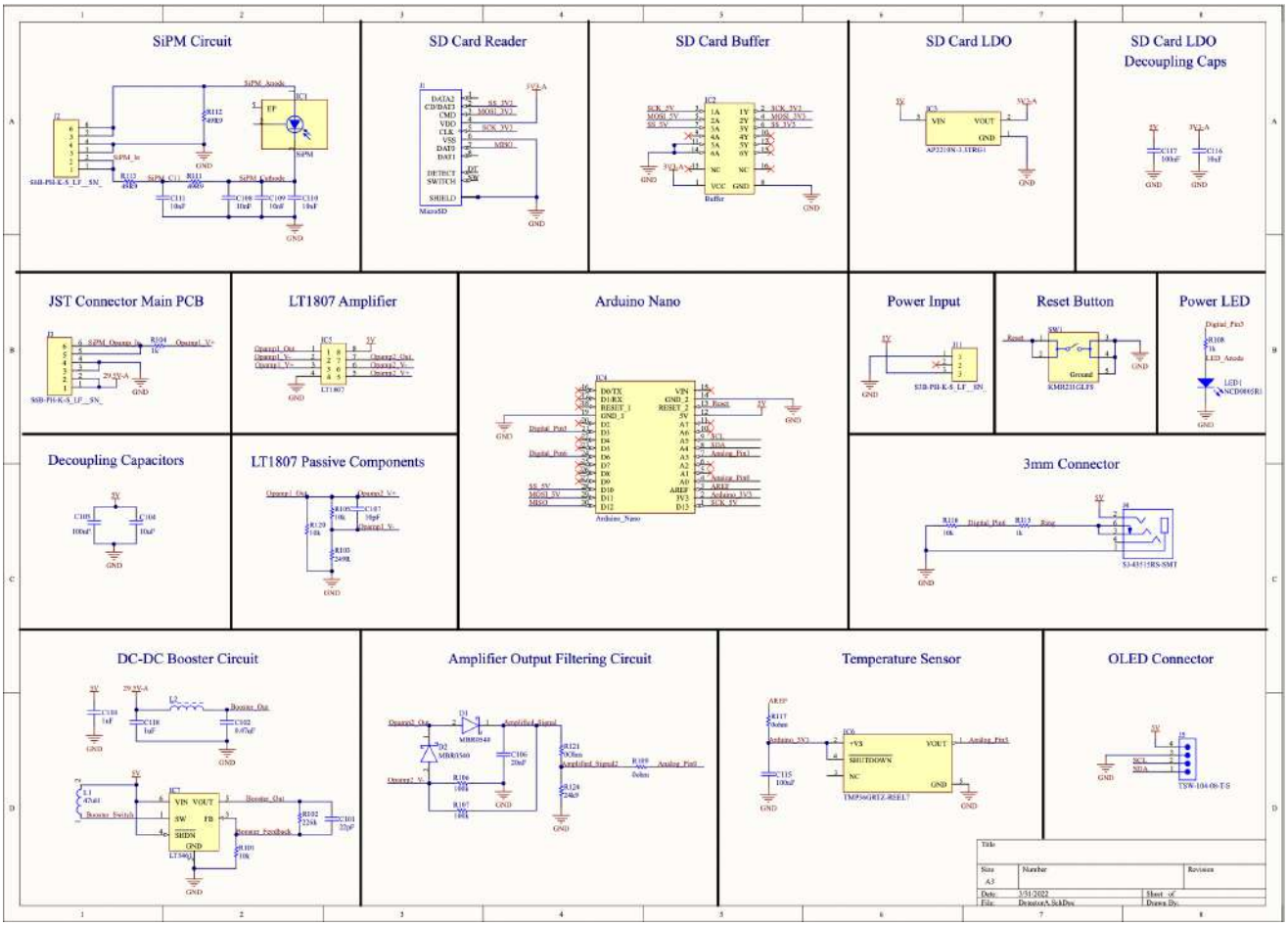
SiPM Circuit
SD Card Reader
SD Card Buffer
SD Card LDO
SD Card LDO Decoupling Caps
JST Connector Main PCB
LT1807 Amplifier
Arduino Nano
Power Input
Reset Button
Power LED
Decoupling Capacitors
LT1807 Passive Components
3mm Connector
DC-DC Booster Circuit
Amplifier Output Filtering Circuit
Temperature Sensor
OLED Connector

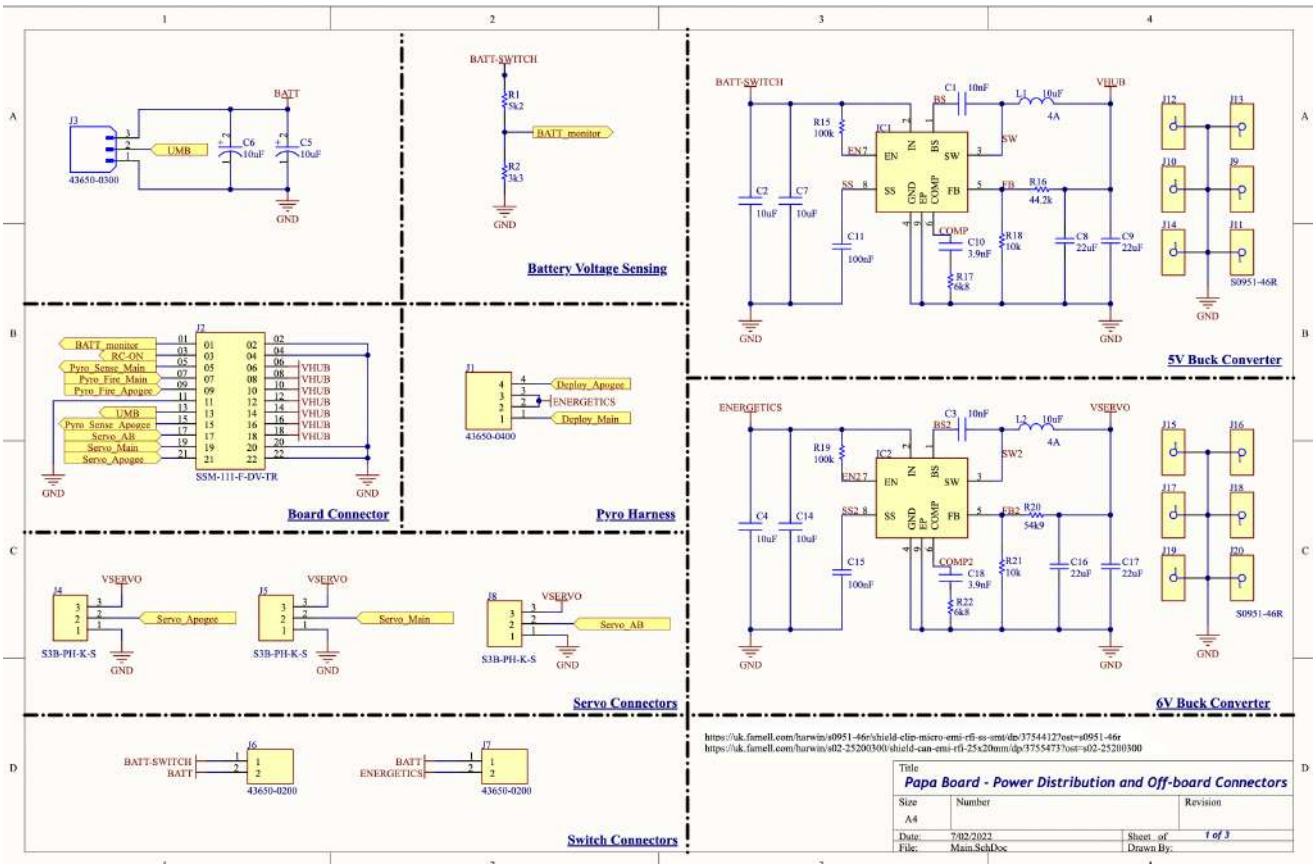
Battery Voltage Sensing
5V Buck Converter
Board Connector
Pyro Harness
Servo Connectors
6V Buck Converter
Switch Connectors
Papa Board - Power Distribution and Off-board Connectors

Current and Voltage Calculations

Assuming FULLY CHARGED battery

Current through Pyro Sense Circuit

Vbat = 12.6V

Total Resistance on Check Line = 13.3k Ohm

Discharge Current: 12.6/13.3 = 1mA

Voltage Div. Output with continuity

Pyro_Sense = Vbat [R8 /(R9+R8)]

'~ 12.6 * (3300 / 13300) ~ 3.12V

Power dissipated by Resistors

P (R7) = (12.6-3.12) * 0.001A = 10 mW

P (R8) = 3.12 * 0.001A = 3.1 mW

V and I limits for Reliable Igniter fire

0.5A < I_ignition < 2A

5V < V_Ignition < 12.6V

Is current Limiting on Igniter needed?

Igniter Resistance: 1<R<10 Ohm

MOSFET RDS: negligible

Without resistors: 12.6/1 = 12.6A DEAD

Without resistors: 12.6/10 = 1.26A OK

Due to variability, the resistance of all the igniters shall be measured. Pending analysis, resistor might be added. Appropriate power dissipation calculations MUST be conducted, together with practical testing of standard 0.25W resistors to check survivablity

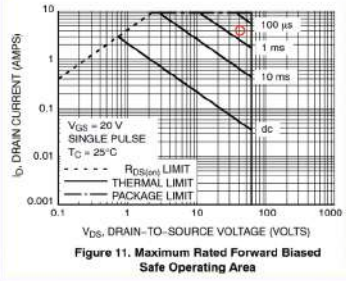

Figure 11. Maximum Rated Forward Biased Safe Operating Area

NVF3055 Datasheet

Pyro Pulse (12.6V, 2A)

Must be 2ms MAX.

Must test this!

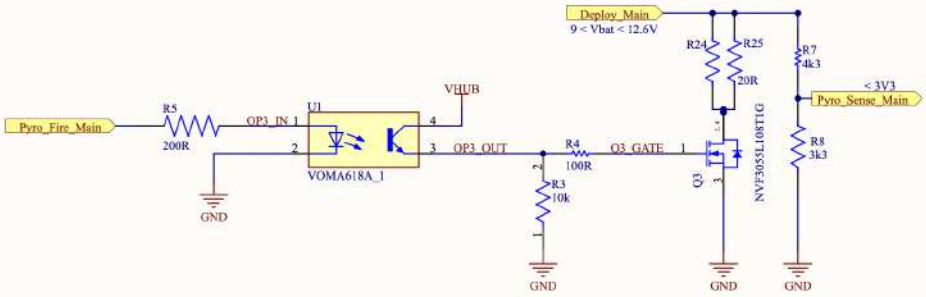

Title: **Papa Board - Main Pyro Ejection and Continuity Check**

Size	Number	Revision
A		
Date: 7/02/2022	Sheet of 2 of 3	
File: Pyro_Main.SchDoc	Drawn By:	

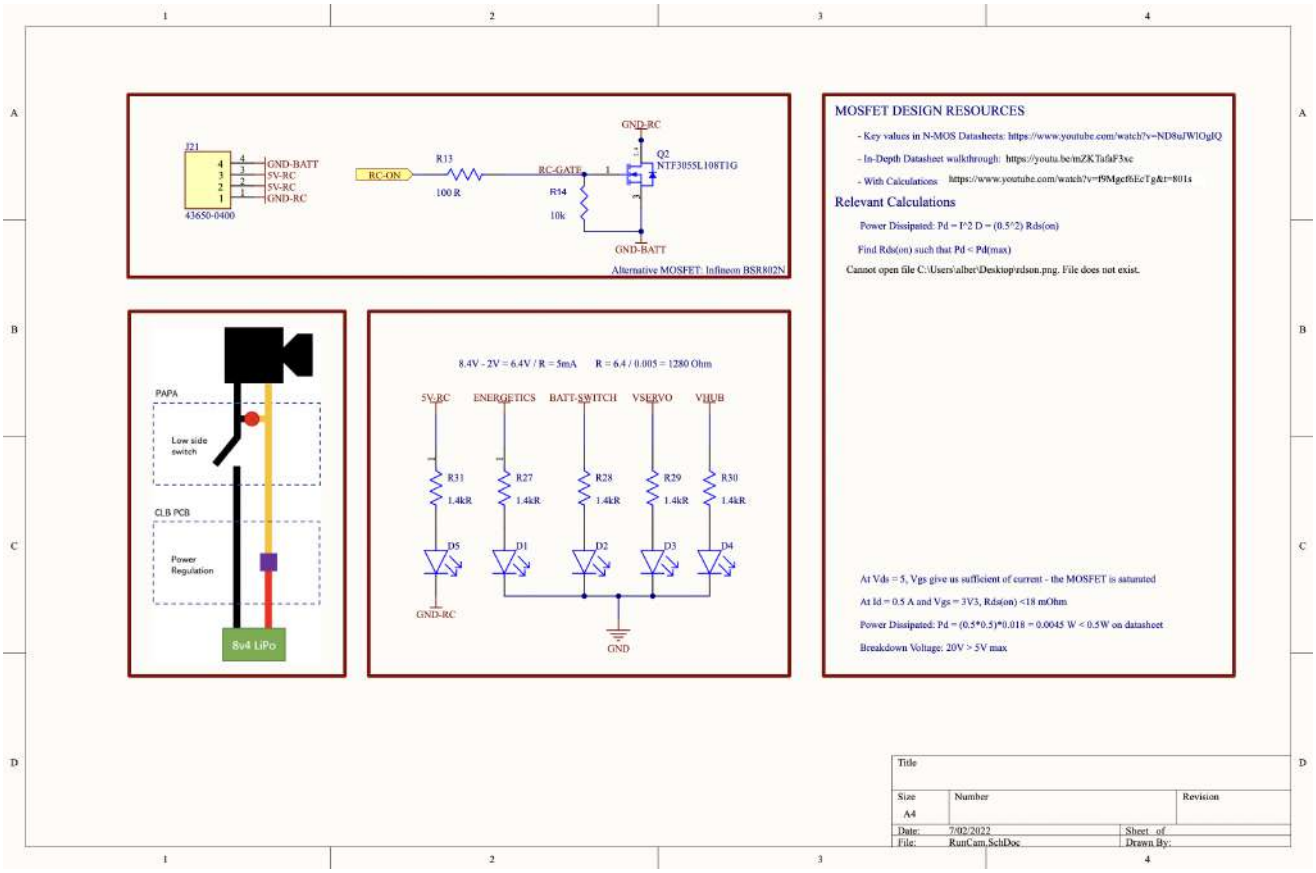
MOSFET DESIGN RESOURCES
- Key values in N-MOS Datasheets: https://www.youtube.com/watch?v=ND8uJWlOgIQ
- In-Depth Datasheet walkthrough: https://youtu.be/mZKTafaF3xc
- With Calculations https://www.youtube.com/watch?v=f9Mgcf6EcTg&t=801s
Relevant Calculations
Power Dissipated: Pd = I^2 D = (0.5^2) Rds(on)
Find Rds(on) such that Pd < Pd(max)
Cannot open file C:\Users\alber\Desktop\rdson.png. File does not exist.
At Vds = 5, Vgs give us sufficient of current - the MOSFET is saturated
At Id = 0.5 A and Vgs = 3V3, Rds(on) <18 mOhm
Power Dissipated: Pd = (0.5*0.5)*0.018 = 0.0045 W < 0.5W on datasheet
Breakdown Voltage: 20V > 5V max
Alternative MOSFET: Infineon BSR802N
8.4V - 2V = 6.4V / R = 5mA R = 6.4 / 0.005 = 1280 Ohm
PAPA
Low side switch
CLB PCB
Power Regulation
8v4 LiPo
Title
Size A4
Number
Revision
Date: 7/02/2022
File: RunCam.SchDoc
Sheet of
Drawn By:

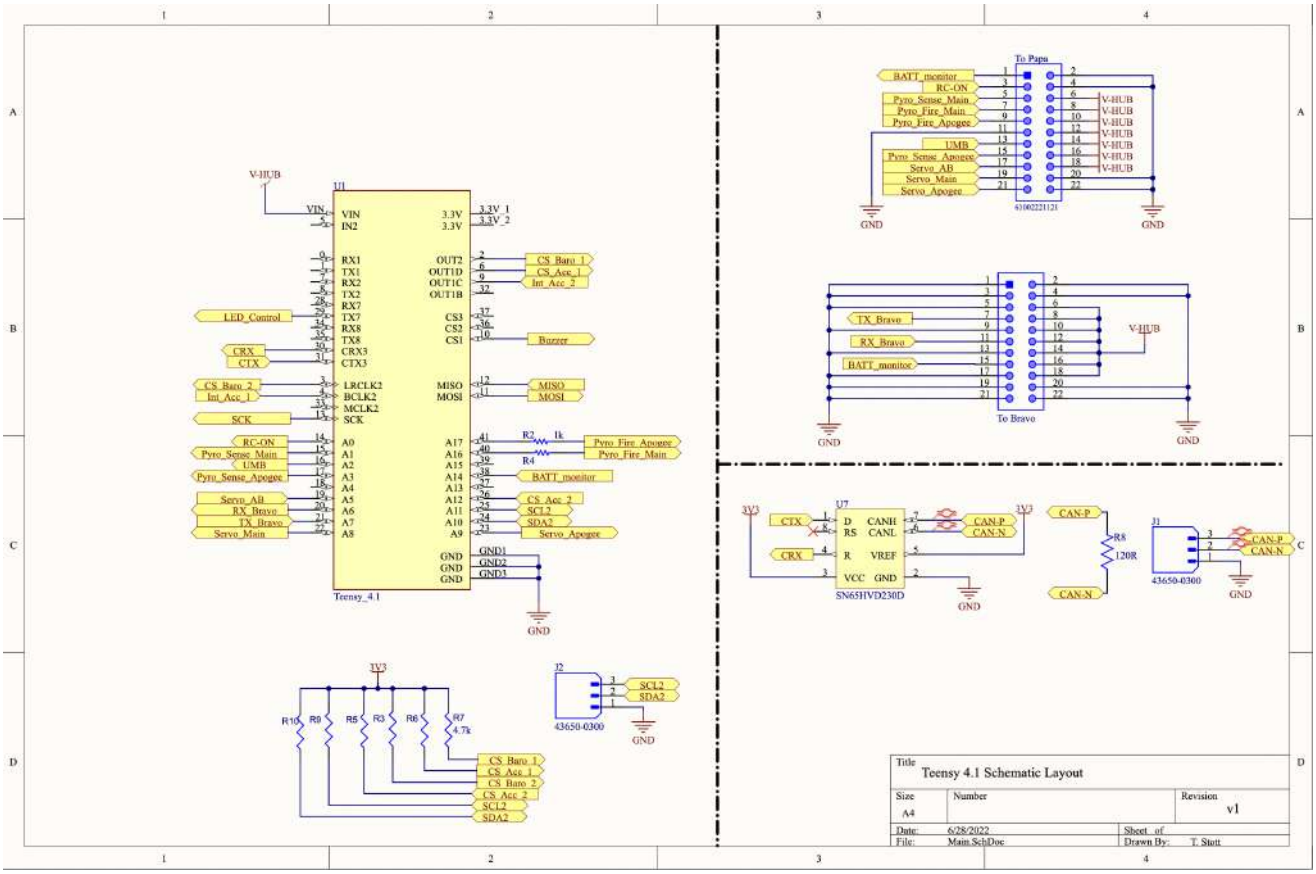
Teensy 4.1 Schematic Layout
Size A4
Number
Revision v1
Date: 6/28/2022
File: Main.SchDoc
Sheet of
Drawn By: T. Stott

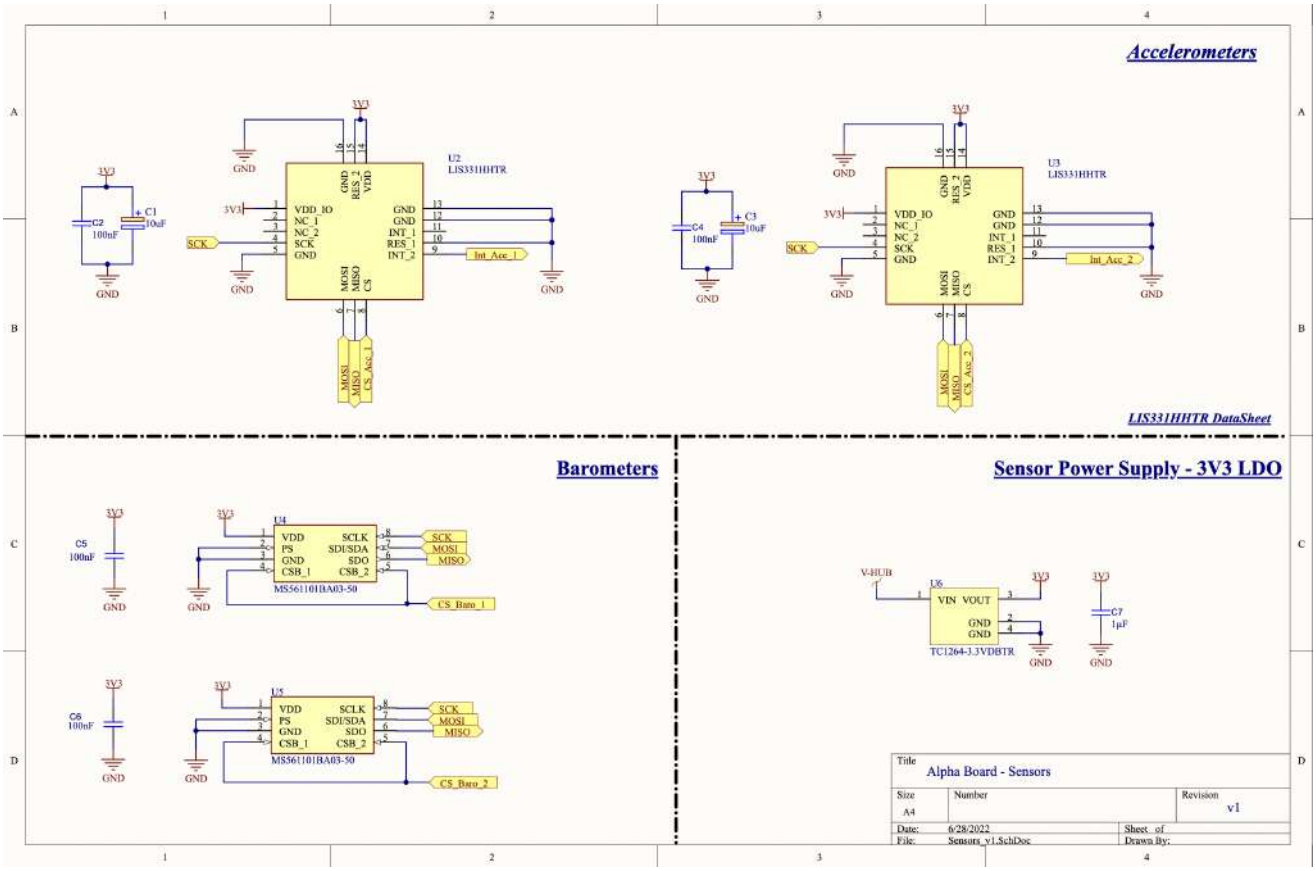
Accelerometers
U2
LIS331HHTR
U3
LIS331HHTR
LIS331HHTR DataSheet
Barometers
U4
U5
MS561101BA03-50
Sensor Power Supply - 3V3 LDO
U6
TC1264-3.3VDBTR
Title
Alpha Board - Sensors
Size
A4
Number
Revision
v1
Date: 6/28/2022
File: Sensors_v1.SchDoc
Sheet of
Drawn By:

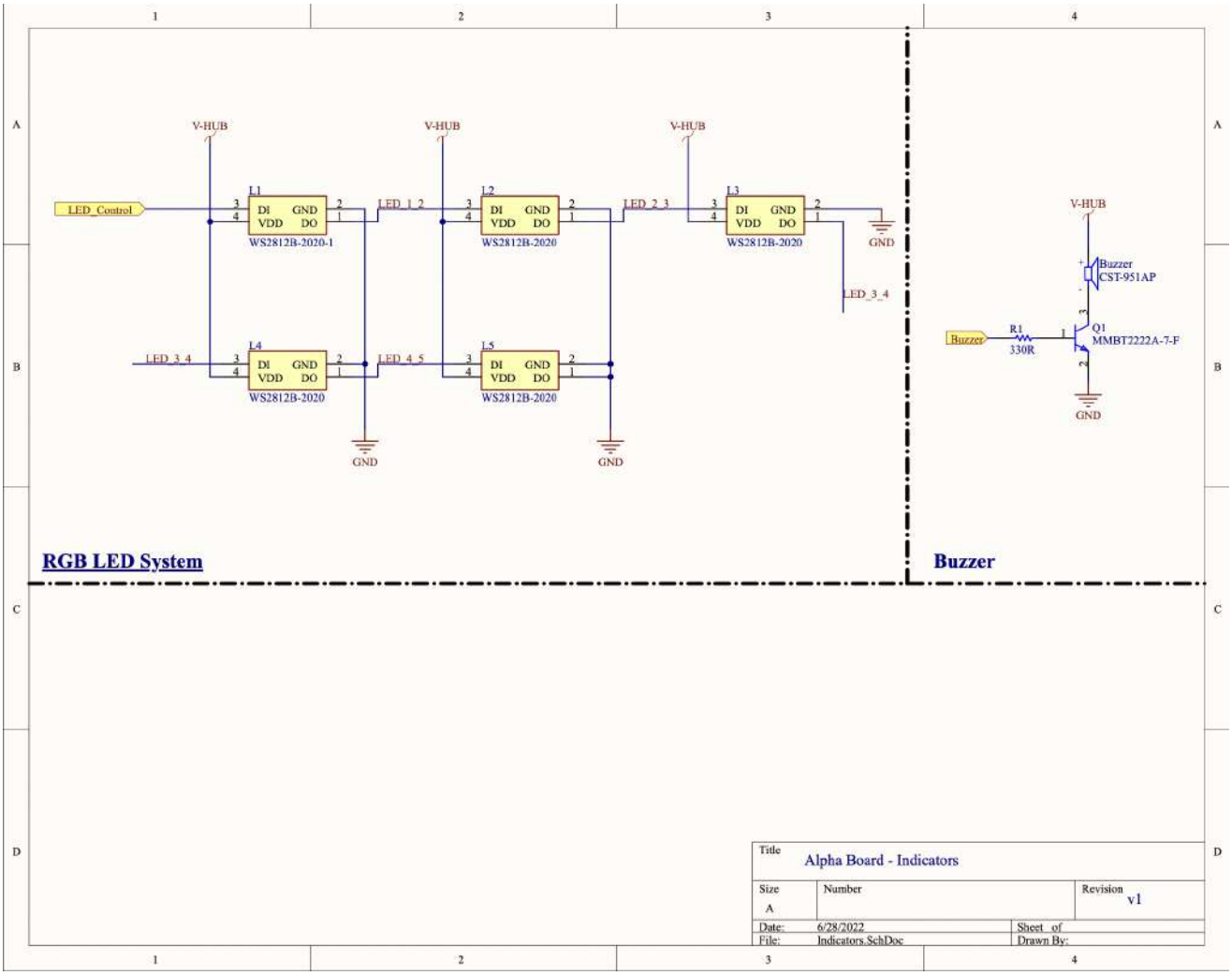
V-HUB
V-HUB
V-HUB
LED_Control
L1
L2
L3
DI GND
VDD DO
WS2812B-2020-1
WS2812B-2020
WS2812B-2020
LED_1_2
LED_2_3
GND
LED_3_4
LED_3_4
L4
L5
LED_4_5
WS2812B-2020
WS2812B-2020
GND
GND
RGB LED System
V-HUB
Buzzer
CST-951AP
Buzzer
R1
330R
Q1
MMBT2222A-7-F
GND
Buzzer
Title
Alpha Board - Indicators
Size
A
Number
Revision
v1
Date:
6/28/2022
Sheet of
File:
Indicators.SchDoc
Drawn By:

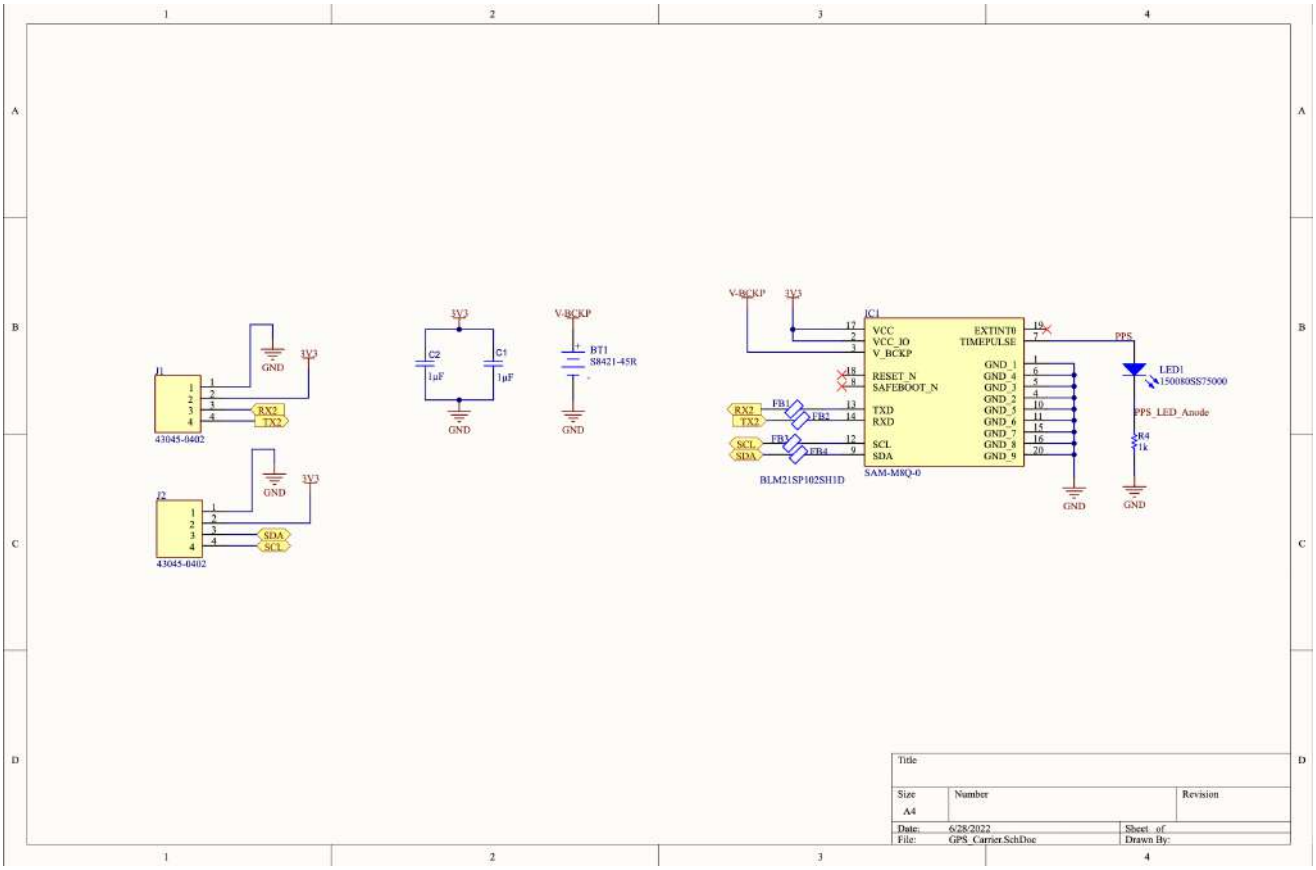
Title
Size
A4
Number
Revision
Date: 6/28/2022
File: GPS_Carrier.SchDoc
Sheet of
Drawn By:
SAM-M8Q-0
BLM21SP102SH1D
43045-0402
S8421-45R
LED1
PPS_LED_Anode

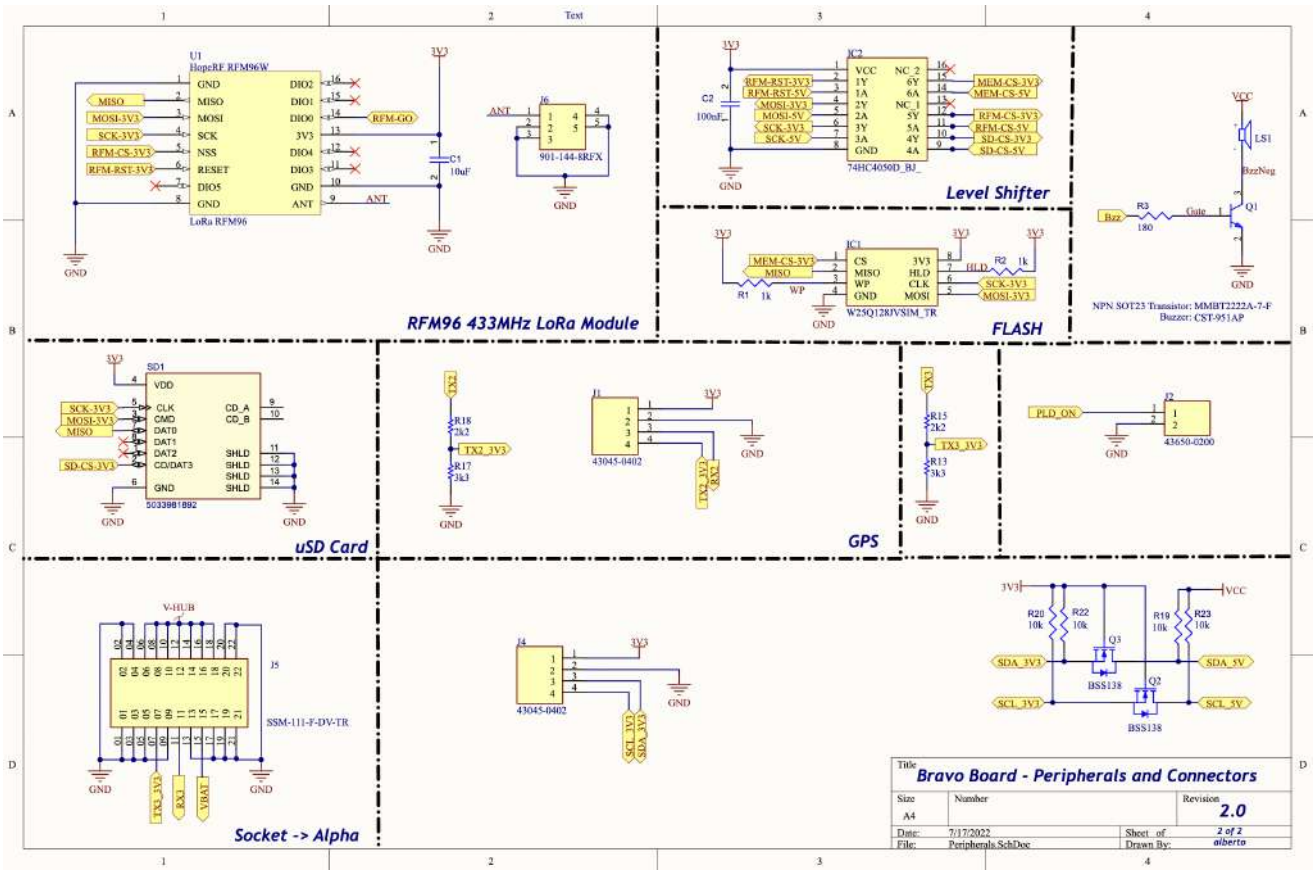
RFM96 433MHz LoRa Module
Level Shifter
FLASH
uSD Card
GPS
Socket -> Alpha
Bravo Board - Peripherals and Connectors
Size
A4
Number
Revision
2.0
Date: 7/17/2022
File: Peripherals.SchDoc
Sheet of
2 of 2
Drawn By:
alberto
HopeRF RFM96W
LoRa RFM96
74HC4050D_BJ_
W25Q128JVSIM_TR
NPN SOT23 Transistor: MMBT2222A-7-F
Buzzer: CST-951AP
SSM-111-F-DV-TR

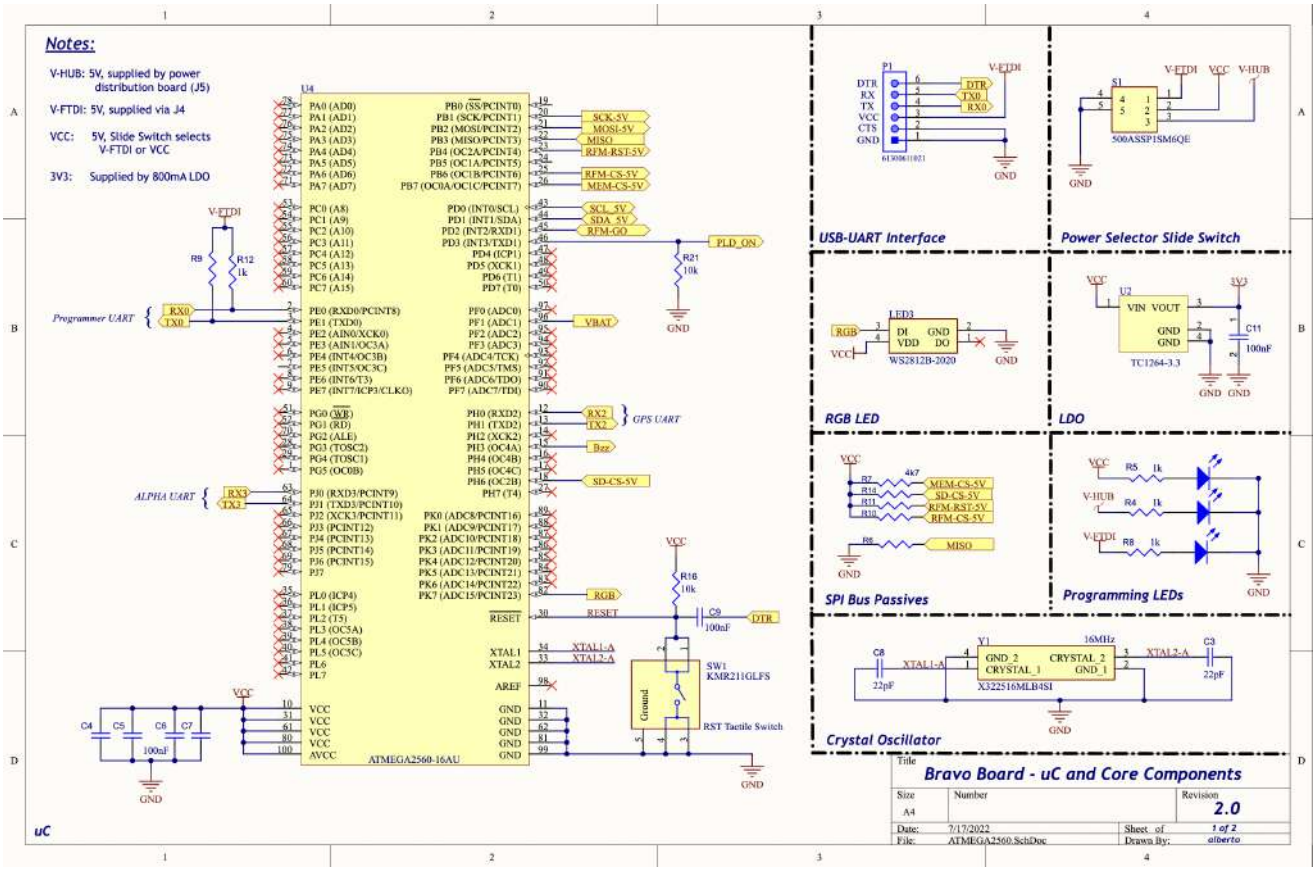
Notes:
V-HUB: 5V, supplied by power distribution board (J5)
V-FTDI: 5V, supplied via J4
VCC: 5V, Slide Switch selects V-FTDI or VCC
3V3: Supplied by 800mA LDO
ATMEGA2560-16AU
uC
USB-UART Interface
Power Selector Slide Switch
RGB LED
LDO
SPI Bus Passives
Programming LEDs
Crystal Oscillator
Bravo Board - uC and Core Components
Size A4
Number
Revision 2.0
Date: 7/17/2022
Sheet of 1 of 2
File: ATMEGA2560.SchDoc
Drawn By: alberto

J — Final launch role definition

Last edited: 13 Oct 2022

Thomas Stott	SRAD avionics deputy
Ann Lee	Recovery deputy
Alberto Progida	Flight director & avionics lead
Zsolt Csonka	Structures lead
Jasper Day	Structures deputy
Matus Komjaty	COTS avionics deputy
Daniel Holler	Software lead
Joseph Azrak	Ground station operator & software deputy
Alex Stevenson	Recovery lead
Jo Shepton	Payload lead
Virginia Cangelosi	Payload electrical deputy lead
Fergus Wilson	Payload mechanical deputy
Phil Henrich	Payload software deputy